



TÉCNICO
LISBOA

Reinforcement Learning for Robust Missile Autopilot Design

Bernardo Gonçalves Ferreira Cortez

Thesis to obtain the Master of Science Degree in

Aerospace Engineering

Supervisor(s): Dr. Florian Ulrich Peter
Prof. Paulo Jorge Coelho Ramalho Oliveira

Examination Committee

Chairperson: Prof. José Fernando Alves da Silva

Supervisor: Dr. Florian Ulrich Peter

Supervisor: Prof. Paulo Jorge Coelho Ramalho Oliveira

Member of the Committee: Prof. Jacinto Carlos Marques Peixoto do Nascimento

December 2020

"Our era needs such wisdom more than bygone ages if the discoveries made by man are to be further humanized. For the future of the world stands in peril unless wiser men are forthcoming."

Pastoral Constitution *Gaudium et Spes*, n.15

AMDG

Acknowledgments

First and foremost, I must thank my family and friends, namely to Mãe, Pai, Kiko, António, Jaime, Maria, Teresa and my grandparents, who have always given me the opportunity to have a fully-integrated and enriching life. They have been specially important in this past months in Germany, to overcome the pandemic times. A special word to my grandfather whose birthday we celebrate in the day I am finishing this writing and who has taught with his example the values of personal and professional responsibility and attentiveness to the others.

Besides, I warmly thank St. Anton parish for welcoming me and also to my dear friends of GVXoxo. They both nourished and promoted my spiritual life, a key side of my eight months stay in Ingolstadt .

Thirdly, I thank the inspiring and interesting lecturers I have come across to in my academic life, namely, professors André Marta, André Martins, António Pascoal, Alex Jung, Nuno Roma, Pedro Batista, Paulo Lopes and Paulo Oliveira. They were a rare breath of fresh air, sharing their knowledge with passion and therefore deserve to be acknowledged.

Fourthly, I want to thank Dr. Florian Peter, who has always achieved a good balance between patience and rigour. A word, as well, to Pascal Kößler for sharing his knowledge and work progress and for his constant availability to answer all my questions.

Finally, I cordially thank Instituto Superior Técnico, TU München and MBDA-D for providing the necessary financial, software and supervising conditions ensuring that I had as much success as possible in this work.

Resumo

Desenvolver controladores de piloto automático de mísseis tem sido uma tarefa complexa, dado o extenso envelope de voo e a sua dinâmica não linear. Permanece desconhecida a solução que seja ótima quer em termos de desempenho nominal quer em robustez a incertezas. Enquanto a Teoria do Controlo acaba por cair em procedimentos de agendamento de parâmetros, a Aprendizagem por Reforço (AR) tem mostrado resultados interessantes em tarefas cada vez mais complexas, desde video-jogos até tarefas robóticas com domínios de ação contínuos. Contudo, falta, ainda, uma maior clarificação sobre como encontrar funções de recompensa e estratégias de exploração adequadas.

Que seja do nosso conhecimento, este trabalho é pioneiro ao propor AR como paradigma para controlo de voo. De facto, visa treinar um agente sem-modelo que controle a dinâmica de voo não linear longitudinal de um míssil, atingindo um desempenho ótimo e robustez. Para tal, sob a metodologia TRPO, a experiência recolhida é aumentada de acordo com HER, guardada num acumulador de amostras e extraída de acordo com a sua pertinência.

Evoluindo o conceito de reprodução prioritizada de experiência para BPER, também reformulamos HER, ativando-os apenas quando o treino converge para políticas subótimas, naquilo a que chamamos a metodologia SER. Finalmente, o processo de Engenharia da Recompensa é detalhadamente exposto.

Os resultados mostram ser possível tanto atingir o desempenho desejado como melhorar a robustez do agente a incertezas (sem consideráveis danos no desempenho nominal) ao treiná-lo em ambientes não nominais, validando, assim, a abordagem proposta e encorajando investigações futuras nesta área.

Palavras-chave: Aprendizagem por reforço, TRPO, HER, controlo de voo, piloto automático de mísseis.

Abstract

Designing missiles' autopilot controllers has been a complex task, given the extensive flight envelope and the nonlinear flight dynamics. A solution that can excel both in nominal performance and in robustness to uncertainties is still to be found. While Control Theory often debouches into parameters' scheduling procedures, Reinforcement Learning has presented interesting results in ever more complex tasks, going from videogames to robotic tasks with continuous action domains. However, it still lacks clearer insights on how to find adequate reward functions and exploration strategies.

To the best of our knowledge, this work is pioneer in proposing Reinforcement Learning as a framework for flight control. In fact, it aims at training a model-free agent that can control the longitudinal non-linear flight dynamics of a missile, achieving target performance and robustness to uncertainties. To that end, under TRPO's methodology, the collected experience is augmented according to HER, stored in a replay buffer and sampled according to its significance.

Not only does this work enhance the concept of prioritized experience replay into BPER, but it also reformulates HER, activating them both only when the training progress converges to suboptimal policies, in what is proposed as the SER methodology. Besides, the Reward Engineering process is carefully detailed.

The results show that it is possible both to achieve the target performance and to improve the agent's robustness to uncertainties (with low damage on nominal performance) by further training it in non-nominal environments, therefore validating the proposed approach and encouraging future research in this field.

Keywords: Reinforcement Learning, TRPO, HER, flight control, missile autopilot.

Contents

Acknowledgments	v
Resumo	vii
Abstract	ix
List of Tables	xiii
List of Figures	xv
Nomenclature	xvii
Acronyms	xvii
1 Introduction	1
1.1 Motivation	1
1.2 Topic Overview	2
1.3 Objectives	3
1.4 Thesis Outline	3
2 Model	5
2.1 Modelled Dynamics	5
2.1.1 Forces and Moments	5
2.1.2 Flight Dynamics	6
2.1.3 Longitudinal Approximation	7
2.1.4 Reference Model	8
2.2 Problem Formulation	8
3 Background	13
3.1 Reinforcement Learning - Basic Concepts	13
3.2 Trust Region Policy Optimization	18
3.3 Reward Engineering	19
3.4 Hindsight Experience Replay	20
3.5 Prioritized Experience Replay	21
4 Application of Reinforcement Learning to the Missile's Flight	23
4.1 Reward Engineering	23
4.1.1 Dense Exponential	24

4.1.2	Dense Sum	26
4.1.3	Sparse	28
4.1.4	Dense Sum with SER	29
4.2	Algorithm	32
4.2.1	Hyperparameters' Configuration	32
4.2.2	Modifications to original TRPO	32
4.2.3	Hindsight Experience Replay	38
4.2.4	Balanced Prioritized Experience Replay	39
4.2.5	Scheduled Experience Replay	40
4.2.6	Algorithm Description	41
4.3	Methodology	43
4.3.1	Command Reference Signal Generation	43
4.3.2	Intermediate Tests	44
4.4	Reproducibility Assessments	45
4.5	Robustness Assessments	46
4.5.1	Robustifying Trains	46
4.5.2	Robustified Agent	48
5	Results and Discussion	49
5.1	Expected Results	49
5.2	Best Found Agent	49
5.2.1	Training Evolution	50
5.2.2	Test Performance	52
5.3	Reproducibility Assessments	53
5.4	Robustness Assessments	53
5.4.1	Latency	53
5.4.2	Estimation Uncertainty	54
5.4.3	Parametric Uncertainty	55
6	Conclusions	59
6.1	Achievements	59
6.2	Future Work	59
	Bibliography	61
	A Reward Engineering	65
	B Nominal Agent used in the Robustness Assessments	66
	C Reproducibility Assessment Experiments	67
	D Nominal and Robustified Agents' Robustness Comparison	77

List of Tables

2.1	Hard Criteria	9
4.1	Hyperparameters' Configuration	33
4.2	Hidden Layers of the Neural Networks	33
4.3	Exploration strategy parameters	36
4.4	Parameters of the Uniform Distribution of the Training Reference Signal Characterization	44
4.5	Testing Reference Signal Characterization	44
4.6	Soft Criteria	45
5.1	Performance achieved by the Best Found Nominal Agent	52
5.2	Robustified Agent success rate in improving the robustness to Latency of the Nominal Agent	54
5.3	Robustified Agent success rate in improving the robustness to Estimation Uncertainty of the Nominal Agent	56
5.4	Robustified Agent success rate in improving the robustness to Parametric Uncertainty of the Nominal Agent	57
A.1	Parameters of the CORF used along the Reward Engineering process	65
B.1	Performance achieved by the 2 nd Best Found Nominal Agent	66

List of Figures

2.1	Shaped and command reference signals	9
2.2	Block diagram including the Reference Model	9
4.1	Suboptimal Agent with oscillatory η in resting periods	28
4.2	Impact of the speed in the sigmoid function	36
4.3	Sigmoid-like decay of $\sigma_{\log,tune}^2$	36
4.4	Testing performance of suboptimal policies	38
4.5	Testing performance of an untrained policy	39
4.6	Evolution of the Amplitude of the Reference Signal during Training	43
4.7	Command Reference Signal	44
5.1	η 's evolution during best found agent's training	50
5.2	η 's resting noise evolution during best found agent's training	50
5.3	η 's transition noise evolution during best found agent's training	51
5.4	Resting tracking error's (acceleration z) evolution during best found agent's training	51
5.5	Transition tracking error's (acceleration z) evolution during best found agent's training	51
5.6	Mean reward per step's evolution during best found agent's training	52
5.7	Test performance of the Best Found Agent	52
5.8	Nominal test performance of the Reproducibility Trials	53
5.9	Mean tracking error of latency robustifying trains	54
5.10	Nominal Performance of the Latency Robustified Agent	54
5.11	Mean tracking error of estimation uncertainty robustifying trains	55
5.12	Nominal Performance of the Estimation Uncertainty Robustified Agent	55
5.13	Mean tracking error of parametric uncertainty robustifying trains	56
5.14	Nominal Performance of the Parametric Uncertainty Robustified Agent	56
B.1	Nominal performance of the $2^n d$ -Best Found Agent used in the Robustness Assessments	66
C.1	Reproducibility assessment training - experiment 1	68
C.2	Reproducibility assessment training - experiment 2	69
C.3	Reproducibility assessment training - experiment 3	70
C.4	Reproducibility assessment training - experiment 4	71

C.5	Reproducibility assessment training - experiment 5	72
C.6	Reproducibility assessment training - experiment 6	73
C.7	Reproducibility assessment training - experiment 7	74
C.8	Reproducibility assessment training - experiment 8	75
C.9	Reproducibility assessment training - experiment 9	76
D.1	Nominal (N) vs. Robustified (R) Agents in Environments with Latency	77
D.2	Nominal (N) vs. Robustified (R) Agents in Environments with Estimation Uncertainty . . .	78
D.3	Nominal (N) vs. Robustified (R) Agents in Environments with Parametric Uncertainty . . .	79

Chapter 1

Introduction

1.1 Motivation

Over the last decades, both the industry and the academic community have been interested in the challenge of controlling the dynamics of non-linear systems, such as missiles. In this specific case, the design of a missiles' autopilot flight controller is dominated by fulfilling demanding requirements concerning performance and robustness over an extensive flight envelope, which, together with the nonlinear dynamic characteristics, make a scheduling of the control parameters over the flight envelope necessary. This leads to tedious design procedures for the selected control architecture and to a very low generalization ability, since the designed control architecture is neither transferable across missile configurations nor flight envelopes.

Reinforcement Learning (RL) constitutes a promising approach to facilitate and standardize the latter for its ability of controlling systems from which it has no prior information.

One could say that the low complexity of the longitudinal flight dynamics is not enough to justify the effort, the time and the resources the present research requires. However, one has to consider, as well, the problem in its whole. Controlling the longitudinal flight dynamics constitutes merely a first step, necessary to the posterior possible expansion of the approach to the whole flight dynamics.

This latter expansion is not exactly direct. On the one side, the complete model is more complex, with possible cross-coupling effects between the several directions of motion. On the other side, the dimension of the state vector will not scale proportionally with the number of dimensions (which triples in the complete model), since the Mach number and the height are not specific to any direction of motion and were already included in the state vector (cf. section 2.2); besides, there is also the plausible hypothesis that the growth in complexity would actually favour a quicker convergence to the optimal policy, since the agent would have a considerably wider range of possible (combinations of) actions.

All in all, weighing all these scenarios tilts in favour of a promising success. This work is, hence, motivated by the will of finding such a RL algorithm. One that can control the longitudinal flight dynamics (cf. section 2.1.2) of a Generic Surface-To-Air Missile (GSAM) with no prior information about it¹, achieving

¹Being, thus, *model-free* (cf. section 3.1).

the desired performance (cf. section 1.3).

1.2 Topic Overview

After the foundations laid out by Sutton et al. [1], Mnih et al. [2] opened the door of the discrete control tasks based on visual inputs for RL. Since then, the Atari 2600 games, the MuJoCo games [3], grasping robots or other classic control problems like the inverted pendulum have become of crosswise usage and are used as benchmarks for assessment of success for new algorithms with the Gym toolkit [4].

It was not long until Schulman et al. [5] proposed TRPO, a model-free on-policy algorithm inspired in the natural policy gradient methods but with increased convergence ability for large non-linear policies, ensuring near monotonic improvements in return by avoiding too drastic policy updates with the objective of avoiding the policy to diverge during training. Perpendicularly to TRPO, Lillicrap et al. [6] proposed DDPG, a model-free off-policy algorithm, revolutionary not only for its ability of learning directly from pixels while maintaining the network architecture simple, which favours its scalability, but mainly because it was designed to cope with continuous domain action. Contrarily to TRPO, DDPG's off-policy nature implied a much higher sample efficiency, resulting in a faster training phase.

Both TRPO and DDPG have been the roots for much of the research work that followed.

On the one side, some authors valued more the benefits of an off-policy algorithm (cf. section 3.1) and took the inspiration in DDPG to develop TD3 [7], addressing DDPG's problem of over-estimation of the states' value. On the other side, others preferred the benefits of off-policy algorithm and proposed interesting improvements to the original TRPO, either by reducing its implementation complexity [8], by trying to decrease the variance of its estimates [9] or even by showing the benefits of its interconnection with replay buffers [10].

Apart from these, a new result began to arise: agents were ensuring stability at the expense of converging to suboptimal solutions. Once again, new algorithms were conceived in each family, on- and off-policy. Haarnoja and Tang proposed to express the optimal policy via a Boltzmann distribution in order to learn stochastic behaviors and to improve the exploration phase within the scope of an off-policy actor-critic architecture: Soft Q-learning [11]. Almost simultaneously, Schulman et al. published PPO [12], claiming to have simplified TRPO's implementation and increased its sample-efficiency by inserting an entropy bonus to increase exploration performance and avoid premature suboptimal convergence. Furthermore, Haarnoja et al. developed SAC [13], in an attempt to recover the training stability without losing the entropy-encouraged exploration and Nachum et al. proposed Smoothie [14], allying the trust region implementation of PPO with DDPG.

Faced with increasingly complex and memory-expensive problems, researchers focused on distributed implementations, which would take advantage of the parallelization of training allowed by the simultaneous operation of multiple agents. This is the motivation for Horgan et al. [15], for D4PG [16], which directly extended the concept of DDPG, and for IMPALA [17].

Finally, there has also been research done on merging both on-policy and off-policy algorithms, trying to profit from the upsides of both, like Interpolated-PG [18], Trust-PCL [19], Q-Prop [20] and PGQL [21].

1.3 Objectives

Having the motivation of section 1.1 in mind and considering all the approaches put forward in section 1.2, this thesis aims at conceiving and implementing a model-free (cf. section 3.1) algorithm within the RL framework to interact with the longitudinal flight non-linear dynamic model of a GSAM using its actuation system (cf. section 2.1.3) in order to achieve certain performance requirements, provided that such a model feeds the RL algorithm back with information about the GSAM's state, thus replacing the autopilot's controller. This algorithm must be designed in the most generic fashion so that it remains pluggable in several different GSAMs/models scenarios.

Finally, the present work also aims at achieving and improving the robustness of the algorithm to conditions different from the training ones (cf. section 4.5).

Performance requirements

The algorithms success will later (cf. section 2.2) be conditioned on whether or not the GSAM's performance achieved the following requirements, whose definition is external to the scope of this thesis:

1. Closed-loop characteristics:
 - (a) Natural frequency = 10 rad.s^{-1}
 - (b) Damping factor = 0.7
2. Static error margin = 0.5%
3. Overshoot $< 20\%$
4. Rise time $< 0.6\text{s}$
5. Settling time (5%) $< 0.6\text{s}$
6. Bounded actuation
7. Smooth actuation

1.4 Thesis Outline

This thesis is structured in four main chapters: an introduction about the model and the formulation of the problem (cf. chapter 2); some theoretical background about concepts that will be crucial to the comprehension of the following chapters (cf. chapter 3); the proposed approach (cf. chapter 4); and its results alongside the respective discussion (cf. chapter 5).

In fact, firstly, after having described the dynamics of the model to be controlled in chapter 2, chapter 3 explains a few brief and intuitive theoretical concepts. Some are basic RL concepts (cf. section 3.1) and other are state-of-the-art RL algorithms and complementary features. This chapter will assume a minimum knowledge about basic Machine Learning (ML), namely that the reader is familiar with basic neural networks and their process of optimization.

In turn, chapter 4 materializes the theory previously exposed by carefully analyzing the proposed algorithm, which is holistically summarized in section 4.2.6 with further details along section 4.2. This chapter also includes descriptions of the methodology followed when training the agent (cf. section 4.3), in the Reproducibility Assessments (cf. section 4.4) and in the Robustness Assessments (cf. section 4.5), whose results are, then, presented in chapter 5. Here, it will be possible to compare the expectations (cf. section 5.1) to the training progress records (cf. section 5.2.1) and to the test performance in the several nominal (cf. section 5.2.2) and non-nominal environments (cf. section 5.4).

After all the latter, the thesis will conclude with a brief summary of the most relevant achievements (cf. section 6.1) and some suggestions of directions for future research (cf. section 6.2).

Chapter 2

Model

The present chapter introduces the dynamics of the system with which the RL agent interacts (cf. section 2.1), including the GSAM's non linear dynamics (cf. section 2.1.2) and the actuator system dynamics (cf. section 2.1.3). After having covered the mentioned dynamics, this chapter also formulates the problem of controlling the described model in the RL framework (cf. section 2.2).

2.1 Modelled Dynamics

The present section follows the nomenclature, coordinate frames and assumptions of Peter et al. [22].

The concept of *flight envelope* is very important, as it loosely refers to the capabilities of the aircraft in terms of airspeed, air density or height. In Control Theory, for example, it is often used for scheduling different designs or parameters' configurations, when facing the impossibility of having the same configuration for the range of possible applications and/or maneuvers.

2.1.1 Forces and Moments

Considering the GSAM as a purely ballistic rigid body, the total forces F_T and moments M_T acting on the it are given by equations (2.1) and (2.2), neglecting any component related with thrust.

$$F_T = F_A + F_G \quad (2.1)$$

$$M_T = M_A \quad (2.2)$$

Notice that the gravitational component of M_T is canceled by considering the GSAM's center of gravity - where the gravitational force is applied - as the reference point. In the North-East-Down (NED) frame, the *O-frame*, it is given by equation (2.3).

$$(F_G)^O = [0, 0, mg]^T \quad (2.3)$$

Together with the chosen geometry and the mass distribution, the aerodynamic force F_A and moment M_A differentiates each GSAM, dictating its dynamic characteristic. In the Body-Fixed frame, the B -frame, F_A and M_A are given by equations (2.4) and (2.5), where \bar{q} , S_{ref} and l_{ref} are the dynamic pressure, the aerodynamic reference area and the reference length.

$$(F_A)^B = \begin{bmatrix} F_{x,A} \\ F_{y,A} \\ F_{z,A} \end{bmatrix}^B = \bar{q} S_{ref} \begin{bmatrix} C_x \\ C_y \\ C_z \end{bmatrix}^B \quad (2.4)$$

$$(M_A)^B = \begin{bmatrix} L_A \\ M_A \\ N_A \end{bmatrix}^B = \bar{q} S_{ref} l_{ref} \begin{bmatrix} C_l \\ C_m \\ C_n \end{bmatrix}^B \quad (2.5)$$

2.1.2 Flight Dynamics

The GSAM is modelled as a rigid body whose non-linear dynamics is composed of four distinct types: translation, rotation, position and attitude. The following equations were extracted from Peter et al. [22], who have carefully detailed their mathematical demonstration.

Translation Dynamics

The translation dynamics is characterized by equation (2.6), in which the dynamics of the velocity of the center of gravity with respect to the Earth-Centered Earth-Fixed frame, the E -frame $V_G^E = \left(\begin{bmatrix} u_G & v_G & w_G \end{bmatrix}^E \right)^T$ is related with the total force applied in the center of gravity $F_{T,G}$ and with GSAM rotation rates with respect to the E-frame ω^E .

$$\dot{V}_G^E = \frac{1}{m} F_{T,G} - \omega^E \times V_G^E \quad (2.6)$$

From $(V_G^E)^E$, the Mach number M is defined as in equation (2.7) (c is the speed of sound), which is used to characterize the flight envelope (cf. section 2.1).

$$M = \frac{|V_G^E|}{c} \quad (2.7)$$

Rotation Dynamics

The rotation dynamics is characterized by equation (2.8), in which the dynamics of the body rate with respect to the E-frame $\omega^E = \left(\begin{bmatrix} p & q & r \end{bmatrix}^E \right)^T$ is related with the total moment applied in the center of gravity M_T^G and with the inertia tensor of the center of gravity J_G .

$$\dot{\omega}^E = (J_G)^{-1} (M_{T,G} - \omega^E \times J_G \omega^E) \quad (2.8)$$

Position Dynamics

As Peter et al. [22] states, under their assumptions, the E-frame is the inertial frame used as the coordinates system for the GSAM position $r_G = [x_G \ y_G \ z_G]$, whose dynamics is characterized by equation (2.9), relating with the the translation dynamics (cf. section (2.6)) and with the total moment applied in the GSAM M_T .

$$\dot{r}_G^E = M_T V_G^E \quad (2.9)$$

In addition to the Mach number (cf. equation (2.7)), the height h , i.e., the distance of the GSAM's center of gravity to the earth surface, will be used for the characterization of the flight envelope. h is calculated using the z coordinate of the position dynamics written in the E-frame z_G^E and the Earth's radius r_o (cf. equation (2.10)).

$$h = z_G^E - r_o \quad (2.10)$$

Attitude Dynamics

The attitude dynamics with respect to the inertial E-frame is described by the Euler angles Φ , Θ and Ψ (cf. equation (2.11)), whose dynamics depend on the rotation dynamics (cf. equation (2.8)).

$$\begin{bmatrix} \dot{\Phi}^E \\ \dot{\Theta}^E \\ \dot{\Psi}^E \end{bmatrix} = \begin{bmatrix} 1 & \sin \Phi^E \tan \Theta^E & \cos \Phi^E \tan \Theta^E \\ 0 & \cos \Phi^E & -\sin \Phi^E \\ 0 & \frac{\sin \Phi^E}{\cos \Theta^E} & \frac{\cos \Phi^E}{\cos \Theta^E} \end{bmatrix} \omega^E \quad (2.11)$$

Due to equation (2.11)'s singularity when $\Theta = \pm 90^\circ$, the attitude is, in truth, described by quaternions q_0, q_1, q_2 and q_3 which are mapped to the Euler angles according to equations (2.12) to (2.14).

$$\Psi = \arctan [2(q_0 q_1 + q_2 q_3), q_0^2 - q_1^2 - q_2^2 + q_3^2] \quad (2.12)$$

$$\Theta = \arcsin 2(q_0 q_2 + q_1 q_3) \quad (2.13)$$

$$\Phi = \arctan [2(q_0 q_3 + q_1 q_2), q_0^2 + q_1^2 - q_2^2 - q_3^2] \quad (2.14)$$

2.1.3 Longitudinal Approximation

The Longitudinal Approximation consists of the hypothesis that the longitudinal ($x0z$ plane) component of the dynamics described in section 2.1.2 written in the B-frame can be considered separately from the remaining ones, not considering the cross-coupling effects.

Actuator Dynamics

Therefore, the model described in section 2.1.2 is actuated by the deflection η of the aerodynamic equivalent elevator, as described by Peter et al. [22], which is mapped from the GSAM's physical control

surfaces¹ deflections δ_i according to equation (2.15).

$$\eta = \frac{\delta_1 - \delta_2 - \delta_3 + \delta_4}{4} \quad (2.15)$$

The actuator system is, thus, the system that receives the desired (commanded) elevator deflection η_{com} and outputs the actual deflection, modelling the dynamic response of the physical fins with its deflection limit of 30° . The latter is assumed to be a second order system with the following closed loop characteristics:

1. Natural frequency ω_n of 150 rad.s^{-1}
2. Damping factor λ of 0.7

2.1.4 Reference Model

The system described in section 2.1.2 is said to be controlled when able of perfectly following a reference signal given to it from the exterior, according to some performance criteria, which, in this case, are defined in section 1.3.

When trying to optimize the achieved performance, one must, however, be aware of the physical limitations imposed by the system being controlled. A commercial airplane, for example, will never have the agility of a fighter jet, regardless of how optimized its controller is. Therefore, it is hopeless to expect the system to follow too abrupt reference signals like step functions. Instead, the system will be asked to follow *shaped reference signals*, i.e., the output of the Reference Model. The latter is hereby defined as the system whose closed loop dynamics is designed to mimic the one desired for the dynamic system being controlled. In this case: natural frequency ω_n and damping factor λ of 10 rad.s^{-1} and 0.7, respectively. Having such a definition, the shaped reference signal, obviously, meets all the tracking performance criteria established in section 1.3 (cf. figure 2.1).

The proper workflow of the interaction between the agent and the the dynamic system being controlled - including a Reference Model - is illustrated in figure 2.2. The *command* reference signal (cf. section 4.3.1) is given as an input to the Reference Model, whose output, the *shaped* reference signal is the input of the agent.

2.2 Problem Formulation

As stated in section 1.3, the proposed algorithm, the agent will assume the role a controller normally has in a control problem. Using standard RL terminology, the GSAM (cf. section 2.1.2) becomes the environment with which the agent iteratively interacts. To do so the dynamics modelled in *Simulink* (cf. section 2.1), was exported to a DLL file and its development is outside the scope of this thesis.

As in a normal control problem, the agent feeds the environment with actions and receives back observations of its state (cf. figure 2.2). Additionally, at each iteration, the agent must also receive a

¹Four fins attached to the missile's tail.

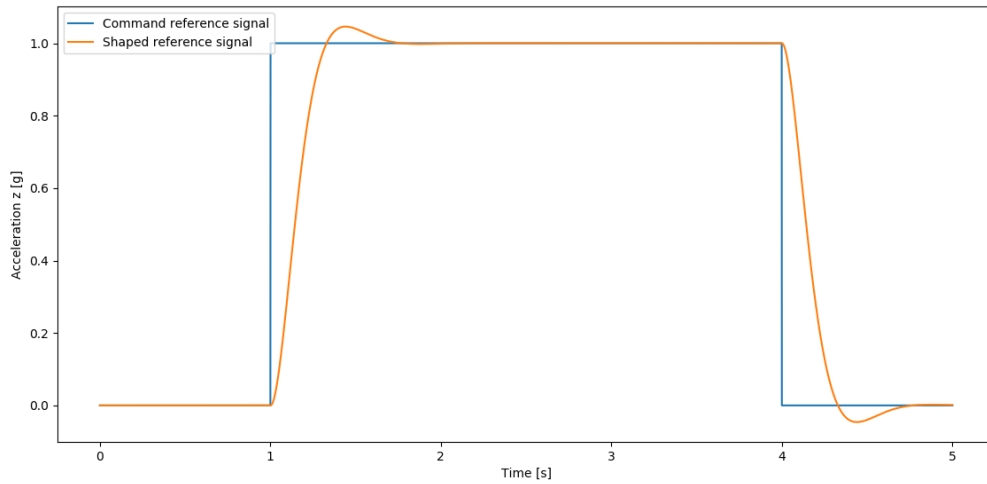


Figure 2.1: Shaped and command reference signals

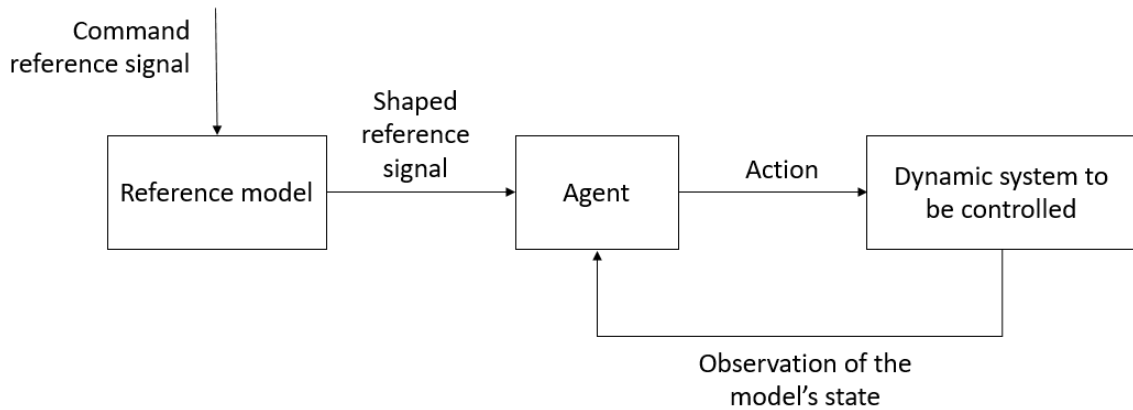


Figure 2.2: Block diagram including the Reference Model

value classifying the observation of the state: the reward r . The closer that observation is from the goal, the higher the reward must be. As it will be discussed in section 3.3, r is the output of the reward function.

Thus, achieving the performance objectives of section 1.3 can be reformulated as the problem of training a RL agent until its performance meets the criteria defined in table 2.1.

Criterion	Threshold
$ e_z _{\max,r}$	5%
overshoot	20%
$ \eta _{\max}$	15°
$\eta_{noise,r}$	1 rad
$\eta_{noise,t}$	0.2 rad

Table 2.1: Hard Criteria

In order to understand how the objectives of section 1.3 give birth to the criteria of table 2.1, it is, first,

necessary to understand the concept of *episode*. In the general RL context, an episode is a sequence of states between two *terminal states*, which is defined as a state in which the agent needs to re-start. In the popular MuJoCo [3] task of the Hopper, for example, the terminal state is commonly defined as the state in which the hopper falls over. In the present case, being 0.001 the sampling time t_s of the environment, and 5s the duration of each reference signal, the episode ends at every 5000 steps when a new reference signal has to be generated (cf. section 4.3.1). No other threshold is used to end the episode.

As it will be further detailed (cf. section 4.3.1), each 5s-long reference signal is composed of two steps of random amplitudes. There is, thus, a total of four transition periods, since each step has got two. A transition period is defined as the period of time after a rise of the command reference signal in which the shaped reference signal is still adapting to the recent change (at 1s and at 4s of figure 2.1) and is allowed to have a higher tracking error e_z . Objectives 4 and 5 (cf. section 1.3) set the transition periods' duration to 0.6s.

Therefore, every value of tracking error e_z measured outside a transition period, in a *resting* period, counts as static error margin (cf. objective 2 of section 1.3) and is subject to $|e_z|_{\max,r}$, or 5% of the amplitude of the reference signal used for testing (cf. section 4.3.1), whereas every e_z measured inside transition periods counts for the computation of the overshoot value (cf. objective 3 of section 1.3).

Moreover, $|\eta|_{\max}$ is set to 15° , because the equivalent fin deflection limit, 30° (cf. section 2.1.3), proved to be too soft as a criteria for ending the train (cf. section 4.3.2), englobing very poor performances.

Finally, e_u is defined as the difference between the equivalent fin deflection η and the output of a filter designed to behave like the ideal η in terms of smoothness and is very useful for the mathematical formulation of the smoothness objective (cf. section 1.3). This filter is modelled as a second order system that, in the transition periods, has got the same characteristics of the actuator system (cf. chapter 2.1.3), but whose natural frequency ω_n is reduced to $5 \text{ rad}\cdot\text{s}^{-1}$ in the resting periods, slowing down its responsiveness to unsmooth actions.

Smoothness is a complex question in so far as we also desire agility. In other words, the objective of a smooth actuation, very important for avoiding energy inefficiency and structural resonance, must not compromise the capacity of the agent to be responsive to changes in the reference signal.

With this in mind, the smoothness goal was split into two criteria: one regarding resting periods, $\eta_{noise,r}$, and another for transition periods, $\eta_{noise,t}$. The former was defined as the L-2 norm of e_u in the four resting periods of the episode (cf. equation (2.16)), whilst the latter as the maximum e_u in transition periods (cf. equation (2.17)), since we want neither any accumulated noise in resting periods nor too big peaks in the transition periods.

$$\eta_{noise,r} = \sqrt{\sum_{t \in \text{resting}} (e_u)_t^2} \quad (2.16)$$

$$\eta_{noise,t} = \max_{t \in \text{transition}} |(e_u)_t| \quad (2.17)$$

Having established these criteria, the state was defined as in equation (2.20), including: (i) the tracking error (cf. equation (2.18)), its integral (cf. equation (2.19)), the reference signal $a_{z,ref}$ and the pitch rate q with the intention to provide the agent with enough information so that it achieves the desired tracking performance; (ii) the previous action η_{t-1} so that the agent can learn smoothness; and (iii) the Mach number M and the height h , identifiers of the flight envelope point, to respect the general implementation principle (cf. section 4.2.2), allowing it to be later expansible to the whole flight envelope.

$$e_z = a_{z,meas} - a_{z,ref} \quad (2.18)$$

$$\left(\int e_z \right)_t = \left(\int e_z \right)_{t-1} + (e_z)_t \cdot t_s \quad (2.19)$$

$$s_t = \left[(e_z)_t, \left(\int e_z \right)_t, (a_{z,ref})_t, q_t, \eta_{t-1}, M_t, h_t \right]^T \quad (2.20)$$

From the latter, the acceleration $a_{z,meas}$ and the pitch rate q are measured by on-board sensors and the Mach number M and the height h are estimated from labelled data.

Chapter 3

Background

The present chapter intends to provide the theoretical background necessary to the comprehension of the proposed implementation that will afterwards be detailed in chapter 4, starting by some basic concepts about the framework of Reinforcement Learning (cf. section 3.1), introducing the algorithm that inspired the proposed approach, Trust Region Policy Optimization (cf. section 3.2), going through the Reward Engineering process (cf. section 3.3) and covering other important implemented features, like Hindsight Experience Replay (cf. section 3.4) and Prioritized Experience Replay (cf. section 3.5).

3.1 Reinforcement Learning - Basic Concepts

Consider the problem of an agent interacting with an environment, having the objective of fulfilling a certain task. RL is the framework in which that agent learns to perform the actions that are helpful towards its objective based on its past experience of interactions. The function that maps state s to the next action a is commonly called the policy $\pi(s)$ (cf. equation (3.1)).

$$\pi(s_t) = a_t \tag{3.1}$$

In this sense, RL is a very broad framework, covering situations from animal learning and brain processes, to simple games with a discrete set of possible actions or more complex robotic tasks with a continuous spectrum of possible states and actions.

Markov Decision Processes

A Markov Decision Process (MDP) is a framework defined by the famous 4-tuple $(\mathbb{S}, \mathbb{A}, T, r)$, in which:

- $\mathbb{S} \equiv \{s_i\}$ is the set of possible states
- $\mathbb{A} \equiv \{a_i\}$ is the action domain
- $T \equiv T(s, a, s')$ is the transition model from which is calculated the probability $P(s'|s, a)$ of being in state s' after having done action a from state s

- $r \equiv r(a, s')$ is the reward function that outputs the reward corresponding to state s' after having done action a

Such processes owe their name to the Markov assumption (3.2), which holds that, when evaluating $s_{t'}, T$ depends only on s_t and a_t and not on previous states or actions.

$$T(s_{t-k}, a_{t-k}, \dots, s_t, a_t, s_{t'}) = T(s_t, a_t, s_{t'}), \forall_k k > 0 \quad (3.2)$$

A RL problem can be studied as a MDP, in which the transition model T of the MDP is used to compute the probability $P(a_t|s_t)$ of taking action a_t in state s_t , filling the role of the policy, which is now said to be stochastic, since it maps states to the probability of taking actions (cf. equation (3.3)). Actions are, hence, sampled from the policy (cf. equation (3.4)), not determined by it (cf. equation (3.1)).

$$\pi(s_t) = P(a_t|s_t) \quad (3.3)$$

$$a_t \sim \pi(s_t) \quad (3.4)$$

Algorithms' Taxonomy

One way of branching all the possible RL algorithms is according to whether, or not, the agent has access to the dynamics of the environment. Model-based agents, in opposition to model-free ones, do have it and use it to better predict the effects of their actions, allowing a faster training process and having achieved state-of-the-art level for several times. However, having to depend on prior information about the environment seriously decreases the number of possible applications. In fact, for most cases, either the environment is not fully observable or there are more unpredictable agents at play. This is exactly the case of controlling a missile's flight, inasmuch as a high level of generalization is desired, meaning that the algorithm must not be specific to one flight situation or missile configuration, but able to fulfill the mission requirements in the widest span of situations, as stated in section 1.3. Hence, the agent must be developed within the model-free paradigm.

Among all the model-free algorithms, one can still distinguish on-policy from off-policy algorithms. According to Sutton et al. [1], off-policy algorithms are those which optimize one policy estimator, the *target*, using experience collected by performing the actions dictated by a different policy estimator, the *behaviour* policy. On the contrary, in the on-policy case, these two roles, *target* and *behaviour*.

Each of the groups has its own advantage: if it is true that off-policy methods are more sample efficient, it is also generally accepted that on-policy algorithms' training is more stable and they are easier to use [18]. Recently, researchers have been investing efforts in taking advantage of the upsides of both types of algorithms, either by directly trying to merge one state-of-the-art algorithm of each kind or by interpolating between on-policy and off-policy with an hyperparameter (cf. section 1.2).

Policy Gradient algorithms

Effectively, an algorithm needs to guarantee convergence to the optimal policy or, otherwise, it will not be applicable to control problems. Policy Gradient algorithms' breakthrough idea is to estimate the policy by its own function approximator, independent from the one used to estimate the value function and to use the total expected reward as the objective function to be maximized. Sutton et al. [23] have shown that this gradient can be written in terms of the observations recorded from the interaction with the environment and of an advantage function (cf. section 3.1), resulting in an iterative policy convergence to a local maximum.

Notice that Policy Gradient algorithms are, by definition, part of the on-policy family, meaning that they tend to be less sample-efficient than off-policy algorithms. Typically, they also struggle to avoid suboptimal convergence and demand a higher number of hyperparameters, being of more complex implementation.

Actor-Critic Architecture

Most of the state-of-the-art RL algorithms subscribe to an actor-critic architecture [10] [24], in which the actions output by the policy, the *actor*, are evaluated by a *critic*. Essentially, the critic is an estimator of the rewards the agent will collect when performing a certain action. Training the agent must, therefore, lead to a situation where the actions receive good critiques and those critiques are close to the rewards actually received.

Sample efficiency

Sample efficiency is a qualitative measure of the amount of observations one algorithm must collect from the environment to achieve a certain goal.

Collecting samples from the environment is often the most time consuming part of a RL learning process and, therefore, the most expensive one. The ability to use at its utmost potential the information collected from the environment is, thus, highly sought after.

Model-based algorithms are, normally, more sample efficient than model-free ones because their prior knowledge allows them to generate accurate synthetic observations, therefore, needing less interactions with the model.

Advantage Function

Being $V_\pi(s_t)$ (cf. equation (3.5)) the expected sum of the discounted future rewards that an agent in state s at time instant t obtains if following a certain policy π until the end of the episode and $Q_\pi(s_t, a_t)$ (cf. equation (3.6)) the expected sum of the discounted future rewards that an agent in state s at time instant t obtains if it executes, action a and, only then, follows a certain policy π until the end of the episode, the advantage function (cf. equation (3.7)) measures the benefit, or *advantage*, of executing action a , when compared with the policy's default behaviour.

$$V_{\pi}(s_t) = \mathbb{E}_{a_t, s_{t+1}, \dots} \left[\sum_{l=0}^{\infty} \gamma^l r(s_{t+l}) \right] \quad (3.5)$$

$$Q_{\pi}(s_t, a_t) = \mathbb{E}_{s_{t+1}, a_{t+1}, \dots} \left[\sum_{l=0}^{\infty} \gamma^l r(s_{t+l}) \right] \quad (3.6)$$

$$A_{\pi, \gamma}(s_t, a_t) = Q_{\pi, \gamma}(s_t, a_t) - V_{\pi, \gamma}(s_t) \quad (3.7)$$

Generalized Advantage Estimation

Let $\delta_{\pi, t}$ (cf. equation (3.8)) be the temporal difference error, TD-error [1]. Equation (3.7) can simply be rewritten as the discounted sum of the TD-errors (cf. equation (3.9)).

$$\delta_{\pi, t} = r_t + \gamma V_{\pi, t+1} - V_{\pi, t} \quad (3.8)$$

$$A_{\pi, \gamma} = \sum_{l=0}^{\infty} \gamma^l \delta_{\pi, t+l} \quad (3.9)$$

Since $A_{\pi, \gamma}$ is unknown, it must be estimated by $\hat{A}_{\pi, \gamma}$. $\hat{A}_{\pi, \gamma}$ can be defined as the sum of the first k elements¹ of the sequence of occurred states and actions (cf. equation (3.10)).

$$\hat{A}_{\pi, \gamma} = \sum_{l=0}^{k-1} \gamma^l \delta_{\pi, t+l} \quad (3.10)$$

Apart from the intuitive meaning of discounting future rewards, γ also has an impact on the bias-variance trade-off, since it can be seen as a variance reduction parameter in an undiscounted rewards problem [9]. In their work, Schulman et al. [9] propose the Generalized Advantage Estimator (cf. equation (3.11)), in which the discount factor, γ , is separated from the variance regulator, λ ($0 < \lambda < 1$).

$$GAE_{\pi, \gamma, \lambda}(s_t) = \sum_{l=0}^{k-1} (\gamma \lambda)^l \delta_{\pi, t+l} \quad (3.11)$$

As they also show, λ becomes the interpolator between two extreme cases: $GAE_{\pi, \gamma, 0}$, which typically has much lower variance at the expense of introducing bias, and $GAE_{\pi, \gamma, 1}$, that has higher variance due to the sum of terms but which bias is low if k is allowed to be high enough. Therefore, equation (3.10) becomes the special case of $GAE_{\pi, \gamma, 1}$, hence the name *Generalized Advantage Estimation*.

Exploration vs. Exploitation

For effects of analogy, consider the task of playing "hot and cold" with one person who hides an object agreed as the target, the Hider, and one person who searches for it, the Seeker. During the game, the Seeker will move around within the bounds defined as the space of the game searching for the target. When getting closer, the Hider will say "Hot" and, obviously, "Cold" otherwise. This is, at its core,

¹In the present case, k is the number of steps considered in one trajectory, *TRAJECTORY_LEN* (cf. section 4.2.1). As Schulman et al. [9] have also stated, the higher k is, the less biased $\hat{A}_{\pi, \gamma}$ is.

a Reinforcement Learning task, being the Seeker the agent, the "Hot"/"Cold" notices the rewards, the Seeker's position the states and the Seeker's decisions of where to go the actions sampled from the policy.

In the beginning, the Seeker, having no hint of where to start searching, will move around randomly, *exploring*, in the hope that, at some point, one of his actions result in a "Hot" notice from the Hider. In Reinforcement Learning terminology, this is said to be the *Exploration* phase, which will end once the Seeker understands where to search in order to receive increasingly loud "Hot" notices, passing to the *Exploitation* phase, in which the Seeker will search in the defined direction, *exploiting* it and making some slight corrections if needed.

This distinction is of utmost importance. In fact, the perfection is in the right balance between both: too much exploration and the agent will never profit from what it has learnt so far and too much exploitation and the agent might converge to suboptimal policies, if converging at all. The challenge is, indeed, how to implement the exploration in the algorithm, given that the method of optimization of the policy proposed by each algorithm deals with the exploitation phase. Notice that exploration is deeply linked to training the agent, since it aims, as explained, at avoiding its suboptimal convergence. Therefore, when being tested, i.e., deployed in the environment to assess its performance, an agent does not explore.

One first option would be to consider fixed periods for each, saying, for example, that the first 20 minutes of the train would always be spent exploring, picking random actions from the set of possible actions. Being easy to implement, this approach is too simplistic: neither can it be properly generalized nor is it clear how to apply it to a continuous action domain task.

For continuous action space problems, the most straightforward approach is to add some noise, often Gaussian noise, to the action sampled from the policy or to use the output of the policy as a mean value of a distribution from which to, then, sample the action. Both this approaches entail an extra hyperparameter that controls the evolution of the magnitude of the noise, in the first case, or of the variance of the distribution, in the second one. This issue has also been addressed more elegantly by authors of algorithms of all families - on-policy algorithms [12], off-policy algorithms [11][13] and hybrids [17][19][21][25] - by introducing an entropy term in the objective function in order to encourage the agent to explore while the other terms have not yet become relevant. Although appealing, this approach also adds an extra hyperparameter, which is harder to tune, in comparison to its afore mentioned analogous since any notion of a proper range given by the physical meaning or by *a priori* understanding of the environment is lost.

Finally, more recently, Plappert et al. [26] have proposed to add noise directly to the parameters of the policy themselves, showing a promising increase in performance when compared to injecting noise in the action space for the state-of-the-art algorithms, often used as benchmark, although not being able to plainly justify this choice apart from the obvious intuition.

Abstract Regions of Train

The training process can be decomposed in three phases, or abstract regions: *far* region, *middle* region and *near* region, whose definitions are more qualitative than accurate. The far region is the first phase

of train, starting from the initialization, where the agent’s performance is very close to random, whereas the near region is the phase where the performance is almost the targetted one, lacking only some small enhancements on one of the performance goals.

These concepts are useful in the reward engineering process (cf. section 4.1) and when designing the exploration strategy (cf. section 4.2.2).

3.2 Trust Region Policy Optimization

Trust Region Policy Optimization (TRPO) has been keystone for researchers, who have used it as benchmark for assessment of new algorithms success or as theoretical launch pad for new ones [9][10][12]. It is an on-policy model-free RL algorithm that aims at maximizing the discounted sum of future rewards (cf. equation (3.12)) following an actor-critic architecture and a trust region search. Its authors argue that TRPO “tends to give monotonic improvement, with little tuning of hyperparameters” [5].

$$R(s_t) = \sum_{l=0}^{\infty} \gamma^l r(t+l) \quad (3.12)$$

While the actor is an estimator of the policy function (cf. equation (3.3)), the critic is an estimator of the value of each state (cf. equation (3.12)). Both are parameterized by neural networks and, hence, called *policy neural network* (Policy NN, with parameters θ) and *value neural network* (Value NN, with parameters ψ), respectively.

In its “single path” estimation procedure, the agent samples actions from the policy, collecting states, actions and rewards in trajectories of arbitrary length. After having collected a batch of trajectories, the interaction with the environment is paused and both neural networks are updated having the latter trajectories as training dataset of a supervised learning process. Schulman et al. [5] have also initially proposed to update the Policy NN with conjugate gradient algorithm followed by a line search. The trust region search would be ensured by a hard constraint on the Kullback-Leibler divergence, D_{KL} (cf. equation (3.13) for the specific case² of D_{KL} between two multivariate normal distributions, $N_0(\mu_0, \Sigma_0)$ and $N_1(\mu_1, \Sigma_1)$, both of dimension n), a statistical measure of the distance between two different probability distributions.

$$D_{KL} = \frac{1}{2} \left(tr(\Sigma_1^{-1}\Sigma_0) + (\mu_1 - \mu_0)^T \Sigma_1^{-1} (\mu_1 - \mu_0) - n + \ln \left(\frac{\det \Sigma_1}{\det \Sigma_0} \right) \right) \quad (3.13)$$

The concept of the trust-region search is truly outstanding in the policy-gradient family of algorithms. Even though the update step is computed from the gradient of the objective function with respect to the policy parameters (meaning that it is aligned in the direction of the objective function maximum - the “right direction”) it can be too high and result in a new policy with worse performance than the previous one. Consider the helpful analogy of the desert races whose accidents caused by wall-like dunes are rather frequent. In these situations, the pilot is driving in the right direction, but he is not expecting the

²This is precisely the case of D_{KL} between two consecutive policies, with an exploration strategy of the type of the one proposed in section 4.2.2.

dune to end abruptly after its top and finds an abyss instead of a smooth slope, falling dangerously.

It was in this context that Trust Region Policy Optimization emerged as an important breakthrough.

As mentioned in section 1.2, briefly after TRPO's original paper, Kangin et al. [10] proposed an enhancement, augmenting the training data by using replay buffers and GAE (cf. section 3.1). Although controversial, under the classic definition [1], this is still an on-policy algorithm. Also contrarily to the original proposal, Kangin et al. train the Value NN with the ADAM optimizer and the Policy with K-FAC [27]. The former was implemented within a regression between the output of the Value NN, \hat{V} , and its target, V' (cf. equation (3.14)), having equation (3.15) as the loss function (being S_{train} the training set), whilst the latter used equation (3.16) as the loss function, which has got a first term concerning the objective function being maximized (cf. equation (3.12)) and a second one penalizing differences between two consecutive policies outside the trust region, whose radius is the hyperparameter δ_{TR} .

$$V'(s_t) = \sum_{l=0}^{k-t} \gamma^l r(s_{t+l}, a_{t+l}) \quad (3.14)$$

$$L_V(S_{train}) = \sum_{s \in S_{train}} \left(V'(s) - \hat{V}(s) \right)^2 \quad (3.15)$$

$$L_P = -\mathbb{E}_{s_0, a_0, \dots} \left[\sum_{t=0}^{\infty} \gamma^t r(s_t, a_t) \right] + \alpha \max(0, \mathbb{E}_{a \sim \pi_{old}} [D_{KL}(\pi_{old}(a), \pi_{new}(a))] - \delta_{TR}) \quad (3.16)$$

For matters of simplicity of implementation, Schulman et al. [5] withdraw the dependency on t , rewriting equation (3.16) in terms of collected experience (cf. equation (3.17)), as a function of two different stochastic policies, π_{new} and π_{old} and the *GAE* (cf. equation (3.11)).

$$L_P = -\mathbb{E}_s \mathbb{E}_{a \sim \pi_{old}} \left[GAE_{\pi_{old}}(s) \frac{\pi_{new}(a)}{\pi_{old}(a)} \right] + \alpha \max(0, \mathbb{E}_{a \sim \pi_{old}} [D_{KL}(\pi_{old}(a), \pi_{new}(a))] - \delta_{TR}) \quad (3.17)$$

Moreover, both versions of TRPO use the same exploration strategy: the output of the Policy NN is used as the mean of a multivariate normal distribution whose covariance matrix is part of the trainable parameters, being learnt as well.

3.3 Reward Engineering

Alongside, perhaps, with the exploration strategy, the reward function is one of the key features to the success of a RL algorithm. Contrarily to the exploration strategy, however, the literature in how to choose a reward function, the so-called Reward Engineering process, is rare, if at all available, due to the fact that most of the classical benchmarks are videogames, having themselves a built-in reward, under the format of game points or surviving duration, depending on the game. Other authors simply state the reward they use with no further details about the thought process behind it. With the rising popularity of RL in robotic simple tasks (like grasping objects with a robotic arm, pushing bricks...), this topic is

gaining importance.

Reward functions can be sparse or dense. On the one hand, sparse rewards are the easiest to understand: they map the set of actions \mathbb{A} and the set of states \mathbb{S} to a countable set (e.g. $\{-100, 0, 1\}$ or $\{-1, 1\}$) representing qualitative levels of failure/.../success. Dense reward functions, on the contrary, are functions that map \mathbb{A} and \mathbb{S} to an uncountable set of reward values. The step function, rising at a certain value of the tracking error, is a common sparse reward function, whereas the opposite of the tracking error is an example of a commonly found dense reward function in robotic applications of RL.

For much appealing that dense reward functions might sound for robotic problems for their similarities to cost functions used in Control Theory³, functions in this subset easily become intractable when the goal simultaneously encapsulates multiple objectives. In fact, even a simple task of moving objects between two positions with a robotic arm unfolds in more than one goal, since, not only do we want to put the object in the final position (in other words: to minimize the error between its position and the desired location), but we also aim at achieving a certain performance when doing so, namely to encourage the agent to follow a certain velocity reference in the robotic arm or to have a smooth transportation, penalizing the reward when observing high values of the first and second derivatives of the position of the arm to achieve the latter. Put together in a sole reward function, these components - and many more could follow - need to be carefully weighted, adding more hyperparameters to the model. These relative weights are key to the success of the agent and finding their optimal values is the most sensitive and time-consuming stage of the design of the algorithm.

Adversely, sparse rewards need not to be weighted. Nonetheless, sparsity is, at the same time, a blessing because of the latter and a curse because, starting from a random initialization, the agent will only experiment "success" during training by pure luck. It might as well never do so, if it happens to take the wrong initial actions. One could think of relaxing the very definition of "success" in order for it appear more often, but the agent would, then, not be accurately taught.

Furthermore, even if observing "successes", the dataset of the collected experience with which the neural networks are updated would be extremely imbalanced. A combined solution that could benefit from the absence of relative weights of a sparse reward and from the robustness to initialization of a dense one, perhaps with some extra features for fighting imbalanced datasets and sparse "success" observations, would certainly be desirable.

3.4 Hindsight Experience Replay

The key idea of Hindsight Experience Replay (HER) is to store in the replay buffers not only the experience collected from interacting with the environment, but also about experiences that would be obtained, had the agent followed a different goal. In fact, since the goal influences the output of the policy but not the environment's dynamics [28], following a different goal would change the collected reward but not the observation each action produced and, hence, it is possible to replay each trajectory and associate its sequence of actions and observation to a different sequence of rewards, ensuring, therefore, that the

³Notice that maximizing a reward function is analogous to minimizing a cost function.

agent encounters success cases when in the update stage.

HER was initially proposed [28] ensembled with sparse rewards and has proved to be beneficial in such cases. However, whether or not HER improves the performance achieved with a dense reward is yet to be demonstrated in the literature and is one of the major contributions of this work (cf. section 6.1).

3.5 Prioritized Experience Replay

Prioritized Experience Replay was initially proposed [29] to achieve a higher efficiency when updating the neural networks, by sampling observations from the replay buffers according to a probability distribution that increases monotonically with their significance. Schaul et al.'s hypothesis is that the significance should be quantified in terms of the Temporal Differences (TD) error (cf. equation (3.8)), since it is the difference between what the model had predicted about the value of a state, V_t , and its updated value after having collected the corresponding instantaneous reward, $r_t + \gamma V_{t+1}$. In other words, Schaul et al.'s hypothesis was that the networks could learn faster by seeing their biggest surprises more often during training.

On the other hand, the required performance (cf. section 2.2), being strict, causes the agent to suffer from very rare successfulness. In agents whose reward is dense (cf. section 3.3) the effects of this rareness are confined to an increase of the convergence time. In agents whose reward is sparse, however, the main issue is that rare results cause the dataset used to update the networks (cf. section 4.2.6) to be extremely imbalanced, since almost all observations are unsuccessful and, thus, the agent fails to learn how to succeed and overfits the "failure" class. Narasimhan et al. have proposed [30] to solve a similar problem by forcing 25% of the training dataset to be sampled from the less represented class.

Chapter 4

Application of Reinforcement Learning to the Missile's Flight

The present chapter presents the approach proposed to solve the problem defined in section 2.2 within the RL framework. To do so, it starts by going through the search for the optimal reward function (cf. section 4.1) to, then, present the proposed algorithm (cf. section 4.2), in which (i) the modifications on the original TRPO (cf. section 4.2.2), (ii) the enhanced proposed exploration strategy (cf. section 4.2.2) and (iii) the complementary added features - SER (cf. section 4.2.5) with an explanation of the reformulation of the concept of HER (cf. section 4.2.3) and the proposed BPER (cf. section 4.2.4) are detailed. Follows the training methodology (cf. section 4.3) and the chapter ends with the experiments made to assess the reproducibility of the results (cf. section 4.4) and the robustness of the best found nominal agent (cf. section 4.5).

4.1 Reward Engineering

The reward function with which the agent met all the performance requirements (cf. table 2.1) will, from now onwards, be referred to as Optimal Reward Function (ORF) and all the others as Candidate to Optimal Reward Function (CORF). When necessary, the relative weights will be denoted by w_i , whose numerical values are described in appendix A.

Noticing the lack of literature in the topic (cf. section 3.3), consider the infinite amount of options available when designing a reward function, which raise the following main challenges:

1. To choose the profile of the reward: linear, exponential or other
2. To decide how to combine the several terms: sum them, multiply them or other
3. To mathematically formulate the performance goals, especially the smooth actuation one
4. To parameterize the relative weights w_i

To the end of providing some guidance to future Reward Engineering processes, the present section presents the thought process behind the search for the ORF.

One could think that the Reward Engineering process would be solved by laying out all the possible options, trying them for the enough amount of time and choosing the best one. However, given the limited amount of resources and unlimited amount of options, such a raw approach becomes intractable, not to mention the difficulty of defining what is the *enough amount of time*. Therefore, the ORF must be found by a well-structured trial and error process, in which the design choices and modifications are grounded both on previously achieved results and on the intuition of the model designer.

In fact, intuition plays a key role in the decision of enhancing/abandoning certain a CORF and can be earned by learning how to define the Abstract Regions of Train (cf. section 3.1) of a specific problem, since that can provide some heuristic of the sort of "abandon all CORF that cannot exit the far region in less than X training episodes". In the present case, all policies that led to unbounded actions η or to tracking errors e_z higher than 40g were considered to be in the far region, whereas policies that could achieve tracking errors e_z below 5g with bounded actions, perhaps lacking some improvement in smoothness, were considered to be in the near region, but having an influence of all of them.

Moreover, it was also observed a tendency for the performance goals (cf. section 2.2) to be interconnected. For example, focusing in improving the policy in terms of boundedness indirectly improved tracking performance in some parts of the training process. Not only that, but also each Abstract Region of Train (cf. section 3.1) was discovered to have its own most critical performance goal, i.e., in each region, one specific performance goal arose as the driving force for indirectly improving the others. In general terms:

- prioritizing boundedness helped a randomly initialized agent to flee the far region;
- prioritizing tracking performance helped an agent already mostly able of boundedness to flee the middle region;
- prioritizing smoothness helped an agent already in the near region to achieve the target performance.

The latter observation does not mean that the CORFs ought to forget the non-principal performance goals of each region, since such a boxed implementation would require a very accurate definition of the Abstract Region of Train. On the contrary, a CORF must be designed in a way such that the right performance goal is highlighted during each region.

4.1.1 Dense Exponential

Dense Exponential CORF belong to the dense subset of reward functions detailed in section 3.3. Starting from a random initialization, the agent's first interactions with the environment typically result in a far from target performance (cf. figure 4.5), which gets iteratively closer to the target. To that end, an exponential profile ensures that the reward's slope does not decrease as the distance to the goal shortens, like it would happen, for example, had the reward function been the one defined in equation (4.1).

$$r = -e_z^2 \quad (4.1)$$

In such cases, the gradient used for updating the agent's parameters (cf. section 4.2.6) would be much lower when closer to the goal than far from it, increasing the convergence time. None of the implementations in this section include HER (cf. section 4.2.3) or BPER (cf. section 4.2.4).

Initial reward

Inspired by the work of Evangelisti [31], whose application was similar to the present one, the first CORF was implemented (cf. equation (4.4)) as an exponential function of the tracking error e_z and the pitch rate q .

$$f_1 = -w_1 \cdot e_z^2 \quad (4.2)$$

$$f_2 = -w_2 \cdot |q| \quad (4.3)$$

$$r = 2e^{f_1+f_2} - 1 \quad (4.4)$$

LQ-cost-like reward

Inspired by the Linear Quadratic Regulator (LQR) control's approach¹ of using the state and the action in the LQ cost, the initial reward function (cf. equation (4.4)) was modified, replacing the pitch rate q by the action η (cf. equation (4.5)). Besides, a third term was added (cf. equation (4.6)) as a discrete penalty to encourage the agent to bound the tracking error.

$$f_2 = -w_2 \cdot |\eta| \quad (4.5)$$

$$f_3 = \begin{cases} 0 & \text{if } |e_z| < 10g \\ -w_3 & \text{otherwise} \end{cases} \quad (4.6)$$

$$r = e^{f_1+f_2} + f_3 \quad (4.7)$$

Several hypotheses were tested upon the configuration introduced in equation (4.7), all of them still being dense functions with an exponential profile and having several terms related with e_z and η , with the main objective of achieving the right balance between perfect tracking and smoothness in the actuation. Effectively, this proved to be the main struggle of the Reward Engineering process, since the agent easily fell either into a bang-bang control [32] situation or into a poor tracking performance, even though smoothly actuated.

¹Control Theory, outside the scope of this thesis.

$\Delta\eta$ reward

f_4 was added (cf. equation (4.9)) to penalize too abrupt variations in η : at each time instant $\Delta\eta$ is the difference between the most recent η and its predecessor. Besides, f_1 's quadratic profile was abandoned in the absence of justification for this extra level of complexity (cf. equation (4.8)).

$$f_1 = -w_1 \cdot |e_z| \quad (4.8)$$

$$f_4 = -w_4 \cdot |\Delta\eta| \quad (4.9)$$

$$r = e^{f_1+f_2+f_4} + f_3 \quad (4.10)$$

Best-fit of past 5 η

f_4 (cf. equation 4.9) was modified, penalizing the best-fit error (cf. equation (4.17)). The latter is defined as the difference between the extrapolation of the last 5 values of η , η_{5past} , and the most recent value of η (cf. equation (4.16)), where t_s is the environment's sampling time (cf. section 2.2).

$$\bar{t}_{past} = \frac{\sum_{i=1}^5 i}{5} t_s = 3t_s \quad (4.11)$$

$$\bar{\eta}_{past}(t) = \frac{\sum_{i=1}^5 \eta_{t-i}}{5} \quad (4.12)$$

$$m(t) = \frac{\sum_{i=1}^5 ((i \cdot t_s - \bar{t}_{past}) \cdot (\eta_{t-i} - \bar{\eta}_{past}(t)))}{\sum_{i=1}^5 (i \cdot t_s - \bar{t}_{past})^2} \quad (4.13)$$

$$b(t) = \bar{\eta}_{past}(t) - m(t) \cdot \bar{t}_{past} \quad (4.14)$$

$$\eta_{5past}(t) = b(t) + 5t_s \cdot m(t) \quad (4.15)$$

$$e_{bf}(t) = \eta(t) - \eta_{5past}(t) \quad (4.16)$$

$$f_4 = -w_4 \cdot |e_{bf}| \quad (4.17)$$

4.1.2 Dense Sum

Dense Sum CORF belong to the dense subset of reward functions detailed in section 3.3. In spite of the advantages mentioned in section 4.1.1, the exponential profile adds an extra level of complexity regarding the relative weights' (w_i , cf. appendix A) tuning process. Hence, the reward function was, instead, defined as a sum of terms (cf. equation (4.18)).

$$r = \sum_{i=1}^n f_i \quad (4.18)$$

None of the configurations proposed in this section include HER (cf. section 4.2.3) or BPER (cf. section 4.2.4), yet.

Four terms, $n = 4$

First of all, the term in η and the discrete penalty (respectively, f_2 and f_3 of section 4.1.1) were replaced by one discrete penalty conditioned on the boundedness of the actions (cf. equation (4.20)), after having observed that the most efficient way of fighting the initial convergence (highly dependent on the networks random initialization) was to penalize the agent for high values of $|\eta|$, since, once it learnt to decrease $|\eta|$, the value of $|e_z|$ would much more easily decrease.

$$f_1 = -w_1 \cdot |e_z| \quad (4.19)$$

$$f_2 = \begin{cases} 0 & \text{if } |\eta| < \eta_{max} \\ -w_2 & \text{otherwise} \end{cases} \quad (4.20)$$

Secondly, in order to encourage smooth actions, f_3 was introduced (cf. equation (4.22)).

$$\eta_{slope} = \frac{\Delta\eta}{t_s} \quad (4.21)$$

$$f_3 = -w_3 \cdot |\eta_{slope}| \quad (4.22)$$

Besides, relating w_3 with $|e_z|$ (cf. appendix A) decreases the time the agent takes to overcome the far-region, since it encourages the agent's policy to be smoother from an early stage, by increasing the relative importance of η_{slope} when $|e_z|$ is high. Notice that this relation between w_3 and $|e_z|$ ends once the agent's performance enters the near-region (here, when $|e_z| < 0.5g$) since it is assumed that the agent would only reach that performance once it had already mastered the action's smoothness.

Finally, having achieved a suboptimal policy marked by an oscillatory behaviour of η in the resting periods (cf. figure 4.1), f_4 (cf. equation (4.23)) was introduced as a bonus only applied in the near-region, encouraging the agent to achieve the optimal policy and conditioned on $|e_u|$ (cf. section 2.2), being $e_{u,max} = 0.03$.

$$f_4 = \begin{cases} w_4 \cdot \frac{e_{u,max} - |e_u|}{e_{u,max}} & \text{if } |e_z| < 3g \wedge |\eta| < 0.2 \wedge |e_u| < e_{u,max} \\ 0 & \text{otherwise} \end{cases} \quad (4.23)$$

Three terms, $n = 3$

Testing the hypothesis that equations (4.22) and (4.23) were redundant, since they both aimed at leading the agent into a smoother policy, the η_{slope} term was dropped, because e_u was designed to be effective in fine-tuning the final stretch of the train. Apart from that, following the success of a discrete penalty in achieving bounded actions, the bonus term for smooth actions (cf. equation (4.23)) was replaced by a discrete penalty for unsmooth ones (cf. equation (4.24)).

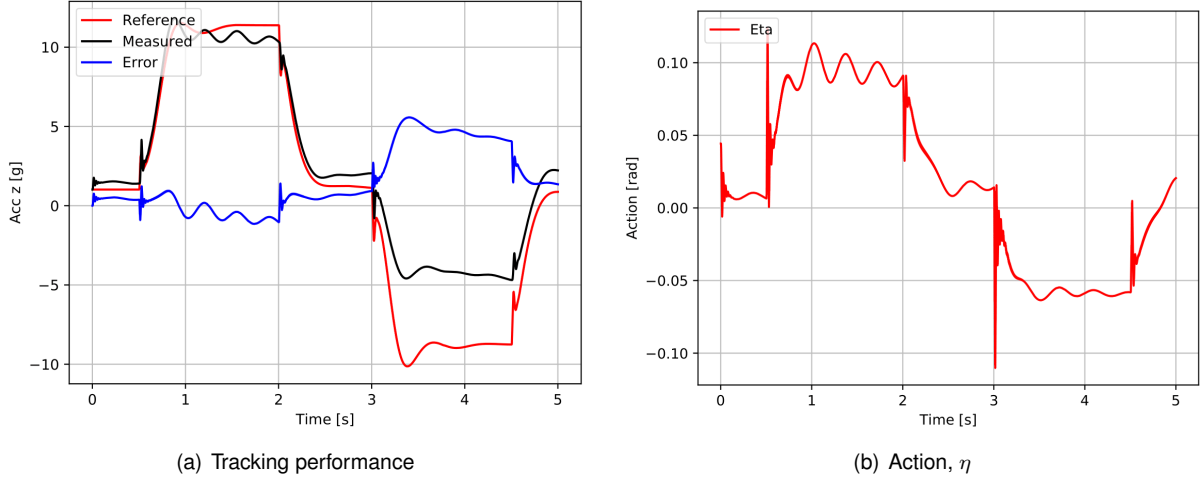


Figure 4.1: Suboptimal Agent with oscillatory η in resting periods

$$f_3 = \begin{cases} 0 & \text{if } |e_u| < e_{u,\max} \\ -w_3 & \text{otherwise} \end{cases} \quad (4.24)$$

Notice that $w_3 \ll w_2$ (cf. appendix A), because it was empirically observed that decreasing η 's magnitude must precede the smoothness goal.

Two terms, $n = 2$ (smoothness)

Encouraged by the success of the previously assumed hypothesis over the $n = 4$ case, the latter was extended to equations (4.20) and (4.24), assuming that encouraging smooth actions would also have the side effect of teaching boundedness and, therefore, replacing them by equation (4.25).

$$f_2 = \begin{cases} 0 & \text{if } |e_u| < e_{u,\max} \\ -w_2 & \text{otherwise} \end{cases} \quad (4.25)$$

Two terms, $n = 2$ (magnitude)

Observing the dependency of the previous agent on the initialization - meaning that, if the initialization is favorable it converges rapidly but, otherwise, it might never converge - its hypothesis was reformulated, assuming, now, that encouraging boundedness would have the side effect of teaching smoothness, replacing f_2 of equation (4.25) for the definition in equation (4.26).

$$f_2 = \begin{cases} 0 & \text{if } |\eta| < \eta_{\max} \\ -w_2 & \text{otherwise} \end{cases} \quad (4.26)$$

4.1.3 Sparse

Sparse CORF belong are the subset of reward functions detailed in section 3.3. Not having achieved the target performance, a perpendicular approach was considered: sparse CORF. As mentioned in section 3.3, sparse rewards suffer from rare observation of successes, tending to overfit the failure class. To

avoid so and provide the agent with successful examples, HER (cf. section 4.2.3) was implemented and activated from the very start of the train. Both CORF described in this section were tested with and without BPER (cf. section 4.2.4).

Binary reward

The most straightforward sparse reward is simply binary under the aforementioned condition (cf. equation (4.27), with $e_{u,\max} = 0.01$).

$$r = \begin{cases} 1 & \text{if } |e_z| < 0.5g \wedge |\eta| < \frac{\eta_{max}}{2} \wedge |e_u| < e_{u,\max} \\ 0 & \text{otherwise} \end{cases} \quad (4.27)$$

The latter agent proved to be highly subdued to the initialization, as it had been the case for the agent with $n = 2$ and f_2 defined in equation (4.25) (cf. section 4.1.2). Hence, an enhanced version of this CORF was implemented by adding a penalty for unbounded actions (cf. equation (4.28)).

$$r = \begin{cases} 1 & \text{if } |e_z| < 0.5g \wedge |\eta| < \frac{\eta_{max}}{2} \wedge |e_u| < e_{u,\max} \\ 0 & \text{otherwise if } |\eta| < \eta_{max} \\ -10 & \text{otherwise} \end{cases} \quad (4.28)$$

Ternary reward

Struggling with the sparsity of the previous CORF, a third level of reward was added to equation (4.27), encouraging the agent to achieve a middle-region (cf. equation (4.29)), i.e., a looser definition of "success".

$$r = \begin{cases} 2 & \text{if } |e_z| < 0.5g \wedge |\eta| < \frac{\eta_{max}}{2} \wedge |e_u| < e_{u,\max} \\ 1 & \text{otherwise if } |e_z| < 10g \wedge |\eta| < \eta_{max} \wedge |e_u| < 3e_{u,\max} \\ 0 & \text{otherwise} \end{cases} \quad (4.29)$$

As for the binary CORF (cf. equation (4.28)), an enhanced version of the ternary CORF was implemented with a discrete penalty of magnitude 10 times higher than the reward value corresponding to success (cf. equation (4.30)).

$$r = \begin{cases} 2 & \text{if } |e_z| < 0.5g \wedge |\eta| < \frac{\eta_{max}}{2} \wedge |e_u| < e_{u,\max} \\ 1 & \text{otherwise if } |e_z| < 10g \wedge |\eta| < \eta_{max} \wedge |e_u| < 3e_{u,\max} \\ 0 & \text{otherwise if } |\eta| < \eta_{max} \\ -20 & \text{otherwise} \end{cases} \quad (4.30)$$

4.1.4 Dense Sum with SER

Although not having achieved the target performance with the approach in section 4.1.3, the experience of implementing HER and BPER raised the hypothesis of their possible benefit within the dense CORF context. In fact, the problems associated with sparse CORF (cf. section 3.3) apply, as well, to dense

rewards if the objective is too strict, i.e., if the goal is too difficult. In this case, the latter could explain why the agent struggled so much with balancing tracking performance and action smoothness.

However, contrarily to sparse rewards (cf. section 4.1.3), dense rewards are, alone, quite efficient in bringing the agent to the middle/near region and, hence, SER (cf. section 4.2.5) was implemented together with some CORF from section 4.1.2 that had shown good train results, possibly with minor changes.

Four terms, $n = 4$

1. Taking the implementation of section 4.1.2, configuration 1 modifies w_3 and w_4 (cf. appendix A), decreasing them when $|e_z|$ grows, so that the agent can be more agile in following rises of the reference signal.
2. Configuration 2 applies the hypotheses of configuration 1 solely to f_3 , assuming that f_4 is not related with agility in the transition periods, only with the oscillations of the resting periods.
3. Configuration 3 takes the implementation of configuration 1 and unfolds w_4 (cf equation (4.31)) in order to progressively encourage the agent to stay inside the near-region, tripling its importance when the agent achieves success with a certain stability, i.e., when the tracking error of the previous episode $|e_z|_{\max, past}$ was already low.

$$w_4 = \begin{cases} 3w_4 & \text{if } |e_z| < 3g \wedge |\eta| < \frac{\eta_{max}}{2} \wedge |e_z|_{\max, past} < 2.5g \\ w_4 & \text{otherwise if } |e_z| < 3g \wedge |\eta| < \frac{\eta_{max}}{2} \end{cases} \quad (4.31)$$

Three terms, $n = 3$

1. f_3 was modified (cf. equation (4.33)), where w_3 decreases with $|e_z|$ in order to allow the agent to be more agile when there is a rise in the reference signal and increases as the agent approaches the target performance (cf. appendix A, with $e_{u, \max} = 0.03$). b (cf. equation (4.32)) is the smoothness bonus.

$$b = \begin{cases} \frac{e_{u, \max} - e_u}{e_{u, \max}} & \text{if } |e_u| < e_{u, \max} \\ 0 & \text{otherwise} \end{cases} \quad (4.32)$$

$$f_3 = \begin{cases} 10w_3.b & \text{if } |e_z| < 2g \wedge |\eta| < \frac{\eta_{max}}{2} \wedge |e_u| < 0.005 \\ 5w_3.b & \text{otherwise if } |e_z| < 2g \wedge |\eta| < \frac{\eta_{max}}{2} \\ w_3.b & \text{otherwise if } |e_z| < 7g \wedge |\eta| < \frac{\eta_{max}}{2} \\ 0 & \text{otherwise} \end{cases} \quad (4.33)$$

2. Different relative weights set (cf. appendix A).
3. f_1 was enhanced with a positive term that grows quadratically with $|e_z|$ (cf. equation(4.34)), in order to encourage the agent to stay inside the near-region.

$$f_1 = \begin{cases} 200 \left(\frac{5g - |e_z|}{5g} \right)^2 & \text{if } |e_z| < 5g \\ -w_1 \cdot |e_z| & \text{otherwise} \end{cases} \quad (4.34)$$

4. With the same intention of configuration 3, configuration 4 encourages the agent to stay inside the near-region using an exponential profile, instead of a quadratic one (cf. equation (4.35)).

$$f_1 = \begin{cases} 200e^{-0.5 \times \frac{|e_z|}{g}} & \text{if } |e_z| < 5g \\ -w_1 \cdot |e_z| & \text{otherwise} \end{cases} \quad (4.35)$$

5. Configuration 5 takes configuration 4 and adds another exponential term, this time replacing f_3 with a function of e_u (cf. equation (4.36), with $e_{u,\max} = 0.03$) in order to encourage the agent to remain in the near-region.

$$f_3 = \begin{cases} 50e^{|e_u|} & \text{if } |e_u| < e_{u,\max} \\ -w_3 & \text{otherwise} \end{cases} \quad (4.36)$$

6. Configuration 6 takes the architecture of configuration 1 and implements it with a different relative weights' set (cf. equation (4.37) and appendix A).

$$f_3 = \begin{cases} \frac{40}{3}w_3.b & \text{if } |e_z| < 2g \wedge |\eta| < \frac{\eta_{\max}}{2} \wedge |e_u| < 0.005 \\ \frac{20}{3}w_3.b & \text{otherwise if } |e_z| < 2g \wedge |\eta| < \frac{\eta_{\max}}{2} \\ w_3.b & \text{otherwise if } |e_z| < 7g \wedge |\eta| < \frac{\eta_{\max}}{2} \\ 0 & \text{otherwise} \end{cases} \quad (4.37)$$

7. Configuration 7 takes the architecture of configuration 1 and implements it with a different relative weights' set (cf. equation (4.38) and appendix A).

$$f_3 = \begin{cases} 20w_3.b & \text{if } |e_z| < 2g \wedge |\eta| < \frac{\eta_{\max}}{2} \wedge |e_u| < 0.005 \\ 10w_3.b & \text{otherwise if } |e_z| < 2g \wedge |\eta| < \frac{\eta_{\max}}{2} \\ 3w_3.b & \text{otherwise if } |e_z| < 7g \wedge |\eta| < \frac{\eta_{\max}}{2} \\ 0 & \text{otherwise} \end{cases} \quad (4.38)$$

8. Configuration 8 takes the architecture of configuration 1 and implements it with a different relative weights' set (cf. equation (4.39) and appendix A).

$$f_3 = \begin{cases} 10w_3.b & \text{if } |e_z| < 2g \wedge |\eta| < \frac{\eta_{\max}}{2} \wedge |e_u| < 0.005 \\ 5w_3.b & \text{otherwise if } |e_z| < 2g \wedge |\eta| < \frac{\eta_{\max}}{2} \\ w_3.b & \text{otherwise if } |e_z| < 7g \wedge |\eta| < \frac{\eta_{\max}}{2} \\ 0 & \text{otherwise} \end{cases} \quad (4.39)$$

Two terms, $n = 2$ (magnitude)

1. Configuration 1 enhances the one of section 4.1.2 by adding an exponential profile to f_1 (cf. equation (4.40)) when the agent is already inside the near-region.

$$f_1 = \begin{cases} 2000e^{-0.5\frac{|e_z|}{g}} & \text{if } |e_z| < 0.5g \\ 1000e^{-0.5\frac{|e_z|}{g}} & \text{if } |e_z| < 2g \\ -w_1|e_z| & \text{otherwise} \end{cases} \quad (4.40)$$

2. Configuration 2 is a continuation of the idea of configuration 1: not only does f_1 have an exponential profile when the agent is in the near-region, but also its far-region's profile evolves quadratically with e_z (cf. equation (4.41)), in an attempt to increase the speed at which the agent learns to abandon this far-region.

$$f_1 = \begin{cases} 2000e^{-0.5\frac{|e_z|}{g}} & \text{if } |e_z| < 0.5g \\ 1000e^{-0.5\frac{|e_z|}{g}} & \text{otherwise if } |e_z| < 10g \\ -(w_1 \cdot e_z)^2 & \text{otherwise} \end{cases} \quad (4.41)$$

4.2 Algorithm

As explained in chapter 1, the current problem required an on-policy model-free RL algorithm. Among them, not only is TRPO a current state-of-the-art algorithm (cf. section 3.2), but it also presents the attractiveness of the trust region search, avoiding sudden drops during the training progress, which is a very interesting feature to be explored by the industry, whose mindset is often aiming at robust results (as section 4.5.2 shows, the trust region is key to the implementation of the robustified agents).

TRPO was, therefore, the most suitable choice to solve the problem stated in section 2.2.

4.2.1 Hyperparameters' Configuration

In the ML context, an hyperparameter is a configuration that needs to be set externally to the model, by its user, in opposition to the model's parameters, which are configurations to which the user is blind since they remain internal to the model and are estimated, updated or predicted from data.

In line with the most recent literature, hyperparameters will henceforward be referred to in upper case words. Due to the limited available computational resources and time, the values shown in table 4.1 were found with a greedy search around the values suggested by Schulman et al. [5] and by Kangin et al. [10]. For the same reason, the configuration was also kept across all the Reward Engineering (cf. section 4.1) process and all the Robustness Assessment Experiments (cf. section 4.5).

4.2.2 Modifications to original TRPO

The present implementation was inspired in the implementations proposed by Schulman et al. [5] and by Kangin et al. [10] (cf section 3.2). There are several differences, though.

Hyperparameter	Value
<i>ALPHA</i>	50
<i>BATCH_SIZE</i>	1
<i>GAMMA</i>	0.995
<i>HID1_MULT</i>	10
<i>KL_TARG</i>	0.003
<i>LAM</i>	0.98
<i>POLICY_EPOCHS</i>	20
<i>POLICY_LAST_HID</i>	10
<i>POLICY_LR_SCALER</i>	0.00075
<i>REPLAY_BUFFER_SIZE</i>	3
<i>TRAJECTORY_LEN</i>	5000
<i>VALUE_EPOCHS</i>	10
<i>VALUE_LAST_HID</i>	5
<i>VALUE_LR_SCALER</i>	0.009

Table 4.1: Hyperparameters' Configuration

Neural Networks Architecture

Firstly, it is of great benefit to architecture the neural networks in the most general possible way so that they can adapt to changes in the observations vector (their input size) or in the actions vector (output size of the Policy NN). Such changes can occur either during the reward engineering (cf. section 4.1) process, in which different reward functions can demand different observations, when scaling to the complete GSAM model (cf. section 6.2) instead of solely the longitudinal model or even if trying to apply this implementation to a different GSAM configuration. Therefore, the present implementation followed the architecture of Patrick Coady², who heuristically tuned it to succeed in ten MuJoCo [3] robotic control environments with different observations and actions. Hence, both neural networks have got three hidden layers whose size is h_1 , h_2 and h_3 (cf. table 4.2), according to the forward orientation.

	h_1	h_2	h_3
Policy NN	$HID1_MULT \times d_o$	$\approx \sqrt{(h_1 \times h_3)_{Policy}}$	$POLICY_LAST_HID \times d_a$
Value NN	$HID1_MULT \times d_o$	$\approx \sqrt{(h_1 \times h_3)_{Value}}$	$VALUE_LAST_HID \times d_a$

Table 4.2: Hidden Layers of the Neural Networks^a

^aCf. section 4.2.1 for details about the hyperparameters.

Normalizing the networks' input

Secondly, as detailed in section 2.2, the observations vector is composed of quantities whose range is drastically different: from the height in the thousands of meters to the past η in the tenths of radians. This variety of ranges within the input of the networks can damage their training because it cannot distinguish whether one neuron's value is very low because it is not important to the prediction being made or

²Available at <https://github.com/pat-coady/trpo>. Last viewed on October 10th 2020.

because the input associated corresponding to a higher weight happens to be a very small number. The observations are, thus, normalized (cf. equation (4.42)) before being fed as input of the neural networks.

$$obs_{norm} = \frac{obs - \mu_{online}}{\sigma_{online}} \quad (4.42)$$

In equation (4.42), μ_{online} and σ_{online} are the mean value and the variance of the set of observations collected along the whole training process, which are updated with information about the newly collected observations obs_{new} after each training episode according to equations (4.43) and (4.44), being m the number of observations collected so far (before that episode) and n the number of observations collected during that last episode.

$$\mu_{new} = \frac{m \cdot \mu_{old} + n \cdot \mu_{obs_{new}}}{m + n} \quad (4.43)$$

$$\sigma_{new}^2 = \frac{m (\sigma_{old}^2 + \mu_{old}^2) + n (\sigma_{obs_{new}}^2 + \mu_{obs_{new}}^2)}{m + n} - \mu_{new}^2 \quad (4.44)$$

Notice that, if $(\mu_{new}, \sigma_{new})$ differed too much from $(\mu_{old}, \sigma_{old})$, equation (4.42) would disrupt the training process, because the neural networks' update, being blind to these parameters, would lose the connection with the unnormalized observations. However, if we can assume that $(\mu_{old}, \sigma_{old}) \approx (\mu_{new}, \sigma_{new})$, then, the normalization of the observations would be a mere linear transformation. The latter assumption is more valid as $m \rightarrow +\infty$, i.e., as train proceeds.

Exploration strategy

The exploration strategy is key to the sampling of new actions, included in stage 1 of algorithm 2 (cf. section 4.2).

As referred in section 3.1, the balance between exploration and exploitation plays a key role in the learning process and it has been addressed by several authors with promising results. The core question, though, is still to be answered: which strategy to choose for each situation, depending on the algorithm, on the reward function or on any other relevant parameter of the model.

In the original TRPO paper, Schulman et al. [5] suggested a policy optimization based on trust-region search, instead of the traditional line search, which, in itself, entails an exploration strategy, since the radius of the trust region is increased when the policy is found not to be optimal, under some criteria, which, although mathematically elegant, is of complex implementation. Facing the latter, Kangin et al. [10] proposed a "replacement of the heuristically calculated trust region parameters, to a single fixed hyperparameter [...] and a trainable diagonal covariance matrix". Both these solutions are a solid progress to the simple addition of Gaussian noise to the action's space or to the policy parameters' space since they directly relate with the training process. Finally, they are also advantageous in comparison to entropy-based techniques, since, with the penalty on KL divergence (cf. section 3.2), they avoid disruptive update steps.

For the aforementioned reasons, the proposed exploration strategy is deeply rooted on Kangin et al.'s

[10] (cf. section 3.2), meaning that, the new action η is sampled from a normal distribution (cf. equation (4.45)) whose mean is the output of the policy neural network and whose variance is obtained according to equation (4.46).

$$\eta \sim N(\mu_\eta, \sigma_\eta^2) \quad (4.45)$$

$$\sigma_\eta^2 = e^{\sigma_{\log}^2} \quad (4.46)$$

Although similar, this strategy differs from the original [10] in σ_{\log}^2 , which will always be a function of $\sigma_{\log,train}^2$ and $\sigma_{\log,tune}^2$ (cf. equation (4.47)), one that is trained with the policy's parameters θ and another that is not trained and needs to be tuned heuristically.

$$\sigma_{\log}^2 = \sigma_{\log,train}^2 + \sigma_{\log,tune}^2(e_z) \quad (4.47)$$

By definition, $\sigma_{\log,tune}^2$ is meant to be set heuristically. Regarding this application, it is reasonable to relate it with the tracking error, encouraging more exploration when the error grows, to allow, for example, an agile response to rises in the reference signal.

This idea raises two questions, though.

First of all, $\sigma_{\log,train}^2$ is updated after each episode whilst e_z changes at every step. How often should $\sigma_{\log,tune}^2$ be updated? By choosing to update it as often as $\sigma_{\log,train}^2$, one would have to decide which e_z of the last episode to use, whereas choosing to do it at every step with the latest e_z would cause disruption, since any outlier would be amplified. In order for $\sigma_{\log,tune}^2$ to follow $\sigma_{\log,train}^2$'s update rate, the former was implemented.

The second question concerns the decay of $\sigma_{\log,tune}^2$ decay with the e_z . Reconsider the principle underlying section 3.1, which sees the training process divided in three regions. A sigmoid-like decay (cf. equation (4.48)), as implemented in equation (4.49), allows the control of the speed of the decay in the hinges between regions with the parameter $s > 0$, being d the drop value of $|e_z|$ defining those hinges and $e_{z,max}$ a normalizing factor close to the maximum $|e_z|$ ever observed.

$$S(e_z) = \left(1 + e^{-(|e_z|-d) \cdot \frac{s}{e_{z,max}}}\right)^{-1} \quad (4.48)$$

$$\sigma_{\log,tune}^2 = \begin{cases} \sigma_{\log,tune,min}^2 + (\sigma_{\log,tune,max}^2 - \sigma_{\log,tune,min}^2) \times \prod_{i=1}^n S_i(e_z) & \text{if } |e_z| > 0.75g \\ -10 & \text{otherwise} \end{cases} \quad (4.49)$$

The higher the value of s , the more abrupt the change between two regions, as shown in figure 4.2.

In the best found nominal agent (cf. section 5.2) and all the reproducibility and robustness assessments (cf. sections 5.3 and 5.4), equation (4.49) was implemented with the configuration of table 4.3 (with $n = 2$), whose decay is illustrated in Figure 4.3.

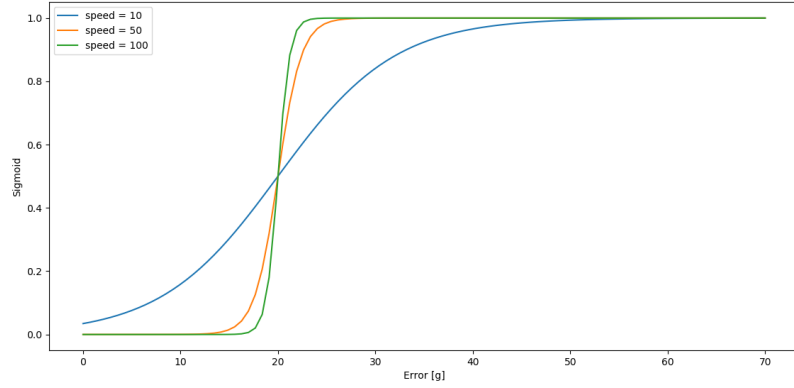


Figure 4.2: Impact of the speed in the sigmoid function

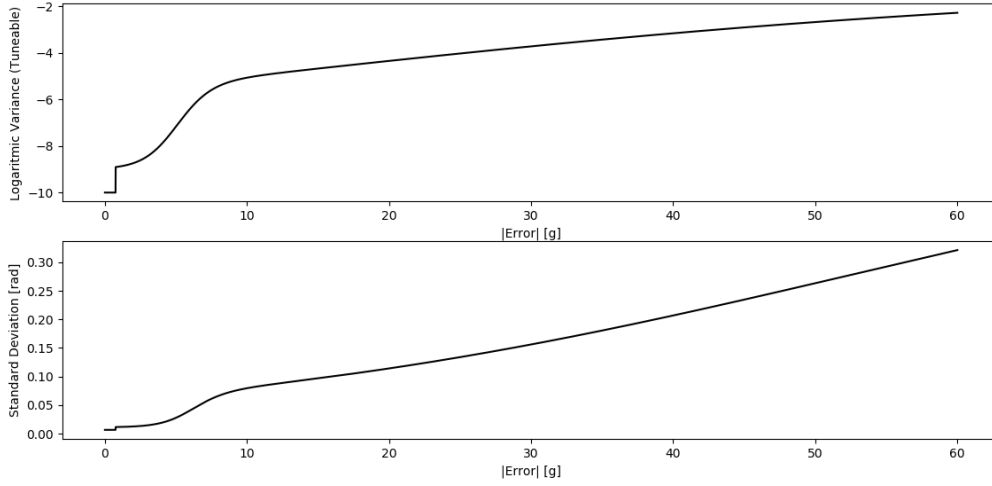


Figure 4.3: Sigmoid-like decay of $\sigma_{\log,tune}^2$

Parameter	$\sigma_{\log,tune,min}^2$	$\sigma_{\log,tune,max}^2$	d_1	s_1	d_2	s_2	$e_{z,max}$
Value	-9	-1	5g	50	10g	2	60g

Table 4.3: Exploration strategy parameters

Loss functions

Fourthly, while keeping the Value NN's loss function proposed by Kangin et al. [10] (cf. equation (3.15)), equation (4.51) was used as the loss function of the Policy NN. The former was kept because it is the most straightforward strategy for the purpose the Value NN was designed with; whereas the latter was modified in order to emphasize the need of reducing D_{KL} . In fact, although the second term of equation (3.17) aimed at penalizing policies outside the trust region, it empirically proved not to be enough in this case, causing the train to diverge too often. It was, therefore, replaced with a term that linearly penalizes D_{KL} and a quadratic term that aims at fine-tuning the D_{KL} so that it is closer to the trust region radius δ_{TR} , encouraging as big update steps as possible. This modification, although functional, has the cost

of one more parameter that needs to be tuned, β .

$$L_1 = \mathbb{E}_{\eta \sim \pi_{\theta_{old}}} [D_{KL}(\pi_{\theta_{old}}(\eta), \pi_{\theta_{new}}(\eta))] \quad (4.50)$$

$$L_P = -\mathbb{E}_s \mathbb{E}_{\eta \sim \pi_{\theta_{old}}} \left[GAE_{\pi_{\theta_{old}}}(s) \frac{\pi_{\theta_{new}}(\eta)}{\pi_{\theta_{old}}(\eta)} \right] + \alpha (\max(0, L_1 - \delta_{TR})^2) + \beta L_1 \quad (4.51)$$

Having the previously mentioned exploration strategy, π_θ is a Gaussian distribution over the continuous action space (cf. equation (4.52), where μ_η and σ_η are defined in equation (4.45)).

$$\pi_\theta(\eta) = \frac{1}{\sigma_\eta \sqrt{2\pi}} e^{-\frac{(\eta - \mu_\eta)^2}{2\sigma_\eta^2}} \quad (4.52)$$

Hence, the first term of equation (4.51) is given by equation (4.53), where n is the number of samples in the training batch, assuming that all samples in the training batch are independent and identically distributed³.

$$\begin{aligned} & \mathbb{E}_s \mathbb{E}_{\eta \sim \pi_{\theta_{old}}} \left[GAE_{\pi_{\theta_{old}}}(s) \frac{\pi_{\theta_{new}}(\eta)}{\pi_{\theta_{old}}(\eta)} \right] = \mathbb{E}_s \left[GAE_{\pi_{\theta_{old}}}(s) \right] \cdot \mathbb{E}_{\eta \sim \pi_{\theta_{old}}} \left[\frac{\pi_{\theta_{new}}(\eta)}{\pi_{\theta_{old}}(\eta)} \right] = \\ & = \left[\frac{1}{n} \sum_{i=1}^n GAE_{\pi_{\theta_{old}}}(s_i) \right] \cdot \left[\frac{\pi_{\theta_{new}}(\eta_1, \dots, \eta_n)}{\pi_{\theta_{old}}(\eta_1, \dots, \eta_n)} \right] = \left[\frac{1}{n} \sum_{i=1}^n GAE_{\pi_{\theta_{old}}}(s_i) \right] \cdot \prod_{i=1}^n \left[\frac{\pi_{\theta_{new}}(\eta_i)}{\pi_{\theta_{old}}(\eta_i)} \right] \end{aligned} \quad (4.53)$$

Moreover, L_1 (cf. equation (4.50)) is given by equation (4.54), being equation (3.13) simplified to equation (4.55) in this specific case.

$$L_1 = \frac{1}{n} \sum_{i=1}^n D_{KL}(\pi_{\theta_{old}}(\eta_i), \pi_{\theta_{new}}(\eta_i)) \quad (4.54)$$

$$D_{KL}(\pi_{\theta_{old}}(\eta), \pi_{\theta_{new}}(\eta)) = \frac{1}{2} \left(\frac{\sigma_{\eta, new}^2}{\sigma_{\eta, old}^2} + \frac{(\mu_{\eta, new} - \mu_{\eta, old})^2}{\sigma_{\eta, new}^2} - 1 + \ln \left(\frac{\sigma_{\eta, new}^2}{\sigma_{\eta, old}^2} \right) \right) \quad (4.55)$$

Optimizers

Finally, given that the two versions of TRPO propose different optimizers for θ (cf. section 3.2), this choice was left to future research (cf. section 6.2) and ADAM [33] was used for its wide cross-range success and acceptability as the default optimizer of most ML application. In both neural networks, ADAM's learning rate was defined as $\frac{s}{\sqrt{h_2}}$, where s is the *POLICY_LR_SCALER* $\times c_{lr_P}$ or the *VALUE_LR_SCALER* (cf. section 4.2.1). Although using ADAM simplifies the update of the policy and value functions' parameters, it leaves the question of the update of the trust region parameters to be separately addressed.

³We can assume they are (i) independent because they are sampled from the replay buffer (stage 5 of algorithm 2, section 4.2.6), breaking the causality correlation that the temporal sequence could entail, and (ii) identically distributed because the exploration strategy is always the same and, therefore, the stochastic policy π_θ is always a Gaussian distribution over the action space (cf. equation (4.52)).

4.2.3 Hindsight Experience Replay

Although promising, implementing HER (cf. stage 2 of algorithm 2) is challenging for the fact that, contrarily to Andrychowicz et al.'s proposal [28], the present goal is not defined by achieving a certain final state, but, instead, by achieving a certain performance in the whole sequence of states that constitutes an episode. For this reason, choosing a different goal must mean, in this case, to follow a different reference signal. Moreover, this reasoning is encouraged by the observation that suboptimal policies often lead the agent to perform "as if" it had, in fact, received a different reference signal: two consecutive steps of amplitudes others than the ones actually given to it, as shown in figure 4.4.

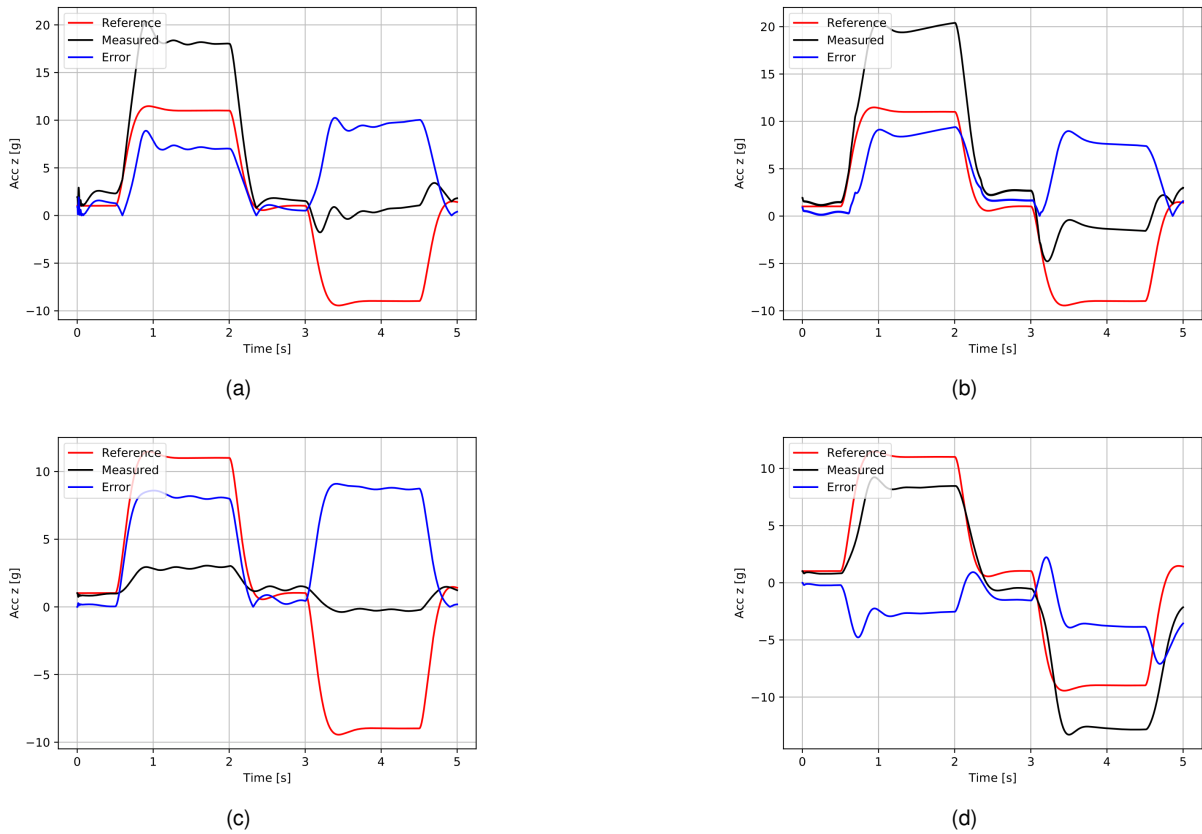


Figure 4.4: Testing performance of suboptimal policies

After collecting enough trajectories to attain a full episode, those trajectories are replayed with new goals, which are sampled according to two different strategies. These strategies dictate the choice of the amplitudes for the two consecutive steps of each new reference signal.

The first strategy, also called *mean* strategy consists of choosing the amplitude of the first and second steps of the command signal (cf. section 2.1.4) as the mean values of the measured acceleration during the first and second resting periods, respectively. Similarly, the second strategy, also called *final* strategy consists of choosing them as the last values of the measured signal during the first and second resting periods. While the first strategy is motivated by the cases where the agent's measured acceleration during the resting periods oscillates around a constant mean value, the second is motivated by those where some overshoot is followed by non-oscillatory steady signal. In both strategies, apart from the step amplitudes, all the other original parameters (cf. section 2.1.4) of the reference signal are kept.

Nevertheless, suboptimal policies such as the ones shown in figure 4.4 are, themselves, the result of some training. In truth, the agent’s performance typically starts as the one shown in figure 4.5, raising the question of the effectiveness of application of HER in such early agents, which will be discussed in section 4.1.

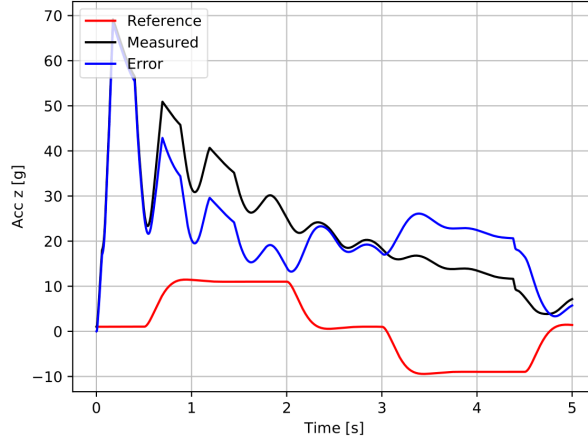


Figure 4.5: Testing performance of an untrained policy

4.2.4 Balanced Prioritized Experience Replay

As explained in 3.5, the motivation behind prioritized experience replay is to find a probability distribution for sampling past experiences from the replay buffers in the way that most efficiently updates the agent’s parameters.

Being l_i the priority level of the experience collected in step i (cf. equation (4.56), with $e_{u,\max} = 0.01$), N_j the number of steps with priority level j and ρ_j the proportion of steps with priority level j desired in the training datasets, Balanced Prioritized Experience Replay (BPER) was implemented according to algorithm 1.

$$l_i = \begin{cases} 1 & \text{if } |e_z|_i < 0.5g \wedge |\eta|_i < \frac{|\eta|_{\max}}{2} \wedge |e_u|_i < e_{u,\max} \\ 0 & \text{otherwise} \end{cases} \quad (4.56)$$

Notice that $P(i)$ and p_i follow the notation of Schaul et al. [29] (assuming $\alpha = 1$), in which $p_i = \frac{1}{\text{rank}(i)}$ matches the rank-based prioritization with $\text{rank}(i)$ meaning the ordinal position of step i when all steps

in the replay buffers are ordered by the magnitude of their temporal differences (cf. equation (3.8)).

Algorithm 1: Hindsight Experience Replay

```

if  $N_1 < 0.25(N_0 + N_1)$  then
   $\rho_1 = 0.25$ 
   $s_j = \sum_i p_i, \forall_i (l_i = j)$  with  $j \in \{0, 1\}$ 
else
   $\rho_1 = 0.5$ 
   $s_0 = s_1 = \sum_i p_i, \forall_i$ 
end

 $\rho_0 = 1 - \rho_1$ 
 $P(i) = \begin{cases} \rho_1 \times \frac{p_i}{s_1} & \text{if } l_i = 1 \\ \rho_0 \times \frac{p_i}{s_0} & \text{otherwise} \end{cases}$ 

```

As condensed in algorithm 1, when there is less than 25% of successful steps in the replay buffers, the successful and unsuccessful subsets of the replay buffers are sampled separately, with 25% coming from the successful subset. In a posterior phase of training, when there is already more than 25% of successful steps, both subsets are molten. In either cases, sampling is always done according to the temporal differences, i.e., a step with higher temporal difference has got a higher chance of being sampled.

Hence, BPER (cf. stage 5 of algorithm 2) constitutes an extension of the Prioritized Experience Replay algorithm described in section 3.5 by the addition of ρ_1 , which is inspired in Narasimhan et al.'s implementation [30], but differs in the sense that its effect is cancelled when there is enough representation of the "success" class.

4.2.5 Scheduled Experience Replay

Having HER (cf. section 4.2.3) and BPER (cf. section 4.2.4) dependent on a condition - the SER condition - is hereby defined as Scheduled Experience Replay (SER). The SER condition is exemplified in equation (4.57), where $\bar{e}_{z,past}$ stands for the mean tracking error of the previously collected episode and ϵ for its threshold (cf. appendix A).

$$\bar{e}_{z,past} \leq \epsilon \tag{4.57}$$

HER was initially proposed as a technique to increase the sample efficiency of algorithms dealing with very sparse rewards (cf. section 3.4). Nevertheless, the reward function that led to the target performance (cf. section 5.2) is not sparse and was already able of achieving the near-region without HER. The hypothesis, in this case, is, therefore, that HER can be a complementary feature activated only when the reward function, on its own, has improved the agent's performance, but converged it to a suboptimal level.

Moreover, if HER has not been activated, BPER adds less benefit, since there is no special reason for the agent to believe that some part of the collected experience is more significant than other, contrarily to what happens once HER takes place.

4.2.6 Algorithm Description

Algorithm 2: Implemented TRPO with a Replay Buffer and SER

Initialization

while *training* **do**

1. Collect experience by interacting with the environment, sampling actions from policy π
2. Augment the collected experience with synthetic successful episodes (SER)
3. $(a_t, s_t, r_t) \leftarrow V'(s_t)$ and $GAE(s_t)$ **for all** (a_t, s_t, r_t) **in** T , **for all** T **in** B
4. Store the newly collected experience in the replay buffer
5. Sample the training sets from the replay buffer (SER)
6. Update all value and policy parameters
7. Update trust region

end

The proposed approach is summarised in algorithm 2, which starts by randomly initializing of the parameters the Policy NN and of the Value NN, by initializing the replay buffer to $R = \{\}$, by setting α (cf. equation (4.51)) to *ALPHA*, by initializing β (cf. equation (4.51)) and c_{lrp} (cf. section 4.2.2) to 1 and by running 5 episodes to initialize μ_{online} and σ_{online} (cf. equation (4.42)).

The information about the agent's interaction with the environment at each step - actions, resulting observations of the state of the environment and respective rewards - is collected in 3-tuples (a, s, r) . A group of consecutive 3-tuples forms a trajectory T and a group of trajectories forms a batch B .

1. One batch of trajectories ($B = \{T_i\}_{i=1}^{BATCH_SIZE}$), each with 3-tuples ($T = \{(a_j, s_j, r_j)\}_{j=1}^{TRAJECTORY_LEN}$), is collected. The actions are sampled according to the policy π and the proposed exploration strategy (cf. section 4.2.2).

When collecting B , every time an episode ends, the performance requirements are checked, possibly deploying intermediate tests (cf. section 4.3.2), $\sigma_{\log, tune}^2$ is updated (using the maximum tracking error registered during the resting periods of the previous episode as e_z in equation (4.49)) and a new reference signal has to be generated (cf. section 4.3.1).

The concept of *trajectory*, however, does not necessarily matches that of *episode*, as defined in section 2.2, the former being more general and the latter specific to the current context. As mentioned before, a trajectory is a sequence of data concerning consecutive time steps of interaction between the agent and the environment, whose length is arbitrarily parameterized by *TRAJECTORY_LEN*. Nevertheless, by matching *TRAJECTORY_LEN* with the length of a full episode, 5000 steps, and setting *BATCH_SIZE* to 1, there is an update of the agent's parameters after each episode, which is reasonable, since it guarantees both (i) that all trajectories have information about all the transient and stationary parts of the episode, which would not happen had *TRAJECTORY_LEN* been defined as less than 5000, and (ii) that the updates are as frequent

as possible.

2. With the aforementioned configuration, after having collected B , the episode is over and, therefore, if the SER condition (cf. section 4.2.5) holds, B is augmented according to HER (cf. section 4.2.3).
3. The targets for the Value NN $V'(s_t)$ (cf. equation (3.14) with $TRAJECTORY_LEN$ as k) and the generalized advantage estimators $GAE(s_t)$ (cf. equation (3.11) with $GAMMA$ and LAM as γ and λ , respectively) are computed and added to the trajectories, augmenting the 3-tuples corresponding to each time step.
4. B is stored in the replay buffer, discarding the oldest batch: the replay buffer R contains data collected from the last $REPLAY_BUFFER_SIZE$ policies and works as a FIFO queue.
5. If the SER condition (cf. section 4.2.5) holds, the training dataset is sampled from R according to BPER (cf. section 4.2.4). Otherwise, the entire information available in R is used as training dataset.
6. The value parameters ψ and the policy parameters θ are updated. ψ 's update is done for $VALUE_EPOCHS$ epochs and θ 's for $POLICY_EPOCHS$ epochs.
7. The trust region parameters are updated according to algorithm 3. The trust region is controlled through the D_{KL} terms of the policy loss function (cf. equation (4.51)). When perfectly weighted, this should be enough for the iterative convergence of D_{KL} to δ_{TR} . However, since α and β are heuristically initialized, the policy loss's terms are far from perfectly weighted and, thus, there might be a need for an adjustment. For matters of simplicity, only β is adjusted, since only the relative size is important.

Indeed, if D_{KL} is far larger than δ_{KL} , a shrinkage of the trust region is needed and, thus, β must be increased. Besides, the latter must also be accompanied by an increased care in the updates, meaning that the learning rate of the policy's optimizer must be reduced, which is indirectly done by its multiplier c_{lr_P} (cf. section 4.2.2). The opposite reasoning applies when D_{KL} is far less than δ_{TR} .

Algorithm 3: Update of the Trust Region Parameters

```

if  $D_{KL} > 2\delta_{TR}$  then
   $\beta = \min(35, 1.5 \times \beta)$ 
  if  $\beta > 30$  and  $c_{lr_P} > \frac{1}{10}$  then
     $c_{lr_P} \leftarrow \frac{c_{lr_P}}{1.5}$ 
else if  $D_{KL} < \frac{\delta_{TR}}{2}$  then
   $\beta = \max\left(\frac{1}{35}, \frac{\beta}{1.5}\right)$ 
  if  $\beta < \frac{1}{30}$  and  $c_{lr_P} < 10$  then
     $c_{lr_P} \leftarrow 1.5 \times c_{lr_P}$ 

```

4.3 Methodology

4.3.1 Command Reference Signal Generation

The command reference signal consists of two consecutive steps, whose amplitudes are either randomly generated or defined as 10g/-10g, depending on whether the agent is in a training or testing situation, respectively. In the former case, the sign of the amplitudes is randomly defined and their absolute values are sampled from a triangular distribution (cf. equation (4.58)), where low and up are given by equations (4.59) and (4.60) and m grows linearly along the first 150 episodes stabilizing in the amplitude of the testing command reference signal, 10g, as shown in figure 4.6.

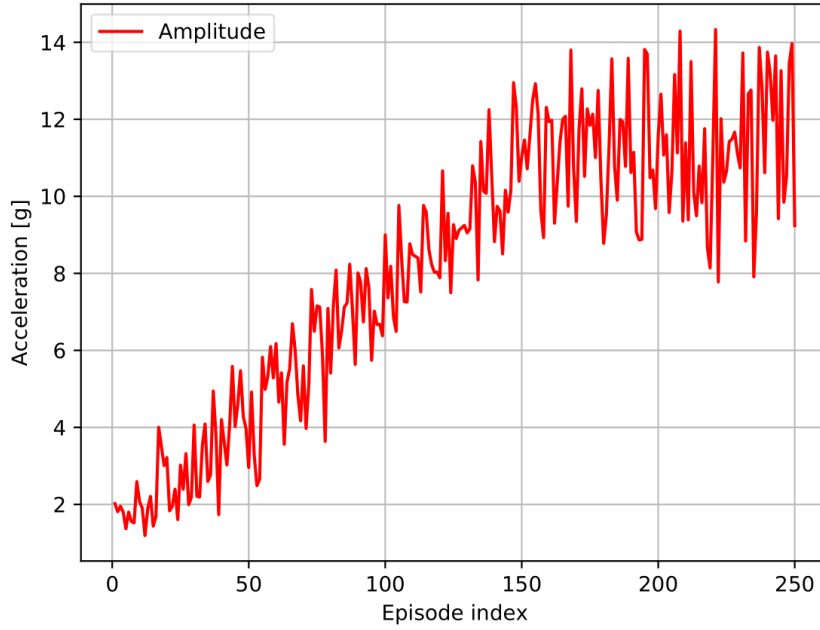


Figure 4.6: Evolution of the Amplitude of the Reference Signal during Training

$$A \sim \text{Triangular}(low, up, m) \quad (4.58)$$

$$low = \max(m - 5g, 1g) \quad (4.59)$$

$$up = m + 5g \quad (4.60)$$

In fact, not varying the reference signal during training would certainly cause the agent to overfit, instead of learning. To avoid so, at training time, in the beginning of each episode, $t1_{start}$, $t1_{len}$, t_{rest} and $t2_{len}$ are sampled from an uniform distribution (cf. equation (4.61)) with table 4.4's parameters, whilst $t1_{end}$, $t2_{start}$ and $t2_{end}$ are defined by equations (4.62), (4.63) and (4.64). All of the latter nomenclature is illustrated in figure 4.7. On the other hand, table 4.5 shows the values established for the testing runs, which are immutable.

$$t_i \sim U(a, b) \quad (4.61)$$

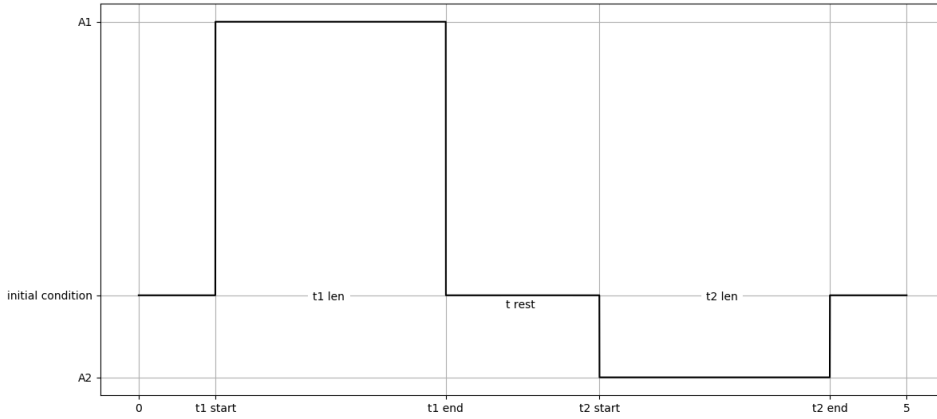


Figure 4.7: Command Reference Signal

	$t1_{start}$	$t1_{len}$	t_{rest}	$t2_{len}$
a	0.5	1	0.6	1
b	1	1.5	1	1.5

Table 4.4: Parameters of the Uniform Distribution of the Training Reference Signal Characterization

$$t1_{end} = t1_{start} + t1_{len} \quad (4.62)$$

$$t2_{start} = t1_{end} + t_{rest} \quad (4.63)$$

$$t2_{end} = t2_{start} + t2_{len} \quad (4.64)$$

$t1_{start}$	$t1_{len}$	t_{rest}	$t2_{len}$
0.5	1.5	1	1.5

Table 4.5: Testing Reference Signal Characterization

4.3.2 Intermediate Tests

The criteria in table 4.6 were established as a softer version of the requirements that define the target performance (cf. section 2.2). The definition of the criteria used for stopping the train is key to the success of the implementation, since, as chapter 5 shows, longer trains do not always mean a performance closer to the target. Furthermore, the need for table 4.6 to present higher thresholds than the ones of section 2.2 lies in that the proposed exploration strategy (cf. section 4.2.2) never allows η 's variance to be null and, hence, the testing performance can be better than the one observed when training.

During training, algorithm 2 is run with periodic interruptions in which it is put on hold and an intermediate test is deployed to keep record of its progress. Apart from the latter, intermediate tests are also

Criterion	Threshold
$ e_z _{\max,r}$	10% $ A_{train} _{\max}$ ^a
overshoot	40%
$ \eta _{\max}$	30°
$\eta_{noise,r}$	5 rad
$\eta_{noise,t}$	0.5 rad

Table 4.6: Soft Criteria

^a A_{train} is the amplitude of one the two steps that constitute the reference signal used during the training process

deployed when the set of criteria in table 4.6 is met after a training episode. In all cases, after any testing episode, in which there is, obviously, no exploration (cf. section 3.1), all the criteria defined in section 2.2 are checked and the train is successfully finished if they are met and resumed otherwise.

4.4 Reproducibility Assessments

The proposed approach has got several stochastic elements:

1. The random initialization of the neural networks parameters
2. The exploration strategy, that samples actions from a normal distribution
3. BPER, that does not use all the past experience to train the networks: instead, samples from the replay buffer. That sampling does follow a distribution related to the Temporal Differences, but it is, nevertheless, stochastic
4. ADAM optimizer, not only because ADAM is a variation of stochastic gradient descent, but also because the policy loss being optimized is stochastic: it is related with D_{KL} .
5. The random amplitude of the steps that compose the reference signal during training contribute to the fact that the experience collected has got a certain level of randomness. Besides, this effect is enlarged by the use of HER, since the new goals defined by the HER's strategies are a direct consequence of the performance of the agent and, therefore, of the reference signal it is given to.

The most relevant is arguably 4, the optimizer's choice, since it is the only one whose substitution could reduce the overall effects of the stochasticity of the algorithm, namely when it comes to reproducibility. In fact, all the others present a higher cost of removal than the cost of the stochasticity they bring about: the initialization of the trainable parameters has to be random in the absence of prior knowledge of a better distribution; the exploration strategy is, in itself, stochastic (if deterministic, the agent would be exploiting); BPER imposes some order in the use of the replay buffers, which would otherwise be sampled randomly or, not sampled at all, resulting in a less efficient training with less informative experience; and the random generation of steps' amplitudes during training is a necessary condition in order to ensure the validity of the training and to avoid overfitting situations.

Due to the several aforementioned factors, the present implementation’s reproducibility is deeply affected. To highlight this issue, nine more training sessions were run with the same configuration, whose results are discussed in section 5.3, making a total of ten agents trained in the same conditions, with the following difference: when training the best found agent (cf. section 5.2), both neural networks were randomly initialized, whereas the remaining nine agents were run loading that very same initialization. Thus, factor 1 cannot be held accountable for conclusions taken from these experiments, whatever they may be. Such a decision has been taken in order to only consider the effects of factors that constitute an algorithm’s design choice and can, therefore, be subject of future research (cf. section 6.2).

Moreover, it has been observed that an agent whose training starts by resuming the training progress of another agent faces some instability in the first few episodes, which may cause its policy to diverge so much from the one of the loaded agent that the benefits of loading it are null. For this reason, in the reproducibility experiments, the configuration described in section 4.2.1 was entirely kept except for the value of $KLTARGET$, which was set to 0.0001, decreasing the trust region radius by a factor of 30, in an attempt of conducting a more cautious training.

4.5 Robustness Assessments

The formal mathematical guarantee of robustness of a RL agent composed of neural networks cannot be done in the same terms as the one of linear controllers.

Defining the model described in section 2 as the nominal environment, with which the agent is trained, robustness can be defined as the ability of the agent⁴ to perform in non-nominal environments. In fact, the latter follows the line of thought of Schain [34], whose work highlights the great value of evaluating the algorithm’s ability to *generalize* the knowledge collected while training, i.e., to understand whether or not the agent can maintain its performance in environments other than the one it was trained in.

Apart from testing the performance of the best found nominal agent in non-nominal environments, the hypothesis that training this agent in the latter can improve its robustness was tested as well. To do so, the train of the best found nominal agent was resumed in the presence of non-nominalities (cf. section 4.5.1) following the same procedure described in section 4.3.2. This train and its resulting best agent are henceforward called *robustifying train* and *robustified agent*, respectively.

4.5.1 Robustifying Trains

Three different modifications were separately made in the provided model (cf. chapter 2), in order to obtain three different non-nominal environments, each of them modelling latency, estimation uncertainty in M and h and parametric uncertainty in the aerodynamic coefficients C_z and C_m .

In the case of non-nominal environments including latency, the range of possible values is $[0, l_{max}] \cap \mathbb{N}^0$, whereas in non-nominal environments including uncertainties, the latter were assumed to be normally distributed, meaning that, following Peter’s [22] line of thought, the range of possible values of

⁴Due to technical issues, the best found nominal agent is not reproducible. Therefore, robustness tests have been deployed with the 2nd-best found nominal agent (cf. figure B.1), which meets the criteria in the whole episode, except for the final 0.25s.

uncertainties is $[\mu - 3\sigma, \mu + 3\sigma]^5$, where l_{max} , μ and 3σ are defined below.

Before each new episode of a robustifying train, the non-nominality new values were sampled from a uniform distribution over the range of possibilities and kept constant during the entire episode. In each case, four different values were tried for the bounds of the range of possibilities (either l_{max} or 3σ) being discarded those whose robustifying train had diverged after 2500 episodes. The remaining were run for a total of 5000 episodes (cf. section 5.4).

Latency

Inserting latency in the system means to delay the effect of the action in the environment. Thus, this non-nominal environment differs from the nominal one in the presence of delay elements at the output of the agent.

Knowing that the environment's sampling time is 1ms, four robustifying trains were run with l_{max} values of 1ms, 3ms, 5ms and 10ms.

Estimation Uncertainty

In common Surface-to-Air missiles, quantities other than the acceleration and the body rates are not measured and need to be estimated from labeled data. Since labeled data is not infinitely accurate, the estimates based on it include some uncertainty, as well. In this case, the M and h , whose dynamics is considerably slower than that of the measured quantities across the considered flight conditions, are estimated.

Again, analogously to Peter [22], the estimation uncertainties in M and h , ΔM and Δh , respectively, have been defined as multiplicative, according to equations (4.65) and (4.66), and follow a normal distribution $N(0, \sigma^2)$.

$$M = (1 + \Delta M) \times M_{nom} \quad (4.65)$$

$$h = (1 + \Delta h) \times h_{nom} \quad (4.66)$$

Four robustifying trains were run with 3σ values of 0.01, 0.02, 0.03 and 0.05.

Parametric Uncertainty

The parametrization of the model's coefficients based on labelled data is not flawless and, therefore, it is important to know the behaviour of the agent in the presence of uncertainty. Aerodynamic coefficients, like C_z and C_m , are of the utmost importance, since on them rely the dynamics of the longitudinal approximation of the GSAM.

The parametric uncertainties were defined as multiplicative, as in equations (4.67) and (4.68), and follow a normal distribution $N(0, \sigma^2)$.

⁵To be accurate, this interval covers only 99.73% of the possible values, but it is assumed to be the whole spectrum of possible values.

$$C_z = (1 + \Delta C_z) \times C_{z,nom} \quad (4.67)$$

$$C_m = (1 + \Delta C_m) \times C_{m,nom} \quad (4.68)$$

Four robustifying trains were run with 3σ values of 0.05, 0.07, 0.10 and 0.15.

4.5.2 Robustified Agent

Similarly to what was argued about the urge of shrinking the trust region radius in section 4.4, *KLTRAGET* was set to 0.00005, halving the value used in the Reproducibility Assessment Experiments due to the fact that, not only did these agents resume previous agents' trains (like in section 4.4), but they also did so in non-nominal, and, therefore, more adverse, conditions, demanding an extra level of prudence.

Finally, the ORF (cf. section 5.2) suffered some fine-tuning as well, so that it could encourage the agent towards the optimal policy again, with two modifications being inserted, motivated by the empirical observation that the original configuration let the performance drift in terms of tracking error and η 's smoothness: w_1 and w_4 were set to $\frac{34}{g}$ and $\frac{240}{\max(\frac{|e_z|}{g}, 3)}$, respectively.

Chapter 5

Results and Discussion

5.1 Expected Results

Empirically, it has been seen that agents that struggle to control η 's magnitude within its bounds (cf. section 2.2) are unable of achieving low error levels without increasing the level of noise, if they can do it at all. In other words, the only way of having good tracking results with unbounded actions is to fall into a bang-bang control-like [32] situation. Therefore, the best found agent will have to start by learning to use only bounded and smooth action values, which will allow it to, then, start decreasing the tracking error.

Notice that, while the tracking error and the noise measures are expected to tend to 0, η 's magnitude is not, since it would mean that the agent had given up actuating in the environment. Hence, it is expected that, at some point in training, the latter stabilizes.

Moreover, the exploration strategy proposed in section 4.2.2 insert some variance in the output of the policy neural network, meaning that the noise measures are also not expected to reach exactly 0. Apart from this effect, the exploration strategy is also meant to avoid suboptimal convergence, whereby occasional drops in performance, i.e., peaks of any of the monitored quantities, may occur, although not often, due to the trust region. In such cases, the exploration is considered successful if the agent can achieve better results afterwards and excessive if such drops cause the policy to diverge.

Finally, the tracking error during transition periods is expected to decrease at a different rate than the one during resting periods. In fact, whilst the latter is expected to tend to 0, the former is not, since the environment is a non-minimum phase system (cf. section 2.1.2) and its transient regime include situations like response delay and undershoot.

5.2 Best Found Agent

The target performance was achieved after training the agent with the reward function detailed in configuration 1 of the "Four terms, $n = 4$ " CORF of section 4.1.4, whose relative weights can be found in appendix A.

5.2.1 Training Evolution

As expected (cf. section 5.1), the agent first learnt to output bounded smooth values for η : figures 5.1, 5.2 and 5.3 show that η 's magnitude and noise peaks drastically decrease after approximately 500 episodes of training, whereas the tracking error (cf. figures 5.4 and 5.5) only starts its decreasing tendency around the 1000th episode of training.

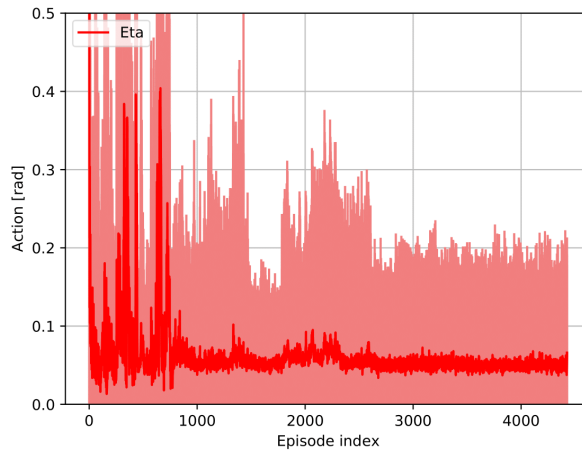


Figure 5.1: η 's evolution during best found agent's training

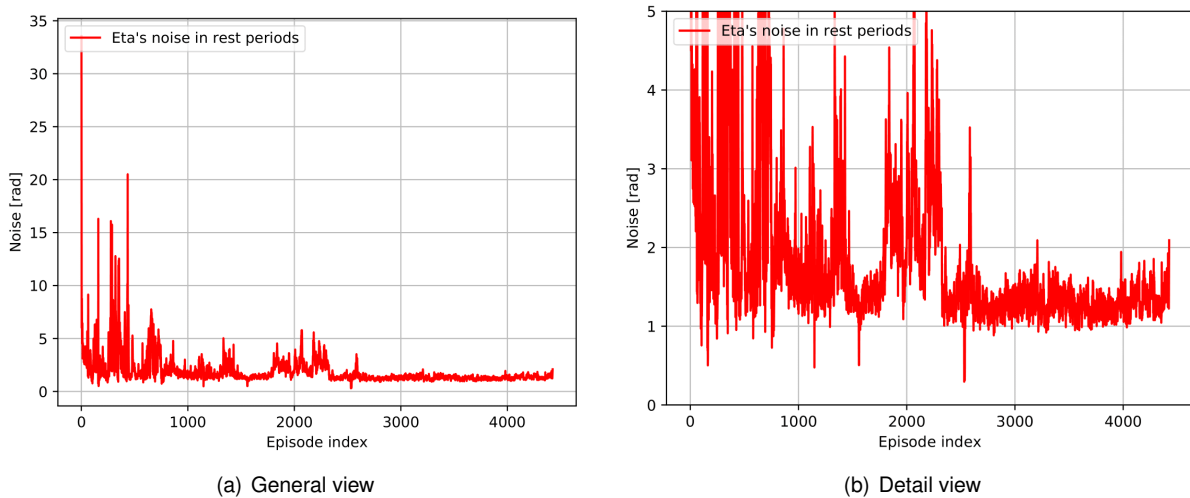
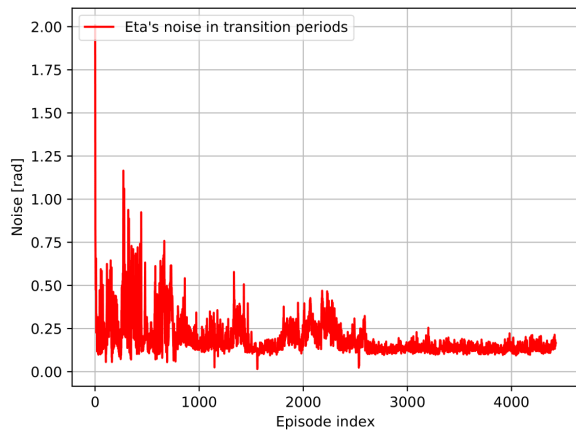


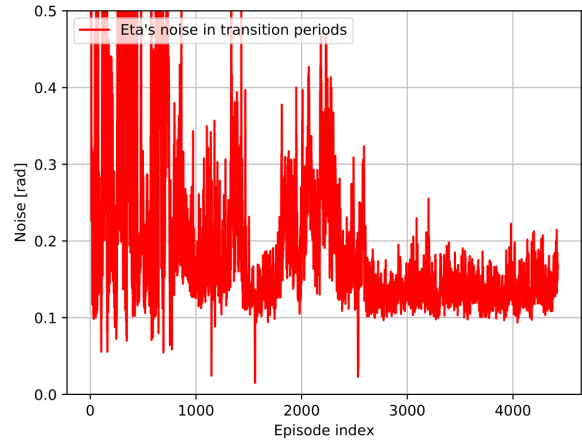
Figure 5.2: η 's resting noise evolution during best found agent's training

Furthermore, the training results evidence occasional higher exploration phases, such as the one occurred between the 2000th and the 3000th episode of training, where there is an odd peak in all the monitored quantities. Since, after this peak, η 's magnitude and noise levels return to their previous stabilized (good) state and that there is a significant decrease in the tracking error during resting periods (cf. figure 5.4), it is reasonable to say that the adopted exploration strategy is properly tuned, being not enough to cause the policy to diverge, as desired.

Finally, figure 5.6 shows that the overall performance indicator, the reward, has got an increasing tendency along the training, meaning that the agent is continuously improving in the direction pointed by the implemented reward function.

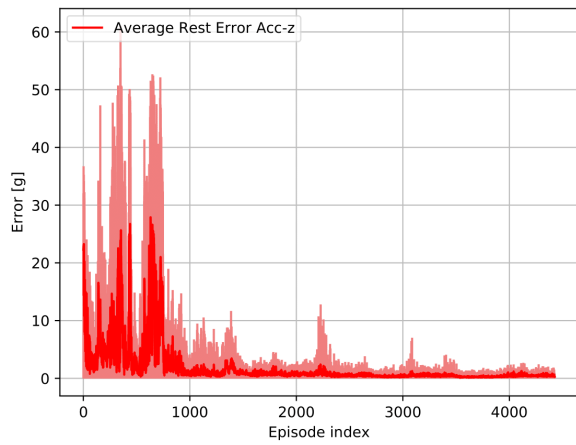


(a) General view

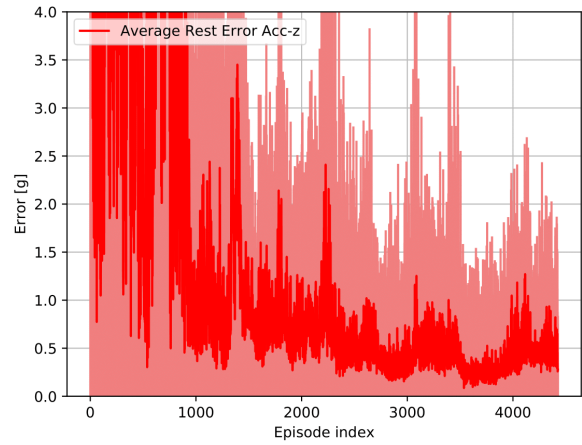


(b) Detail view

Figure 5.3: η 's transition noise evolution during best found agent's training

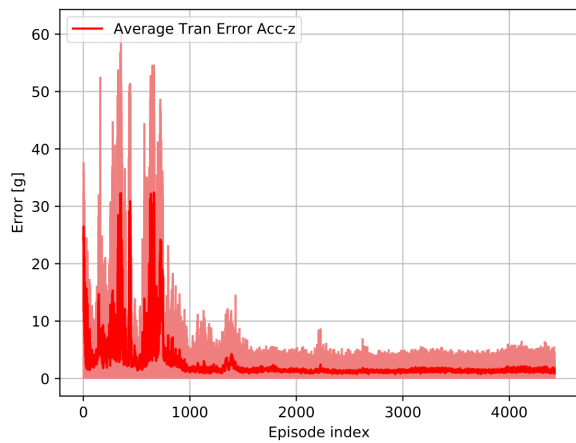


(a) General view

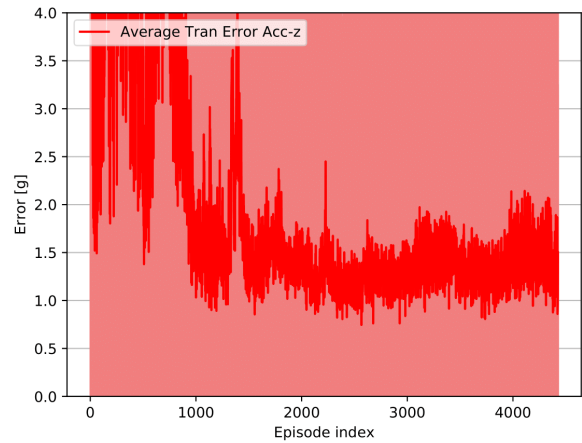


(b) Detail view

Figure 5.4: Resting tracking error's (acceleration z) evolution during best found agent's training



(a) General view



(b) Detail view

Figure 5.5: Transition tracking error's (acceleration z) evolution during best found agent's training

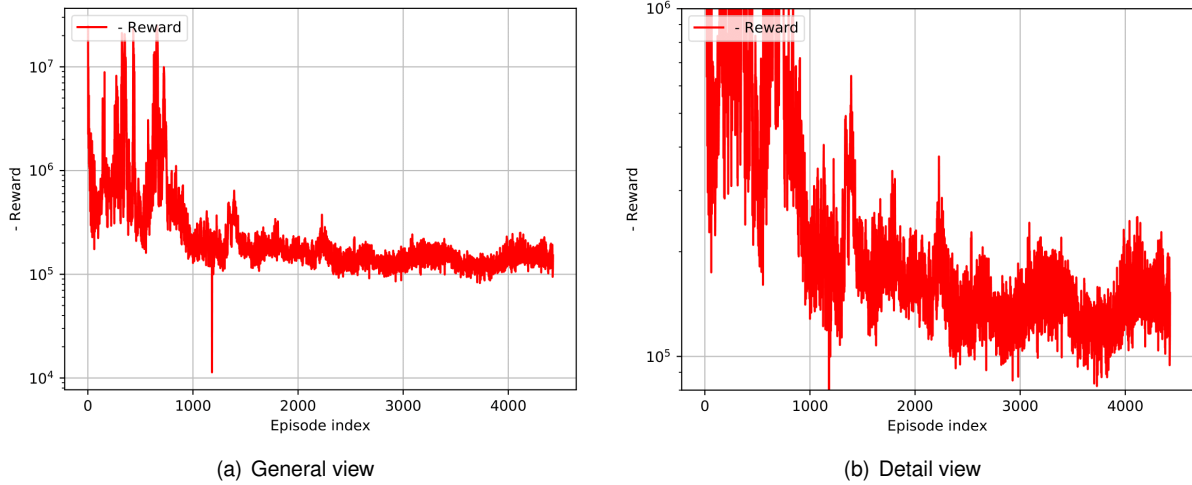


Figure 5.6: Mean reward per step's evolution during best found agent's training

5.2.2 Test Performance

As defined in section 4.3.1, the agent's performance is assessed with a double step reference signal with an amplitude of 10g.

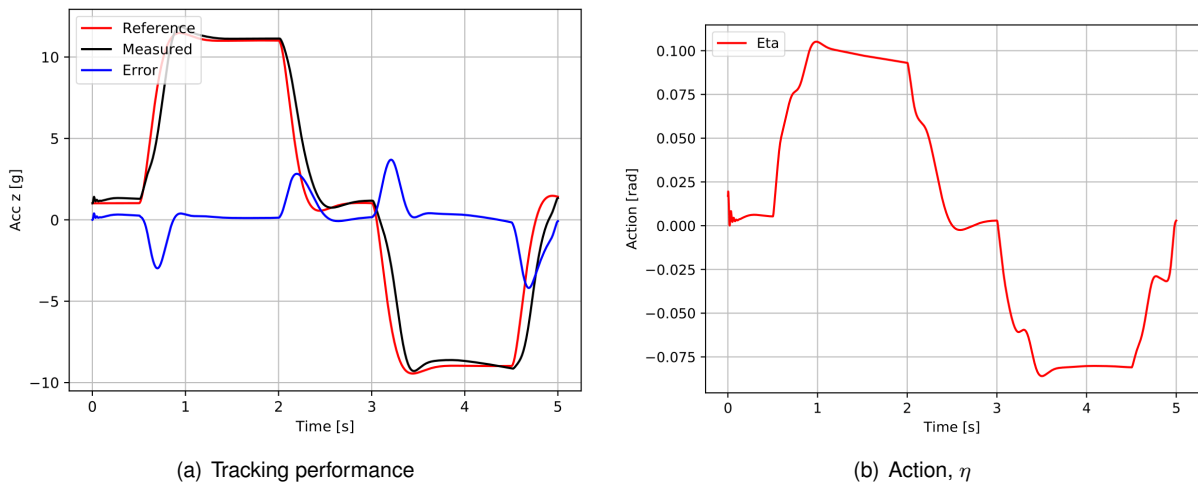


Figure 5.7: Test performance of the Best Found Agent

As figure 5.7 evidences, the agent is clearly able of controlling the measured acceleration and to track the reference signal it is fed with, satisfying all the performance requirements defined in section 2.2 (cf. table 5.1).

Performance requirement	[Unit]	Value
$ e_z _{\max,r}$	[g]	0.4214
Overshoot	[%]	8.480
$ \eta _{\max}$	[rad]	0.1052
$\eta_{noise,r}$	[rad]	0.04222
$\eta_{noise,t}$	[rad]	0.005513

Table 5.1: Performance achieved by the Best Found Nominal Agent

5.3 Reproducibility Assessments

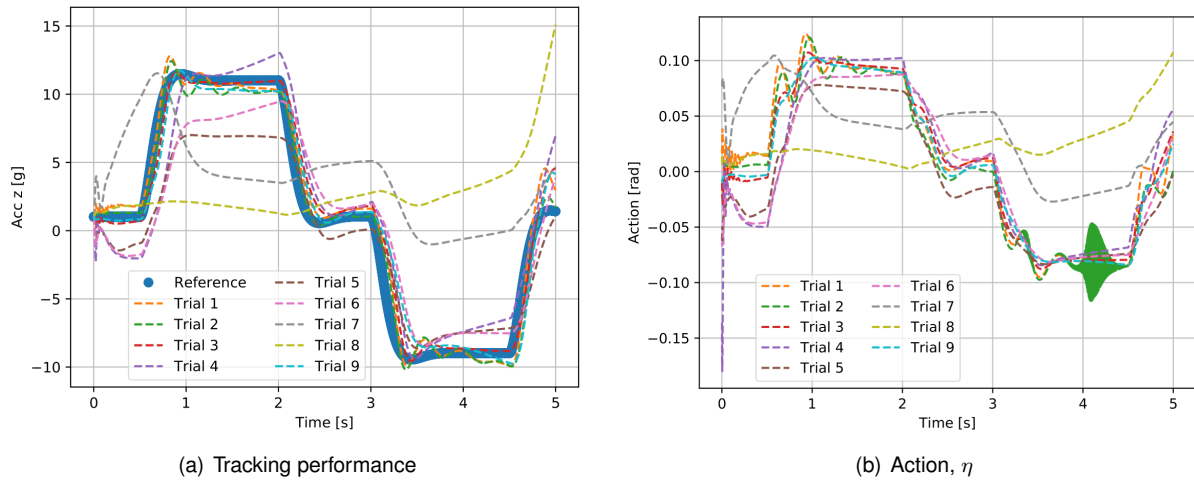


Figure 5.8: Nominal test performance of the Reproducibility Trials^a

^aCf. appendix C for further detailed statistics about the trains of these agents.

Figure 5.8 shows the tests of the best agents obtained during each of the nine trains run to assess the reproducibility of the best found nominal agent (cf. section 5.2) and it is possible to see that none of them achieved the target performance, i.e., none meets all the performance criteria established in section 2.2. Although most of the trials can be considered between the middle and the near regions, it is, in fact, possible to verify that trials 7 and 8 present a very poor tracking performance and that trial 2's action signal is not smooth. The reproducibility of the best found nominal agent is, thus, an important future research topic (cf. section 6.2).

5.4 Robustness Assessments

5.4.1 Latency

As figure 5.9 shows, from the four different values of l_{max} tried, only 5ms converged after 2500 episodes, meaning that it was the only robustifying train being run for a total of 5000 episodes, during which the best agent found was defined as the Latency Robustified Agent. When compared to the nominal agent (cf. figure B.1), the latter's nominal performance (cf. figure 5.10) is damaged, having a less stable action signal and a poorer tracking performance.

Furthermore, its performance in environments with latency (0ms to 40ms) did not provide any enhancement, as its success rate is low in all quantities of interest (cf. table 5.2).

Since the Latency Robustified Agent was worse than the Nominal Agent in both nominal and non-nominal environments, it lost in both Performance and Robustness categories. Thus, it is possible to say, in general terms, that, concerning latency, the robustifying trains failed.

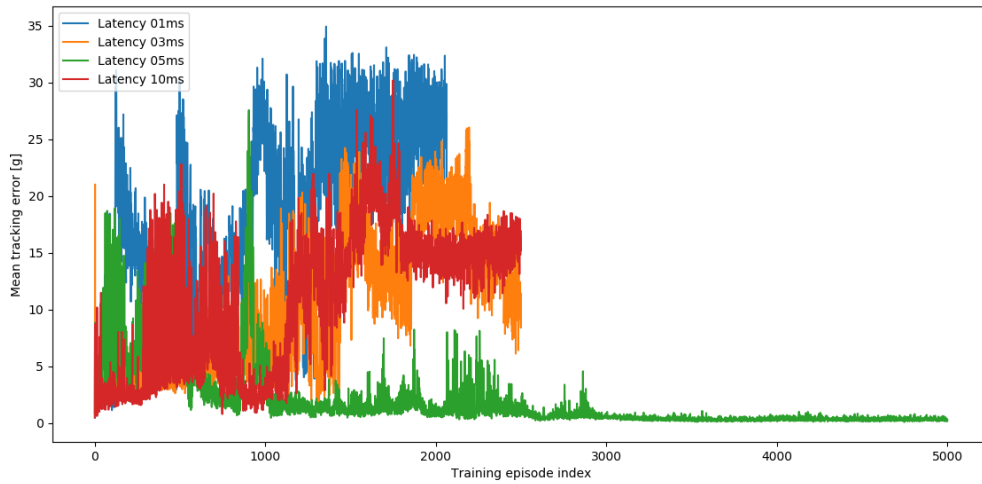


Figure 5.9: Mean tracking error of latency robustifying trains

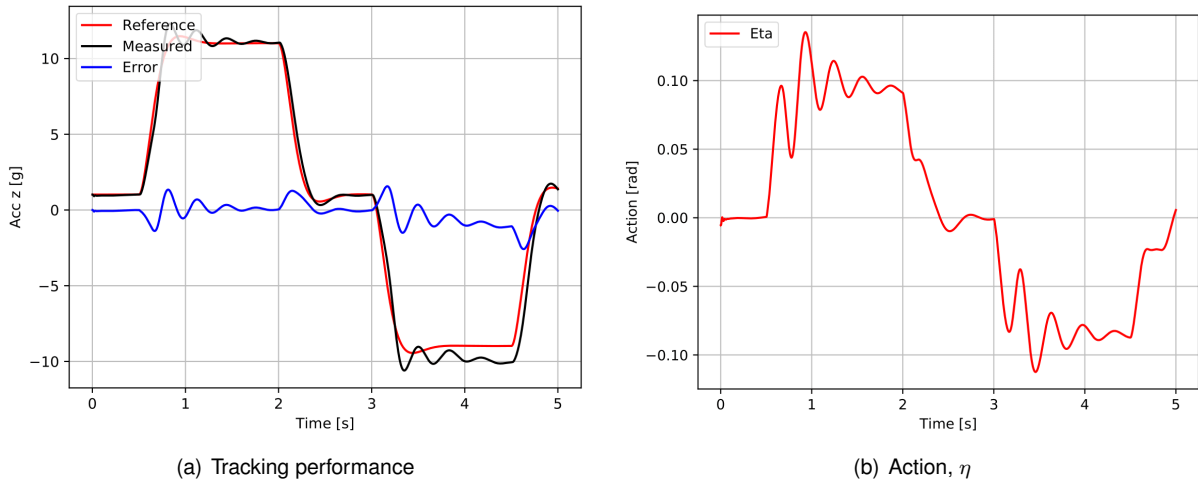


Figure 5.10: Nominal Performance of the Latency Robustified Agent

Performance requirement	Success %
$ e_z _{\max,r}$	0.00
Overshoot	25.00
η_{\max}	0.00
$\eta_{noise,r}$	7.50
$\eta_{noise,t}$	5.00

Table 5.2: Robustified Agent success rate in improving the robustness to Latency of the Nominal Agent^b

^aCf. figure D.1 for further details

^bCf. figure D.1 for further details

5.4.2 Estimation Uncertainty

As figure 5.11 shows, from the four different values of 3σ tried, only the 3% one converged after 2500 episodes, meaning that it was the only robustifying train being run for a total of 5000 episodes, during which the best agent found was defined as the Estimation Uncertainty Robustified Agent. When com-

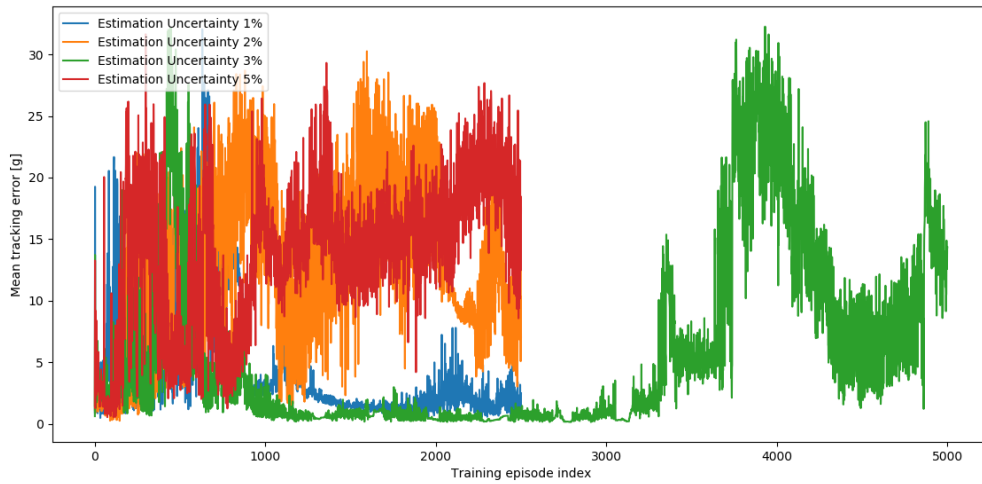


Figure 5.11: Mean tracking error of estimation uncertainty robustifying trains

pared to the nominal agent (cf. figure B.1), the latter's nominal performance (cf. figure 5.12) is improved, having a lower overshoot and a smoother action signal.

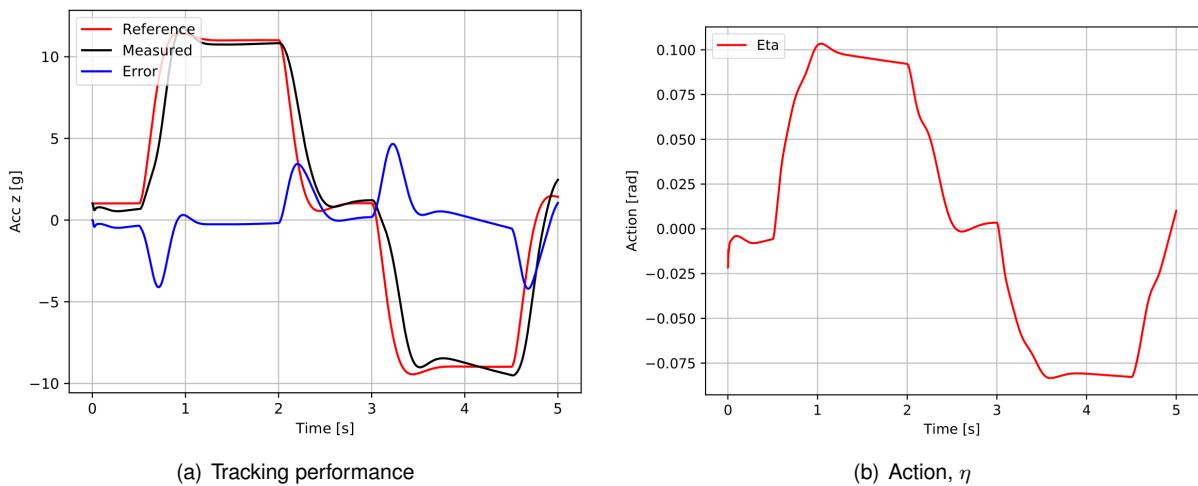


Figure 5.12: Nominal Performance of the Estimation Uncertainty Robustified Agent

Furthermore, it enhanced the performance of the Nominal Agent in environments with estimation uncertainty (-10% to 10%), having achieved high success rates in all quantities of interest (cf. table 5.3).

Since the Estimation Uncertainty Robustified Agent was better than the Nominal Agent in both nominal and non-nominal environments, it won in both Performance and Robustness categories. Thus, it is possible to say, in general terms, that, concerning estimation uncertainty, the robustifying trains succeeded.

5.4.3 Parametric Uncertainty

As figure 5.13 shows, from the four different values of 3σ tried, only the 5% one converged after 2500 episodes, meaning that it was the only robustifying train being run for a total of 5000 episodes, during

Performance requirement	Success %
$ e_z _{\max,r}$	60.38
Overshoot	66.39
η_{\max}	91.97
$\eta_{noise,r}$	77.51
$\eta_{noise,t}$	82.33

Table 5.3: Robustified Agent success rate in improving the robustness to Estimation Uncertainty of the Nominal Agent^b

^aCf. figure D.2 for further details

^bCf. figure D.2 for further details

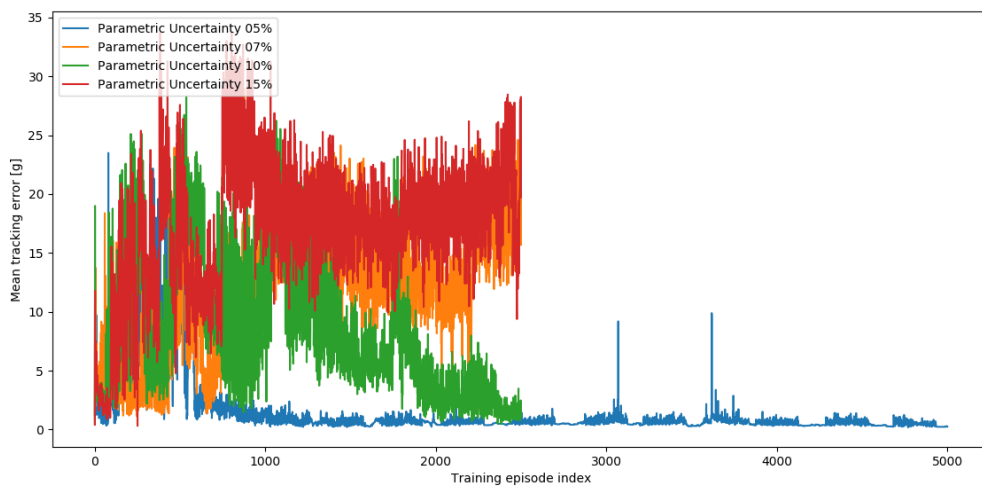


Figure 5.13: Mean tracking error of parametric uncertainty robustifying trains

which the best agent found was defined as the Parametric Uncertainty Robustified Agent. When compared to the nominal agent (cf. figure B.1), the latter's nominal tracking performance is damaged, but the action signal is smoother (cf. figure 5.14).

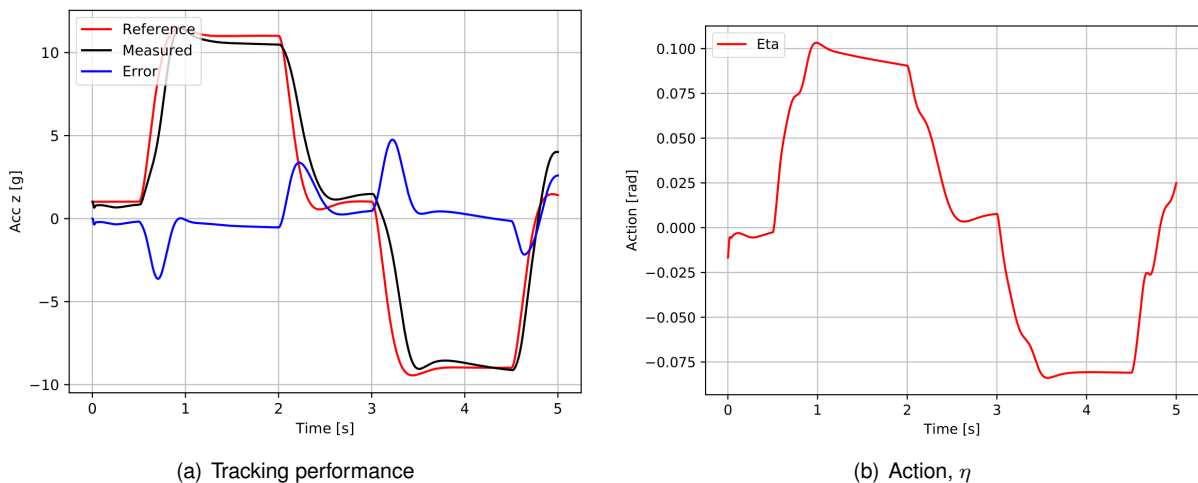


Figure 5.14: Nominal Performance of the Parametric Uncertainty Robustified Agent

Furthermore, it enhanced the performance of the Nominal Agent in environments with parametric uncertainty (-40% to 40%), having achieved high success rates in all quantities of interest (cf. table 5.4).

Performance requirement	Success %
$ e_z _{\max,r}$	61.55
Overshoot	83.16
η_{\max}	98.28
$\eta_{noise,r}$	100.00
$\eta_{noise,t}$	99.31

Table 5.4: Robustified Agent success rate in improving the robustness to Parametric Uncertainty of the Nominal Agent^b

^aCf. figure D.3 for further details

^bCf. figure D.3 for further details

Since the Parametric Uncertainty Robustified Agent was better than the Nominal Agent in non-nominal environments, it won in the Robustness categories, remaining acceptably the same in terms of performance in nominal environments. Thus, it is possible to say, in general terms, that, concerning parametric uncertainty, the robustifying trains succeeded.

Chapter 6

Conclusions

6.1 Achievements

The proposed algorithm has been considered successful, since all the objectives established in section 1.3 were accomplished, confirming the motivations put forth in section 1.1. Three main achievements must be highlighted:

1. the best found nominal performance (cf. section 5.2) achieved by the proposed algorithm with the non-linear model of the dynamic system (cf. chapter 2);
2. the ability of SER (cf. section 4.2.5) in boosting a previously suboptimally converged performance;
3. the success achieved by the Robustifying Trains (cf. section 4.5.1) whose Robustified Agents (cf. section 4.5.2) show very sound rates of success in overtaking the performance achieved by the best found nominal agent (cf. sections 5.4.2 and 5.4.3). RL has confirmed to be a promising learning framework for real life applications, where the concept of Robustifying Trains can bridge the gap between training the agent in the nominal environment and deploying it in reality.

6.2 Future Work

The first direction of future work is to expand the current task to the control of the whole flight dynamics of the GSAM, instead of solely the longitudinal one. Such an expansion would require both (i) straightforward modifications in the code and in the training methodology and (ii) some conceptual challenges, concerning the expansion of the reward function and of the exploration strategy. This direction of research is considered to be primary because it fulfills the purpose the hereby proposed algorithm was designed with (cf. section 1.1). Notice, for example, that the neural networks' architectures were already designed so that their size scales in accordance with different dimensions of the state and action vectors (cf. section 4.2.2).

Secondly, it would be interesting to investigate how to tackle the main challenges faced during the design of the proposed algorithm, namely:

1. to avoid the time consuming reward engineering (cf. section 4.1) ;
2. the definition of the exploration strategy (cf. section 4.2.2);
3. the reproducibility issue (cf. section 5.3);
4. the high number of hyperparameters (cf. section 4.2.1).

In fact, the reward engineering (cf. 1) is the most time consuming stage of the entire process and its avoidance is a priority. To this end, approaches like having sparse reward functions [28] or no reward functions at all [35], can be source of inspiration. As section 4.1.3 showed, it is highly likely that a so drastic simplification of the reward function requires deeper modifications in the RL algorithm itself even to the point where the algorithm to implement - in this case, TRPO - is chosen as a consequence of the reward function and not the opposite. For instance, Andrychowicz et al. proposed HER [28] has a key feature for DQN [36] to deal with sparse rewards. Knowing, however, that DQN is not suitable for the present task for its discrete action space, it would be interesting to implement DDPG [6], DQN's continuous action space child algorithm, with a sparse reward and HER.

Besides, it would be interesting to find an exploration strategy (cf. 2) able of following the evolution in terms of all the goals (cf. section 2.2), conditioning it, for example, on the reward r instead of only the tracking error e_z (cf. equation (4.47)). This is especially important if the goals grow in complexity once the implementation is expanded to the whole flight dynamics model, as suggested before.

Regarding 3, research could be done in order to find different techniques for the neural network's optimization phase, instead of ADAM, since they surely have a strong impact on the unfolding of the parameters' training, which dictate the reproducibility of the results.

Finally, there is also space for improvement concerning the hyperparameterization (cf. 4), more specifically, to identify optimality domains of each hyperparameter and the benefits of search algorithms like Random Search [37] in the tuning process.

Bibliography

- [1] R. S. Sutton and A. G. Barto. *Reinforcement Learning: An Introduction*. The MIT Press, 2 edition, 2018. ISBN 9780262039246. URL <https://lccn.loc.gov/2018023826>.
- [2] V. Mnih, K. Kavukcuoglu, D. Silver, A. Graves, I. Antonoglou, D. Wierstra, and M. Riedmiller. Playing Atari with Deep Reinforcement Learning. pages 1–9, 2013. URL <http://arxiv.org/abs/1312.5602>.
- [3] E. Todorov, T. Erez, and Y. Tassa. MuJoCo: A physics engine for model-based control. In *IEEE International Conference on Intelligent Robots and Systems*, pages 5026–5033, 2012. ISBN 9781467317375. doi: 10.1109/IROS.2012.6386109.
- [4] G. Brockman, V. Cheung, L. Pettersson, J. Schneider, J. Schulman, J. Tang, and W. Z. Openai. OpenAI Gym. Technical report, 2016.
- [5] J. Schulman, S. Levine, P. Moritz, M. Jordan, and P. Abbeel. Trust region policy optimization. *32nd International Conference on Machine Learning, ICML 2015*, 3:1889–1897, 2015.
- [6] T. P. Lillicrap, J. J. Hunt, A. Pritzel, N. Heess, T. Erez, Y. Tassa, D. Silver, and D. Wierstra. Continuous control with deep reinforcement learning. *4th International Conference on Learning Representations, ICLR 2016 - Conference Track Proceedings*, 2016.
- [7] S. Fujimoto, H. Van Hoof, and D. Meger. Addressing Function Approximation Error in Actor-Critic Methods. *35th International Conference on Machine Learning, ICML 2018*, 4:2587–2601, 2018.
- [8] Y. Wu, E. Mansimov, S. Liao, R. Grosse, and J. Ba. Scalable trust-region method for deep reinforcement learning using Kronecker-factored approximation. *Advances in Neural Information Processing Systems*, 2017-Decem(Nips):5280–5289, 2017. ISSN 10495258.
- [9] J. Schulman, P. Moritz, S. Levine, M. I. Jordan, and P. Abbeel. High-dimensional continuous control using generalized advantage estimation. *4th International Conference on Learning Representations, ICLR 2016 - Conference Track Proceedings*, pages 1–14, 2016.
- [10] D. Kangin and N. Pugeault. On-Policy Trust Region Policy Optimisation with Replay Buffers. pages 1–13, 2019. URL <http://arxiv.org/abs/1901.06212>.
- [11] T. Haarnoja, H. Tang, P. Abbeel, and S. Levine. Reinforcement learning with deep energy-based policies. *34th International Conference on Machine Learning, ICML 2017*, 3:2171–2186, 2017.

- [12] J. Schulman, F. Wolski, P. Dhariwal, A. Radford, and O. Klimov. Proximal Policy Optimization Algorithms. pages 1–12, 2017. URL <http://arxiv.org/abs/1707.06347>.
- [13] T. Haarnoja, A. Zhou, P. Abbeel, and S. Levine. Soft actor-critic: Off-policy maximum entropy deep reinforcement learning with a stochastic actor. *35th International Conference on Machine Learning, ICML 2018*, 5:2976–2989, 2018.
- [14] O. Nachum, M. Norouzi, G. Tucker, and D. Schuurmans. Smoothed action value functions for learning Gaussian policies. *35th International Conference on Machine Learning, ICML 2018*, 8: 5941–5953, 2018.
- [15] D. Horgan, J. Quan, D. Budden, G. Barth-Maron, M. Hessel, H. Van Hasselt, and D. Silver. Distributed prioritized experience replay. *6th International Conference on Learning Representations, ICLR 2018 - Conference Track Proceedings*, pages 1–19, 2018.
- [16] G. Barth-Maron, M. W. Hoffman, D. Budden, W. Dabney, D. Horgan, T. B. Dhruva, A. Muldal, N. Heess, and T. Lillicrap. Distributed distributional deterministic policy gradients. *6th International Conference on Learning Representations, ICLR 2018 - Conference Track Proceedings*, pages 1–16, 2018.
- [17] L. Espeholt, H. Soyer, R. Munos, K. Simonyan, V. Mnih, T. Ward, B. Yotam, F. Vlad, H. Tim, I. Dunning, S. Legg, and K. Kavukcuoglu. IMPALA: Scalable Distributed Deep-RL with Importance Weighted Actor-Learner Architectures. *35th International Conference on Machine Learning, ICML 2018*, 4:2263–2284, 2018.
- [18] S. Gu, T. Lillicrap, Z. Ghahramani, R. E. Turner, B. Schölkopf, and S. Levine. Interpolated policy gradient: Merging on-policy and off-policy gradient estimation for deep reinforcement learning. *Advances in Neural Information Processing Systems, 2017-Decem(Nips)*:3847–3856, 2017. ISSN 10495258.
- [19] O. Nachum, M. Norouzi, K. Xu, and D. Schuurmans. TruST-PCL: An off-policy trust region method for continuous control. *6th International Conference on Learning Representations, ICLR 2018 - Conference Track Proceedings*, pages 1–14, 2018.
- [20] S. Gu, T. Lillicrap, Z. Ghahramani, R. E. Turner, and S. Levine. Q-PrOP: Sample-efficient policy gradient with an off-policy critic. *5th International Conference on Learning Representations, ICLR 2017 - Conference Track Proceedings*, pages 1–13, 2019.
- [21] B. O’Donoghue, R. Munos, K. Kavukcuoglu, and V. Mnih. Combining policy gradient and q-learning. *5th International Conference on Learning Representations, ICLR 2017 - Conference Track Proceedings*, pages 1–15, 2019.
- [22] F. Peter. *Nonlinear and Adaptive Missile Autopilot Design*. PhD thesis, Technischen Universität München, Munich, 5 2018.

- [23] R. S. Sutton, D. Mcallester, S. Singh, and Y. Mansour. Policy Gradient Methods for Reinforcement Learning with Function Approximation. Technical report, 2000.
- [24] R. H. Crites and A. G. Barto. An Actor/Critic Algorithm that Equivalent to Q-Learning. In *Advances in Neural Information Processing Systems*, pages 401–408. 1995.
- [25] M. Jaderberg, V. Mnih, W. M. Czarnecki, T. Schaul, J. Z. Leibo, D. Silver, and K. Kavukcuoglu. Reinforcement learning with unsupervised auxiliary tasks. *5th International Conference on Learning Representations, ICLR 2017 - Conference Track Proceedings*, pages 1–14, 2019.
- [26] M. Plappert, R. Houthoofd, P. Dhariwal, S. Sidor, R. Y. Chen, X. Chen, T. Asfour, P. Abbeel, M. Andrychowicz, and â. Openai. Parameter Space Noise for Exploration. Technical report.
- [27] J. Martens and R. Grosse. Optimizing neural networks with Kronecker-factored approximate curvature. *32nd International Conference on Machine Learning, ICML 2015*, 3:2398–2407, 2015.
- [28] M. Andrychowicz, F. Wolski, A. Ray, J. Schneider, R. Fong, P. Welinder, B. McGrew, J. Tobin, P. Abbeel, and W. Zaremba. Hindsight Experience Replay. In *Advances in Neural Information Processing Systems*, 2017. URL <https://goo.gl/SMrQnI>.
- [29] T. Schaul, J. Quan, I. Antonoglou, and D. Silver. Prioritized experience replay. *4th International Conference on Learning Representations, ICLR 2016 - Conference Track Proceedings*, pages 1–21, 2016.
- [30] K. Narasimhan, T. D. Kulkarni, and R. Barzilay. Language Understanding for Text-based Games using Deep Reinforcement Learning. Technical report, Massachusetts Institute of Technology, 2015. URL <http://mudstats.com/>.
- [31] L. Evangelisti. *Asynchronous Advantage Actor-Critic Deep Reinforcement Learning applied to Quadcopter Control*. PhD thesis, Technische Universität München, 2019.
- [32] R. Bellman, I. Glicksberg, and O. Gross. On the 'bang-bang' control problem. *Quarterly of Applied Mathematics*, 14(1):11–18, 4 1956. ISSN 0033-569X. doi: 10.1090/qam/78516. URL <https://www.ams.org/qam/1956-14-01/S0033-569X-1956-78516-4/>.
- [33] D. P. Kingma and J. L. Ba. Adam: A method for stochastic optimization. *3rd International Conference on Learning Representations, ICLR 2015 - Conference Track Proceedings*, pages 1–15, 2015.
- [34] M. Schain. *Machine Learning Algorithms and Robustness*. PhD thesis, Tel Aviv University, 2015. URL https://www.tau.ac.il/~mansour/students/Mariano_Scain_Ph.d.pdf.
- [35] B. Eysenbach, A. Gupta, J. Ibarz, and S. Levine. Diversity is All You Need: learning skills without a reward function. 2018. URL <https://sites.google.com/view/diayn/>.
- [36] V. Mnih, K. Kavukcuoglu, D. Silver, A. A. Rusu, J. Veness, M. G. Bellemare, A. Graves, M. Riedmiller, A. K. Fidjeland, G. Ostrovski, S. Petersen, C. Beattie, A. Sadik, I. Antonoglou, H. King,

D. Kumaran, D. Wierstra, S. Legg, and D. Hassabis. Human-level control through deep reinforcement learning. *Nature*, 2015. doi: 10.1038/nature14236.

[37] J. Bergstra and Y. Bengio. Random search for hyper-parameter optimization. *Journal of Machine Learning Research*, 13:281–305, 2012. ISSN 15324435.

Appendix A

Reward Engineering

CORF	w_1	w_2	w_3	w_4	ϵ
ES ^a Initial	$4g^{-2}$	10			
ES LQ-cost-like	$(10g)^{-1}$	$\frac{6}{\pi}$	20		
ES $\Delta\eta$	$(10g)^{-1}$	$\frac{6}{\pi}$	20	0.01	
ES Best-fit of past 5 η	$(7g)^{-1}$	$\frac{6}{\pi}$	3	20	
DS ^b $n = 4$	$30g^{-1}$	10^4	$0.1 \max\left(\frac{ e_z }{g}, 0.5\right)$	20	
DS $n = 3$	$30g^{-1}$	10^5	10^3		
DS $n = 2$ (smoothness)	$30g^{-1}$	10^3			
DS $n = 2$ (magnitude)	$30g^{-1}$	10^5			
DS SER $n = 4$ (conf. 1)	$30g^{-1}$	10^4	$\frac{0.08}{\max\left(\frac{ e_z }{g}, 0.5\right)}$	$\frac{20}{3 \max\left(\frac{ e_z }{g}, 3\right)}$	$2g$
DS SER $n = 4$ (conf. 2)	$40g^{-1}$	10^4	$\frac{0.1}{\max\left(\frac{ e_z }{g}, 0.5\right)}$	20	$10g$
DS SER $n = 4$ (conf. 3)	$30g^{-1}$	10^4	$\frac{60}{\max\left(\frac{ e_z }{g}, 3\right)}$	20	$8g$
DS SER $n = 3$ (conf. 1)	$40g^{-1}$	5×10^4	$\frac{20}{\max\left(\frac{ e_z }{g}, 3\right)}$		$10g$
DS SER $n = 3$ (conf. 2)	$40g^{-1}$	10^5	10^3		$5g$
DS SER $n = 3$ (conf. 3)	$120g^{-1}$	10^5	10^3		$2g$
DS SER $n = 3$ (conf. 4)	$120g^{-1}$	10^5	10^3		$7g$
DS SER $n = 3$ (conf. 5)	$120g^{-1}$	10^5	10^3		$5g$
DS SER $n = 3$ (conf. 6)	$42g^{-1}$	10^5	$\frac{60}{\max\left(\frac{ e_z }{g}, 3\right)}$		$8g$
DS SER $n = 3$ (conf. 7)	$40g^{-1}$	10^5	$\frac{20}{\max\left(\frac{ e_z }{g}, 3\right)}$		$6g$
DS SER $n = 3$ (conf. 8)	$40g^{-1}$	10^5	$\frac{60}{\max\left(\frac{ e_z }{g}, 3\right)}$		$10g$
DS SER $n = 2$ (magnitude, conf. 1)	2	10^4			$10g$
DS SER $n = 2$ (magnitude, conf. 2)	2	5×10^4			$8g$

Table A.1: Parameters of the CORF used along the Reward Engineering process

^aExponential Sum

^bDense Sum

Appendix B

Nominal Agent used in the Robustness Assessments

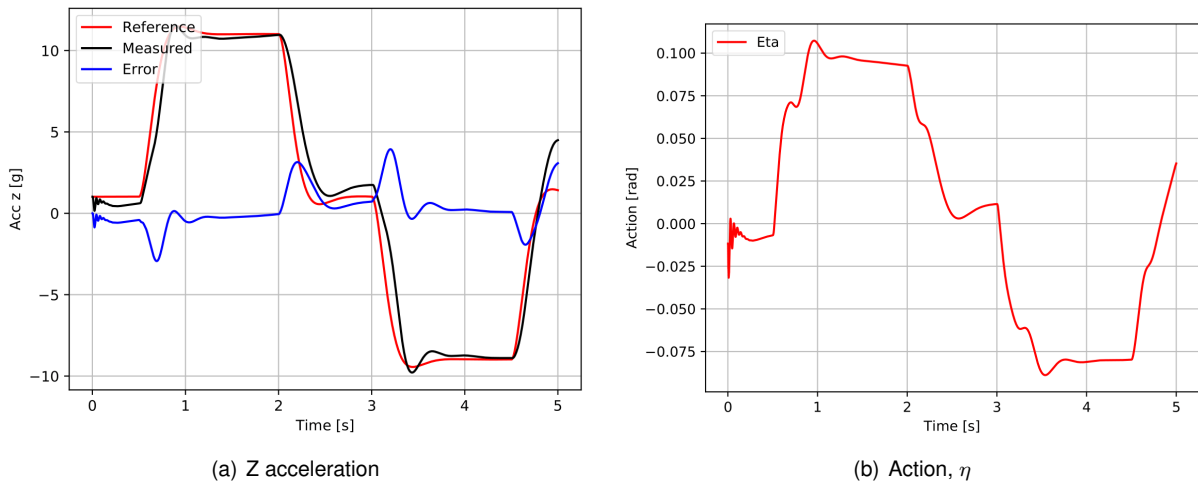


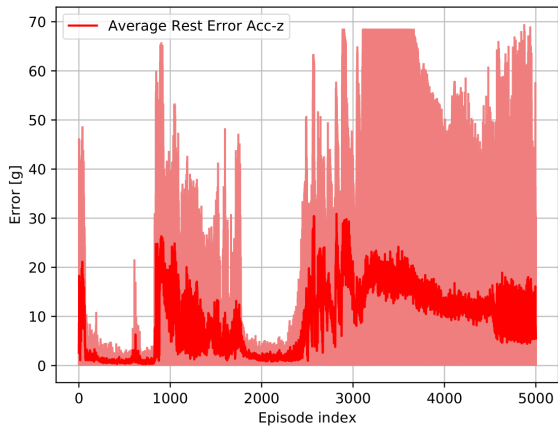
Figure B.1: Nominal performance of the 2^{nd} -Best Found Agent used in the Robustness Assessments

Performance requirement	[Unit]	Value
$ e_z _{\max,r}$	[g]	0.8666
Overshoot	[%]	34.76
η_{\max}	[rad]	0.1073
$\eta_{noise,r}$	[rad]	0.09285
$\eta_{noise,t}$	[rad]	0.006574

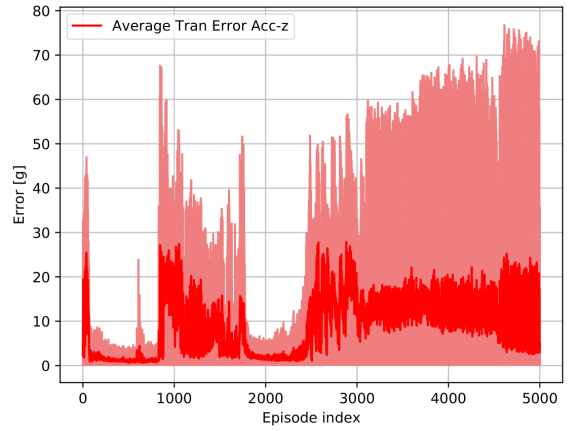
Table B.1: Performance achieved by the 2^{nd} Best Found Nominal Agent

Appendix C

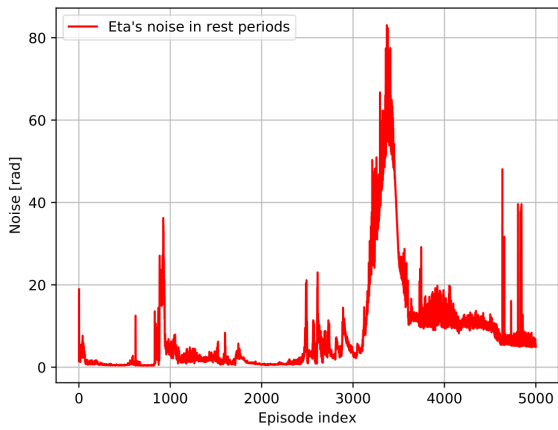
Reproducibility Assessment Experiments



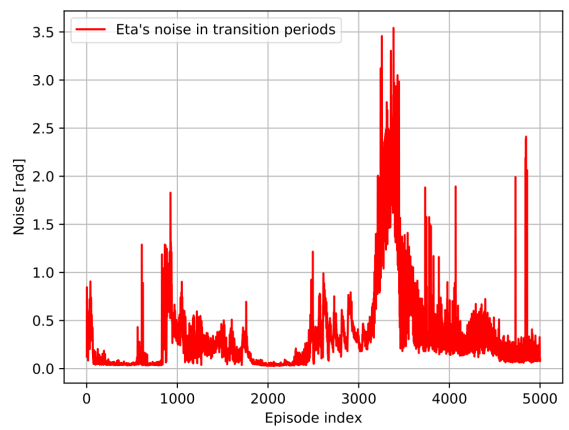
(a) Tracking error in resting periods



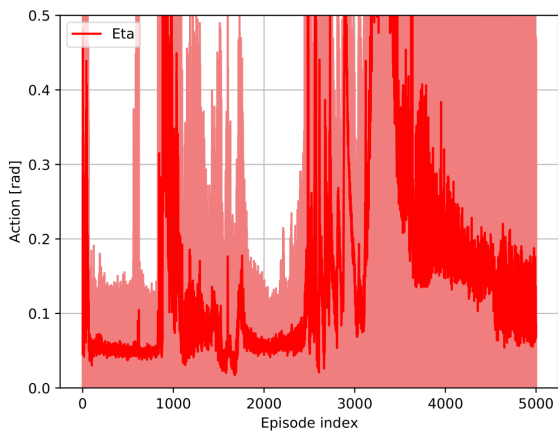
(b) Tracking error in transition periods



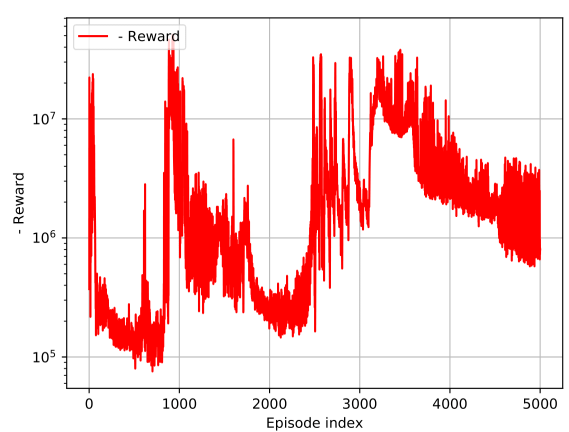
(c) η 's noise in resting periods



(d) η 's noise in transition periods

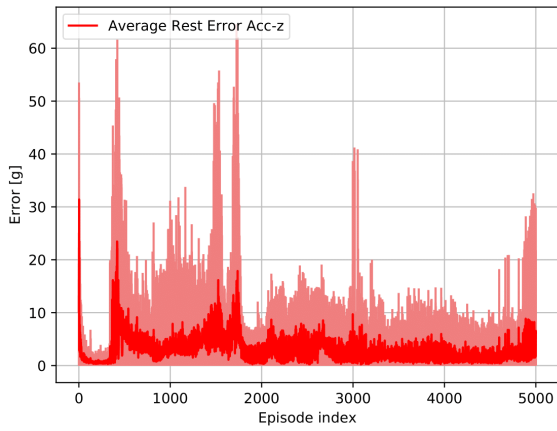


(e) η 's magnitude

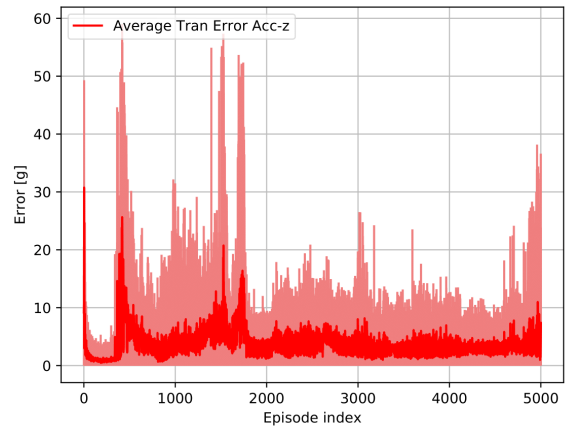


(f) Reward

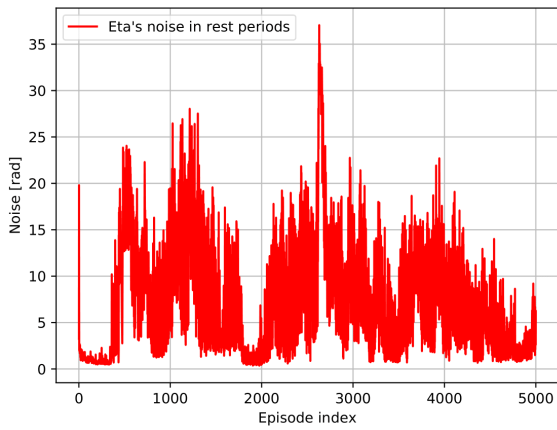
Figure C.1: Reproducibility assessment training - experiment 1



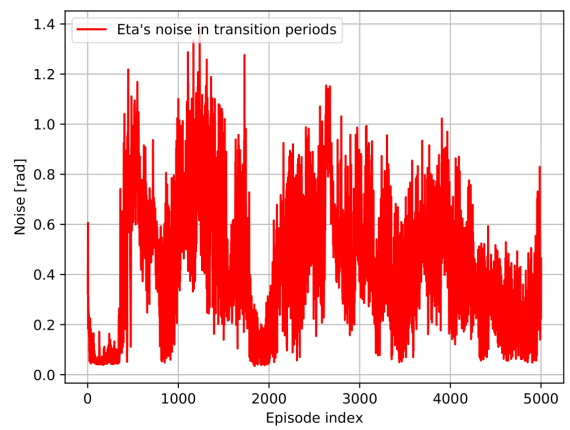
(a) Tracking error in resting periods



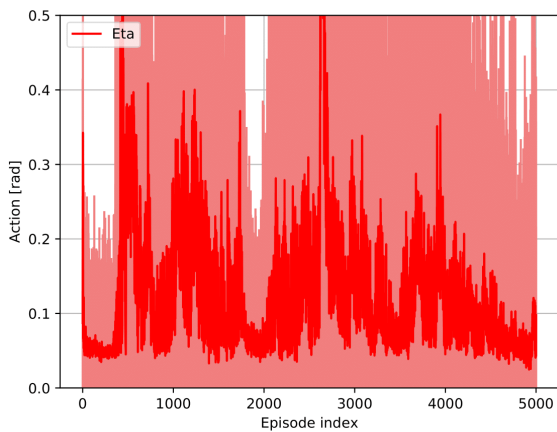
(b) Tracking error in transition periods



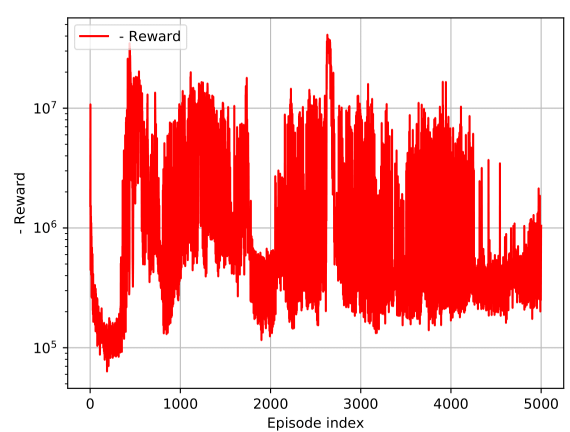
(c) η 's noise in resting periods



(d) η 's noise in transition periods

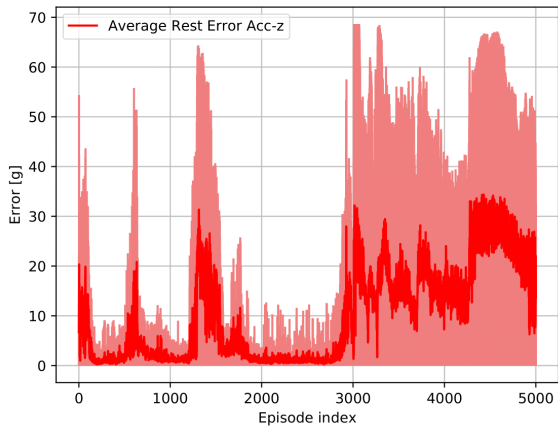


(e) η 's magnitude

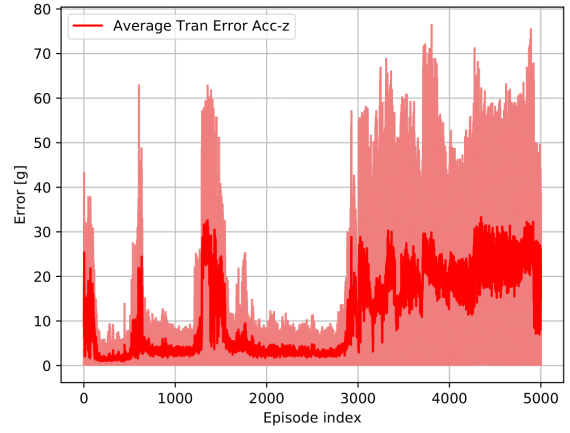


(f) Reward

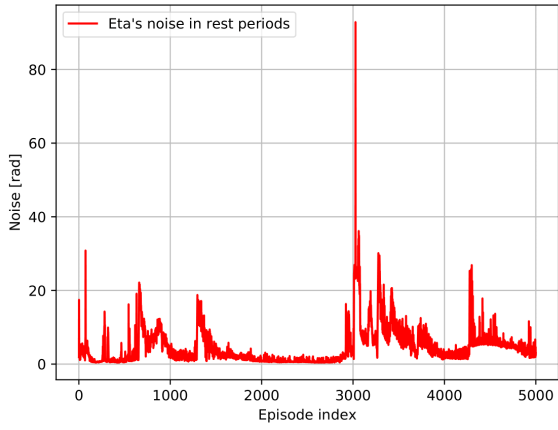
Figure C.2: Reproducibility assessment training - experiment 2



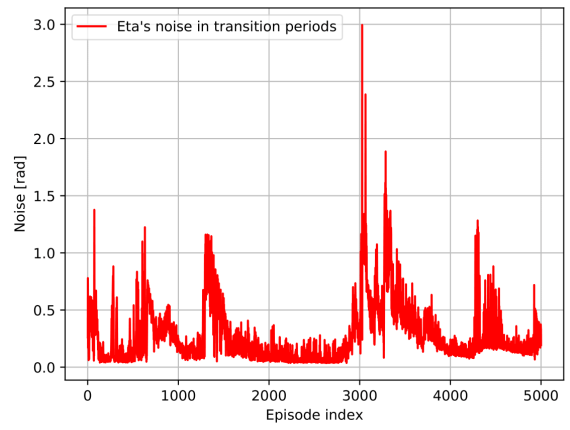
(a) Tracking error in resting periods



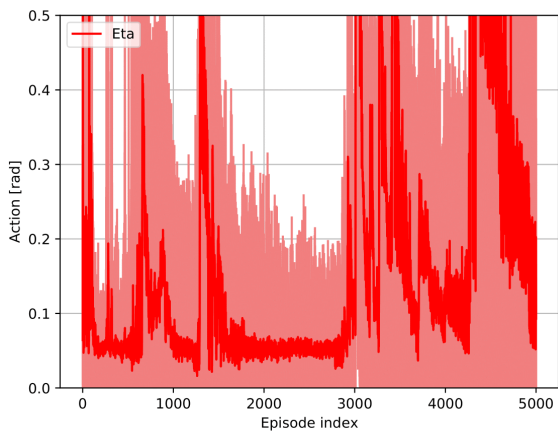
(b) Tracking error in transition periods



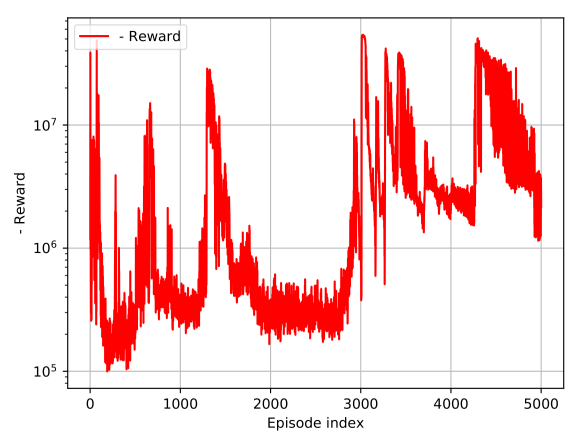
(c) η 's noise in resting periods



(d) η 's noise in transition periods

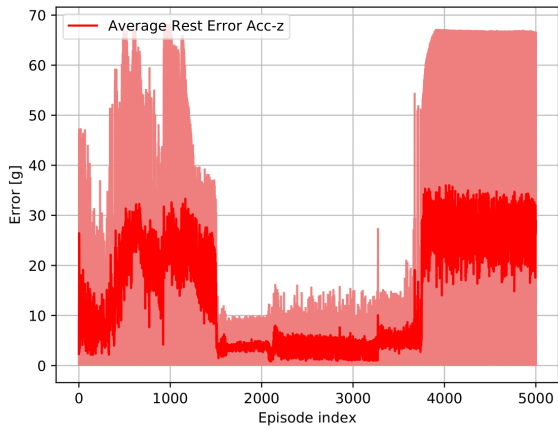


(e) η 's magnitude

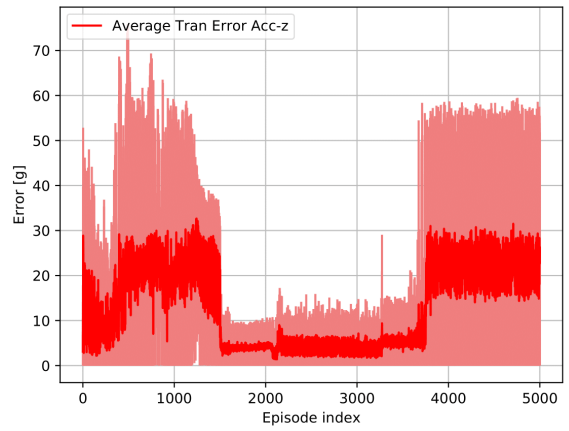


(f) Reward

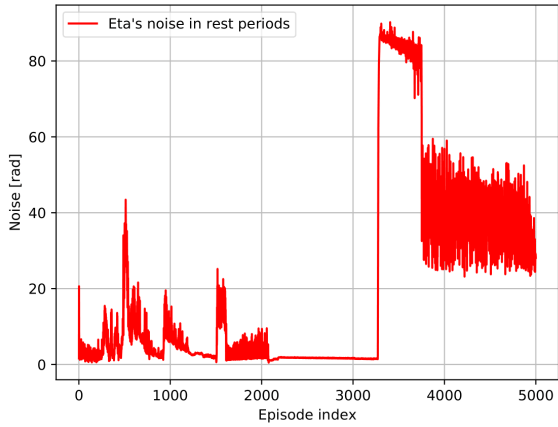
Figure C.3: Reproducibility assessment training - experiment 3



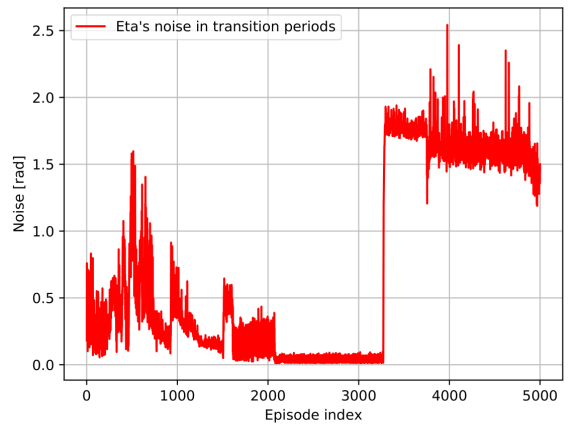
(a) Tracking error in resting periods



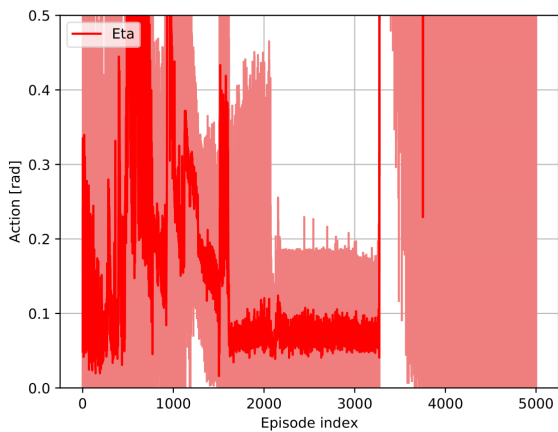
(b) Tracking error in transition periods



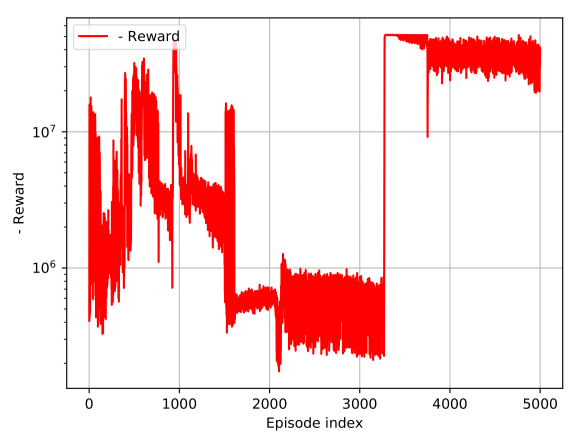
(c) η 's noise in resting periods



(d) η 's noise in transition periods

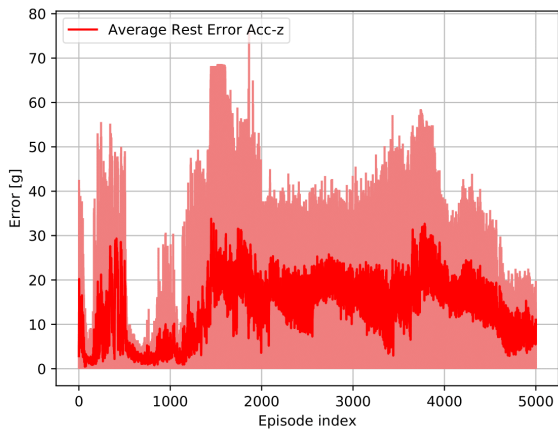


(e) η 's magnitude

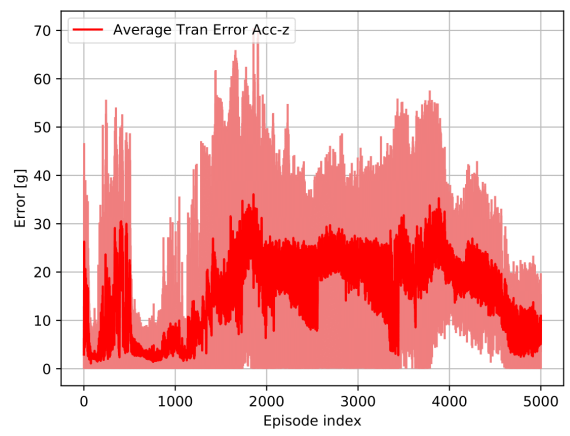


(f) Reward

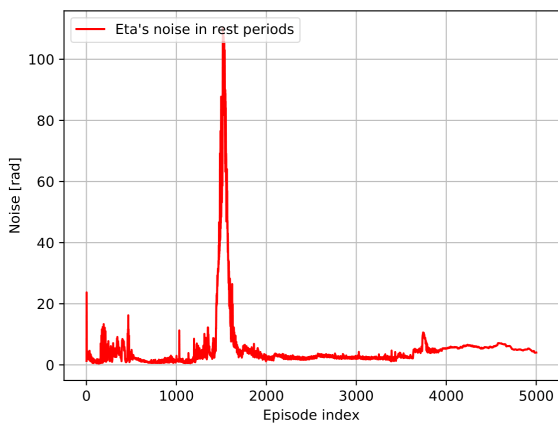
Figure C.4: Reproducibility assessment training - experiment 4



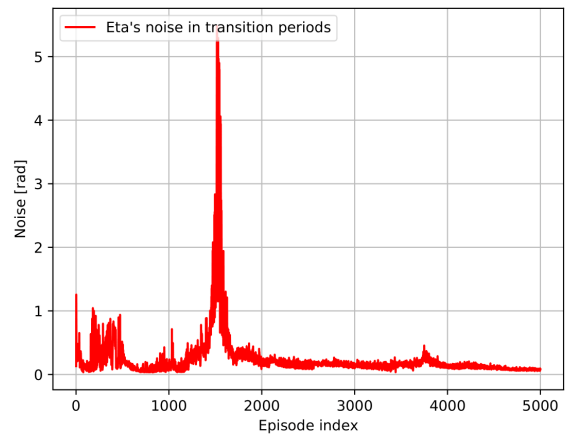
(a) Tracking error in resting periods



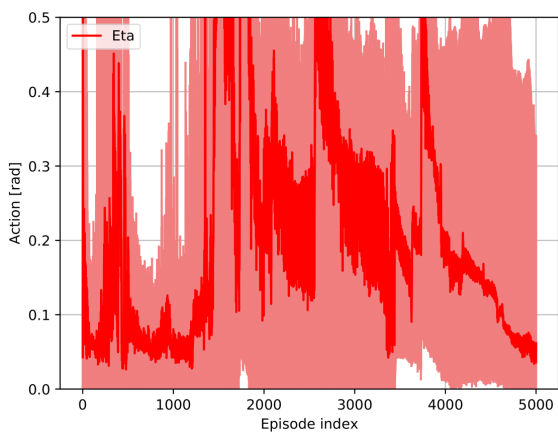
(b) Tracking error in transition periods



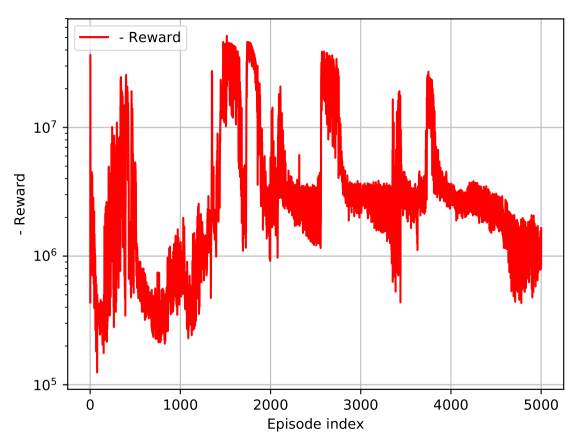
(c) η 's noise in resting periods



(d) η 's noise in transition periods

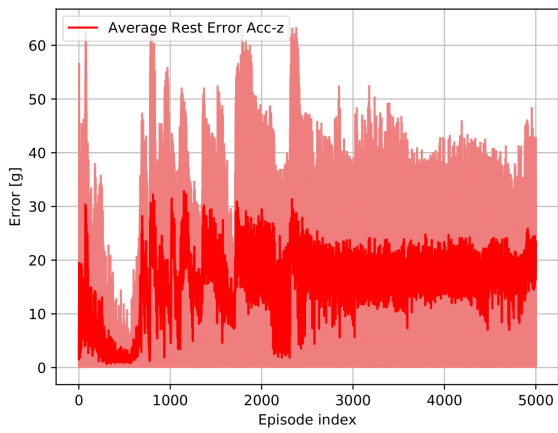


(e) η 's magnitude

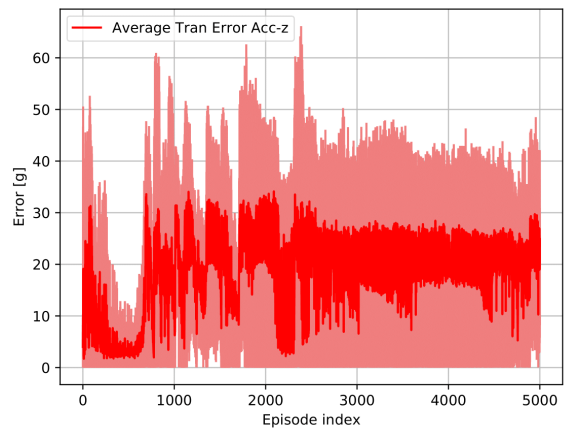


(f) Reward

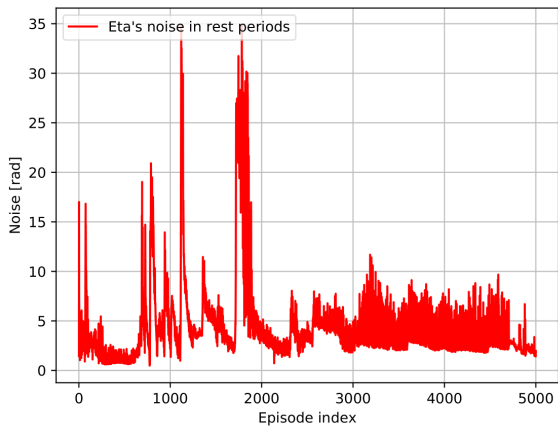
Figure C.5: Reproducibility assessment training - experiment 5



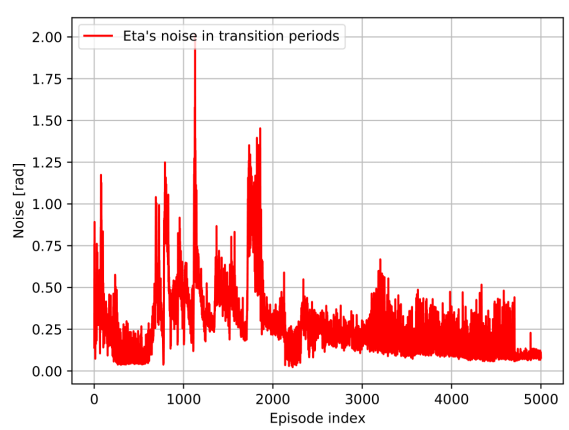
(a) Tracking error in resting periods



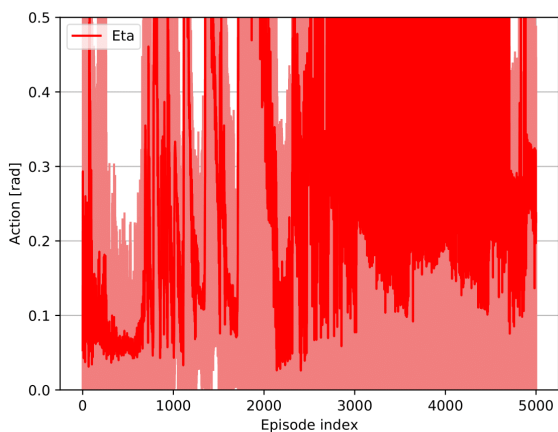
(b) Tracking error in transition periods



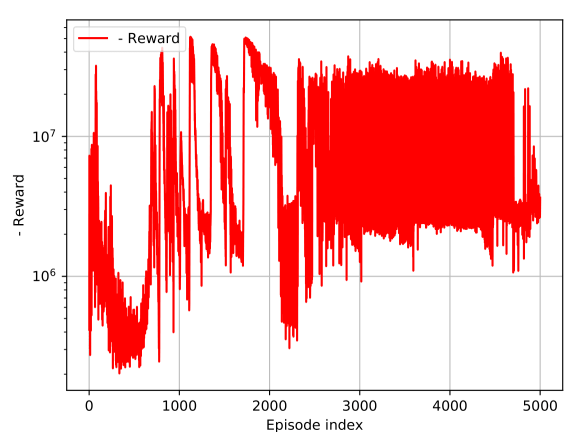
(c) η 's noise in resting periods



(d) η 's noise in transition periods

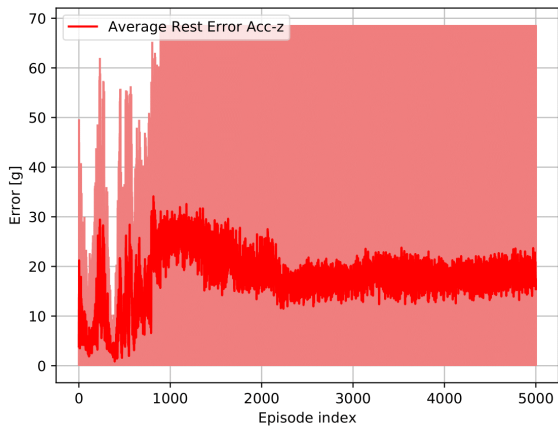


(e) η 's magnitude

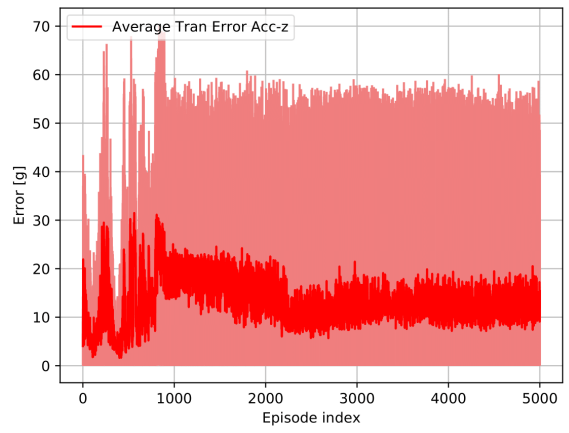


(f) Reward

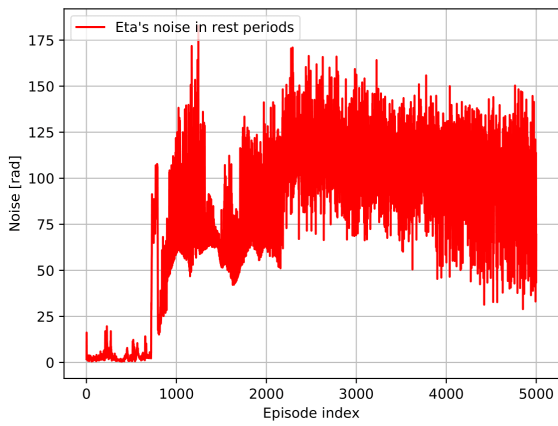
Figure C.6: Reproducibility assessment training - experiment 6



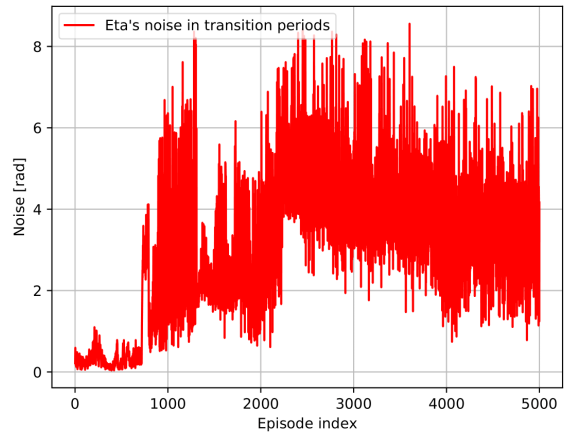
(a) Tracking error in resting periods



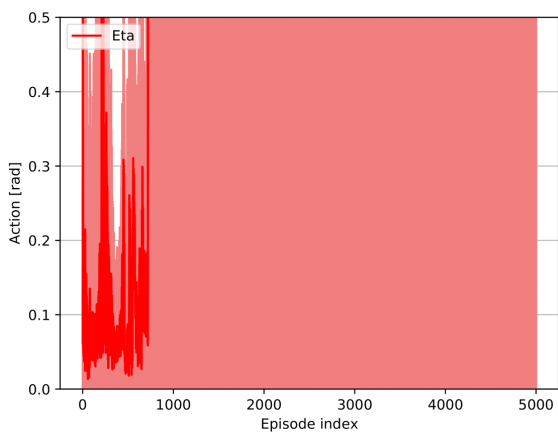
(b) Tracking error in transition periods



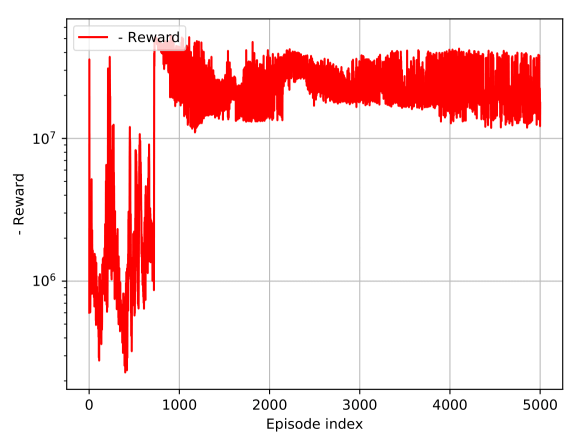
(c) η 's noise in resting periods



(d) η 's noise in transition periods

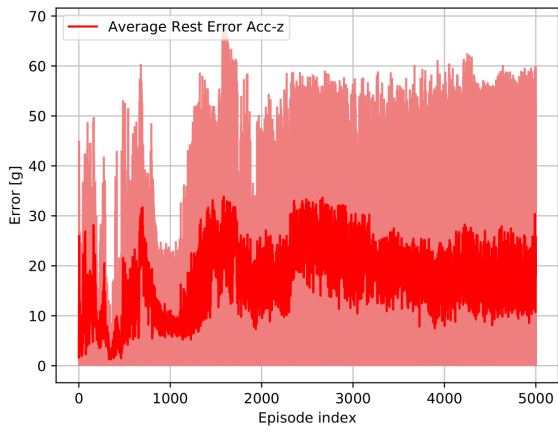


(e) η 's magnitude

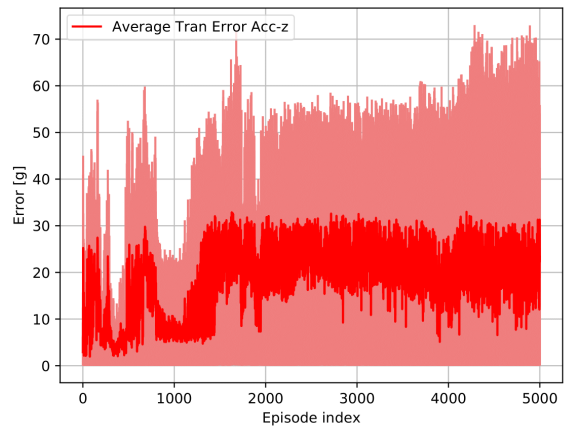


(f) Reward

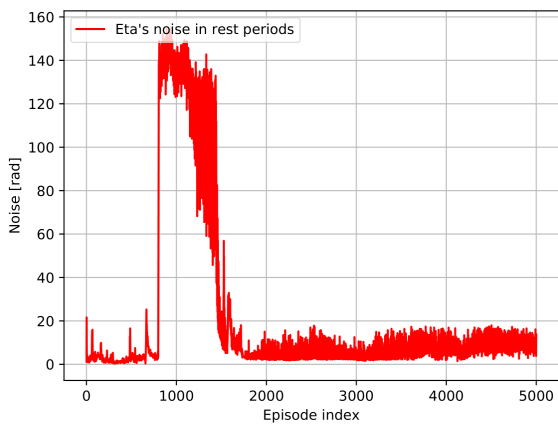
Figure C.7: Reproducibility assessment training - experiment 7



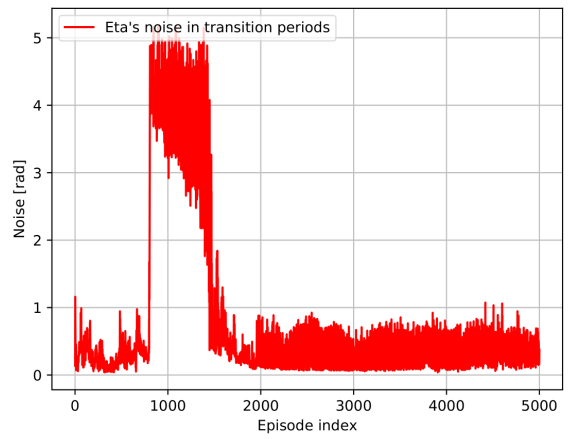
(a) Tracking error in resting periods



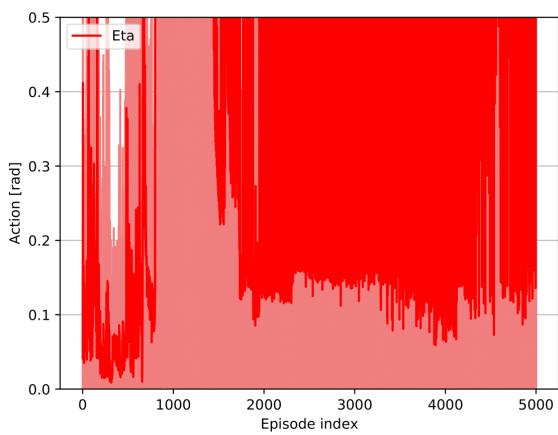
(b) Tracking error in transition periods



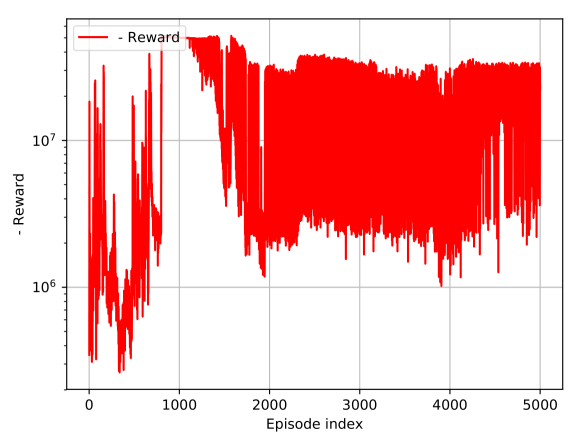
(c) η 's noise in resting periods



(d) η 's noise in transition periods

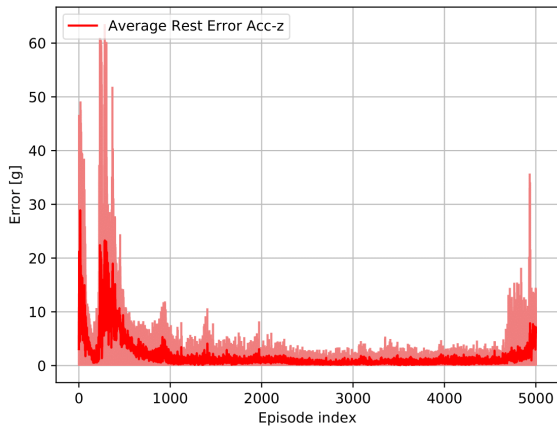


(e) η 's magnitude

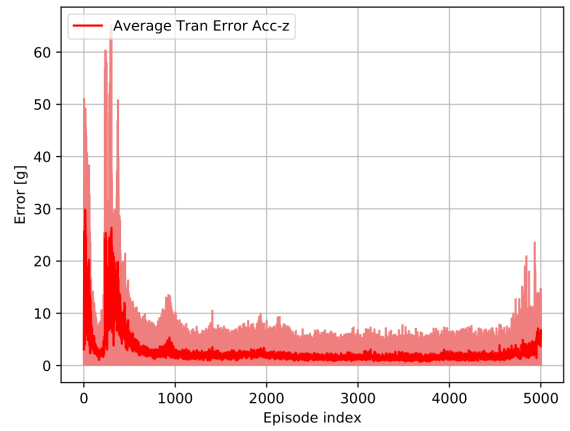


(f) Reward

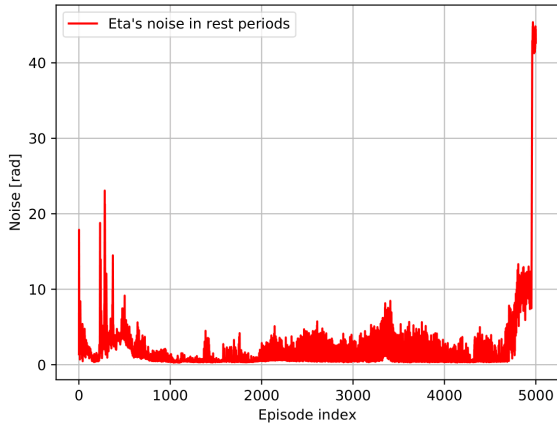
Figure C.8: Reproducibility assessment training - experiment 8



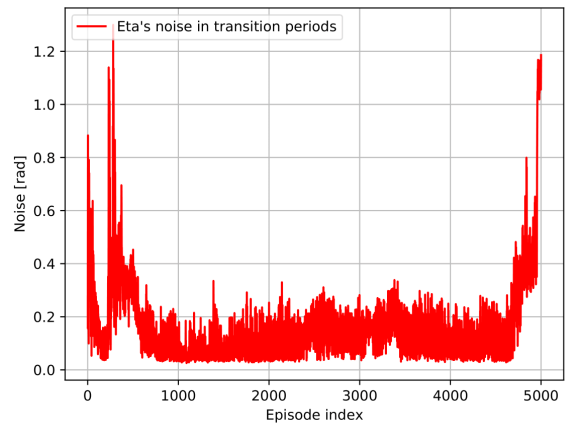
(a) Tracking error in resting periods



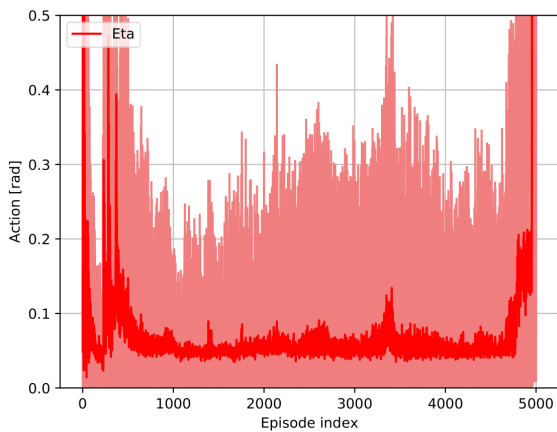
(b) Tracking error in transition periods



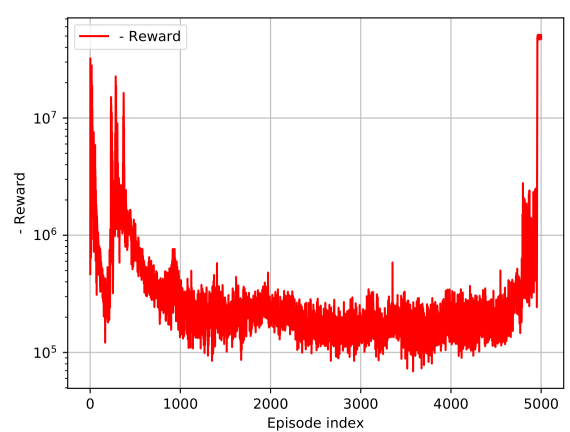
(c) η 's noise in resting periods



(d) η 's noise in transition periods



(e) η 's magnitude



(f) Reward

Figure C.9: Reproducibility assessment training - experiment 9

Appendix D

Nominal and Robustified Agents' Robustness Comparison

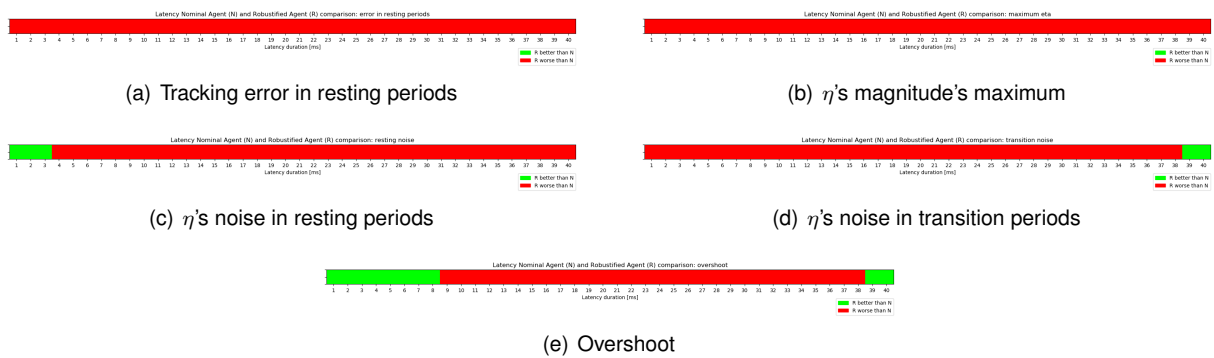
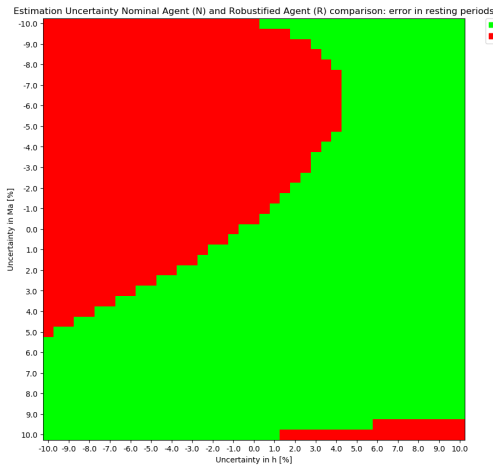


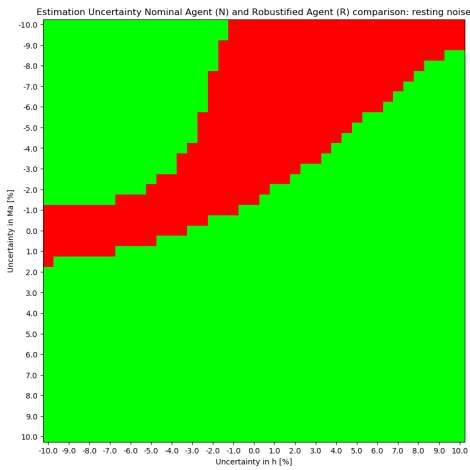
Figure D.1: Nominal (N) vs. Robustified (R) Agents in Environments with Latency



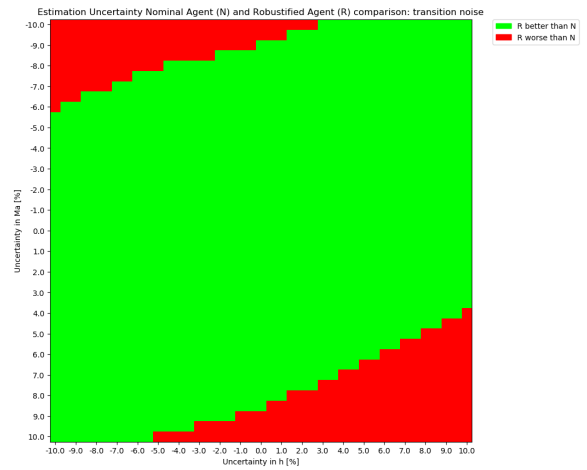
(a) Tracking error in resting periods



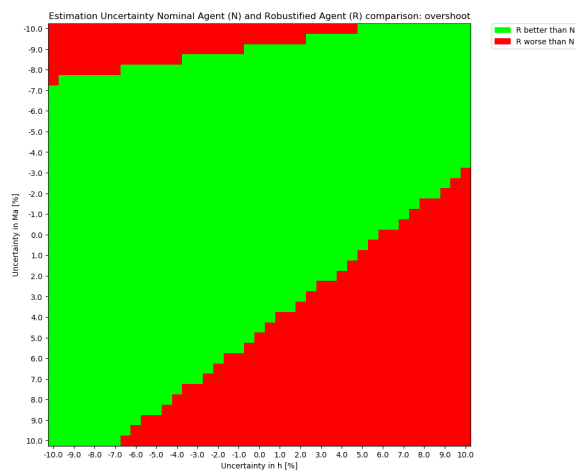
(b) η 's magnitude's maximum



(c) η 's noise in resting periods

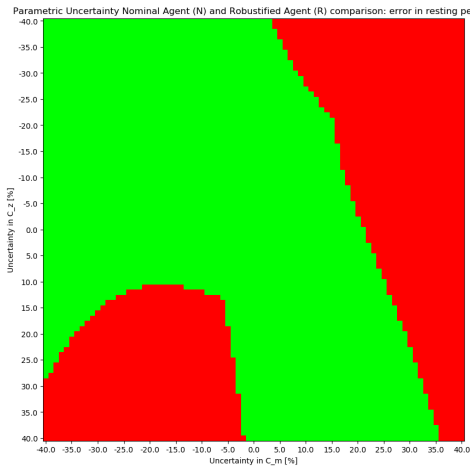


(d) η 's noise in transition periods

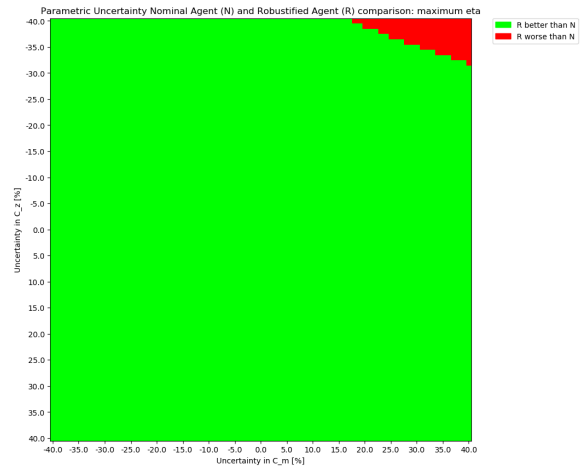


(e) Overshoot

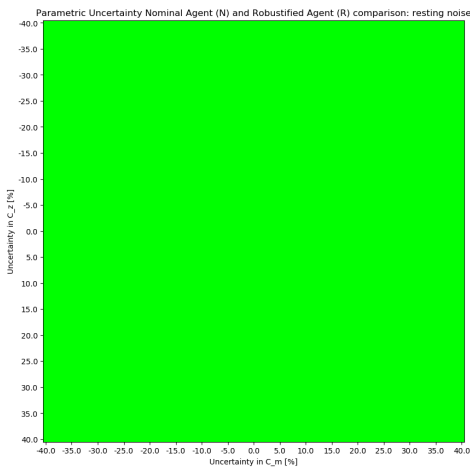
Figure D.2: Nominal (N) vs. Robustified (R) Agents in Environments with Estimation Uncertainty



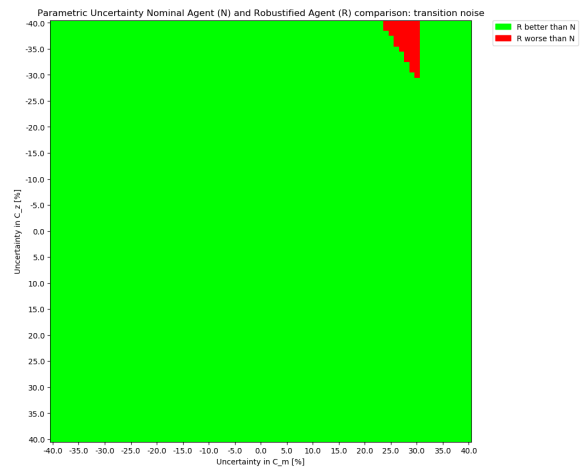
(a) Tracking error in resting periods



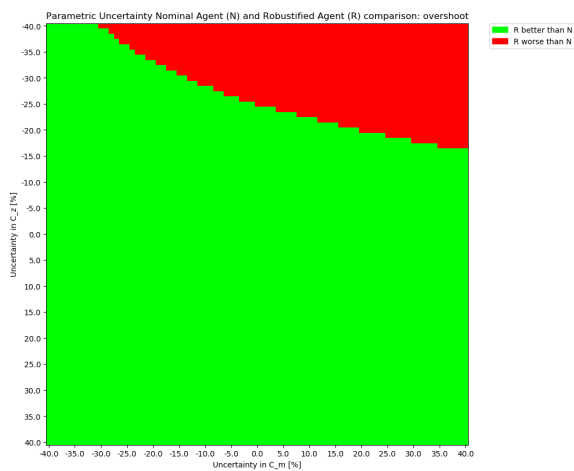
(b) η 's magnitude's maximum



(c) η 's noise in resting periods



(d) η 's noise in transition periods



(e) Overshoot

Figure D.3: Nominal (N) vs. Robustified (R) Agents in Environments with Parametric Uncertainty

